CHALMERS
UNIVERSITY OF TECHNOLOGY

A Numerical Investigation of the Slamming Event Through FSI Analysis

Master's thesis in the International Master´s Programme in Naval Architecture and Ocean Engineering

MARION AKU ATSINE ZU

Department of Mechanics and Maritime Sciences
CHALMERS UNIVERSITY OF TECHNOLOGY
Gothenburg, Sweden 2019

MASTER'S THESIS IN THE INTERNATIONAL MASTER'S PROGRAMME IN NAVAL ARCHITECTURE AND OCEAN ENGINEERING

A Numerical Investigation of the Slamming Event Through FSI Analysis

MARION AKU ATSINE ZU

Department of Mechanics and Maritime Sciences

Division of Marine Technology

CHALMERS UNIVERSITY OF TECHNOLOGY

Göteborg, Sweden 2019

A Numerical Investigation of the Slamming Event Through FSI Analysis
MARION AKU ATSINE ZU

Master's Thesis 2019:84
Department of Mechanics and Maritime Sciences
Division of Marine Technology
Chalmers University of Technology
SE - 412 96 Göteborg
Sweden
Telephone: + 46 (0)31-772 1000

ACKNOWLEDGEMENTS

As per the requirements for a Master's Degree in Naval Architecture and Ocean Engineering at Chalmers University of Technology, Göteborg, this Master Thesis on "A Numerical Investigation of the Slamming Event Through FSI Analysis" was carried out at the Division of Marine Technology, Department of Mechanics and Maritime Sciences between January 2019 and July 2019 under the supervision of Professor Carl-Erik Janson.

I would like to take this opportunity to acknowledge the relentless efforts, support and patience of Professor Carl- Erik Janson and his effective supervision throughout the period of my research.

I would also like to take this opportunity to register my respect to all authors and researches from whose work I have made reference to during this research.

To my family, friends, I am very grateful for the morale support given me during this period.

Göteborg, July 2019.

Marion Aku Atsine Zu

A Numerical Investigation of the Slamming Event Through FSI Analysis
Master's Thesis in the International Master's Programme in Naval Architecture and Ocean Engineering
MARION AKU ATSINE ZU
Department of Mechanics and Maritime Sciences
Division of Marine Technology
Chalmers University of Technology

ABSTRACT

Consciously, the Maritime Industry / Classification Societies / Marine Engineers / Naval Architects have over the century engaged in progressive research work in the subject area of hull slamming to understand its complexity and the physics behind / underlying it. This is evident owing to the number of publications and literature in this subject area over the decade only. Achieving this global aim will ensure that slamming and slamming induced whipping are incorporated and its effects accounted for in Classification Rules pertaining to structural design and hull integrity in the early stages.

Different theories, methods and approaches have been utilized in the various research studies into hull slamming that include momentum theory, boundary element methods, statistical methods, analytical methods computational fluid dynamics – CFD, SPH methods, experimental techniques and full scale experiments. However, each of these methods have limitations and challenges though helping to bridge the gap from what was unknown about slamming in the past to what is being known about the phenomenon in recent times. The future of research and analysis in slamming is through the use of numerical methods most specifically CFD.

In view of this, the current research study which is focused on a "Numerical Investigation of the Slamming Event Through FSI Analysis" was carried out by means of a co-simulation using STAR-CCM+, a CFD software and ABAQUS, a FE Software. Investigations were made into the effect of deadrise angles, the effect of the compressibility of air and water (the fluid) and the effect of the magnitude of the water entry velocity / impact velocity.

Results from the simulations on the three different focus areas indicate that the unlikely event of slamming / the phenomenon is sensitive to the deadrise angles, compressibility of the fluid and the magnitude of the impact velocity.

Keywords: Numerical analysis, FSI analysis, slamming, hull slamming, impact velocity, deadrise angles, compressibility of air, compressibility of water, air cushion.

LIST OF ABBREVIATIONS

BEM	Boundary Element Method
CFD	Computational Fluid Dynamics
FE	Finite Element
FSI	Fluid Structure Interaction
SPH	Smooth Particle Hydrodynamics
UN	United Nations

LIST OF SYMBOLS

$^\circ$	Degrees

LIST OF UNITS ABBREVIATIONS

m	Metres
mm	Millimetres
MN	Mega-Newton
N	Newton

TABLE OF CONTENT

LIST OF FIGURES

LIST OF APPENDICES

1. INTRODUCTION

With reference to the effects of hull slamming which include issues of structural integrity (Cheon *et al.*, 2016) and causes of accidents as that of the MSC Napoli and the ferry Estonia (Marine Accident Investigation Branch, 2008; Kapsenberg, 2011), the subject area of slamming has over the years been addressed through focused and dedicated research, trying to understand its complex phenomenon (Kapsenberg, 2011). This is evident owing to the number of different publications in the subject area of slamming, with some placing more focus on the theoretical methods and others focusing on the feasibilities of practical application of the postulated theoretical models or methods (Faltinsen, 2001; Faltinsen, Landrini and Greco, 2004; Hirdaris and Temarel, 2009).

Though accidents are not the only central focus for extensive research work in the subject area of slamming, it is a noteworthy fact that in seamanship operations, the event of slamming and/or the predicted perils of slamming are the primary reasons for reduction in speed or change in heading in rough seas or rough weather. Hence, the question of whether to accept certain design parameters arises since there exists no criteria on how to account for slamming-induced pressures in the design stages (Faltinsen, 2005; Kapsenberg, 2011; Cheon *et al.*, 2016). Then again, it is credible and clearly evident from the report of the accident of the MSC Napoli (Marine Accident Investigation Branch, 2008) that slamming and slamming-induced whipping are not yet soundly incorporated in the Classification rules; owing to the fact that presently, "an estimated factor of the calculated maximum bending moment is used to account for these dynamic effects" (Kapsenberg, 2011).

The start of research in the area of slamming, to understand its complexity dates back to the 20th Century and is to this day still ongoing since the problem is far from being solved (Kapsenberg, 2011). It is undisputed that credible results and findings have been made in the subject area, however, these are not enough to be incorporated as parameters or set criteria in the design of a ship for an intended route as may be the desired case (Faltinsen, 2005; Kapsenberg, 2011; Cheon *et al.*, 2016).

Slamming is generally defined as water impact, the impact of the hull or a section of the hull as it re-enters water (waves) (Abrate, 2013). The physical process of slamming involves an interaction between a structure and a fluid with a free surface (Faltinsen, 2005; Abrate, 2013). In view of this, analysis or research in the subject area of slamming must always be carried out as a combination of structural mechanics and hydrodynamics (Faltinsen, 2005); in other words, a fluid-structure interaction- FSI analysis or hydroelasticity. Hydroelasticity in context reflects the fact that the structural elastic reaction and the nature of the flow of the fluid (mixture of air and water) are considered concurrently, with the implication of an interaction between both the fluid flow and the structure.

Understanding Slamming, How Far Has the Industry Come

Slamming could either be a risk for ship accidents or an influence on the operational limits of a vessel (Faltinsen, 2005; Kapsenberg, 2011; Cheon *et al.*, 2016) since ship masters mostly reduce speed to avoid slamming. An extensive scope of work in the area of slamming (hull slamming) has been executed and have produced credible and feasible solutions, however, these solutions are not sufficient to furnish the Industry with the necessary criteria to adopt for particular ship designs on designated sea routes (Cheon *et al.*, 2016).

It is without doubt that ships are being designed to have more flexibility and also larger in size compared to yesterday. The structural designs of ships have also been influenced by the introduced use of high-tensile steel allowing for the reduction in the dimensions of structural members. These developments give rise to the concern of the effect of flexural deformations on the bending moments influenced by waves as well as fatigue of the structural members influenced by slamming and slamming induced loads (Kapsenberg, 2011).

In view of this, continued research in the subject area of slamming is encouraged to help in understanding the phenomenon of slamming to adapt future designs of ship hulls to ensure structural integrity and also safety of crew, passengers and cargo against the effect of slamming and slamming induced loads.

Several methods / theories have been used in performing structural analysis from the slamming / water impact perspective; these include the use of analytical methods, boundary element methods, numerical methods and even full scale experiments. However, there are limitations that come with using any of these methods. In comparison, numerical methods provide more accurate solutions though it is not efficient as compared to the other traditional methods. The use of CFD techniques in numerical analysis will offset the downsides of numerical approaches in the rather near future though it requires more sophisticated computer systems and several days of running simulations.

The Maritime Industry / Classification Societies through conscious efforts are working on the developments of these different theories / methods to have well-established criteria or requirements in the class rules that will include the effect of impact loads and the corresponding structural dynamic responses in the unlikely event of slamming. Achieving this will coherently fulfil part of target eight (8) of Goal fourteen (14) of the UN Sustainable Development Goals envisioned for 2030 which is focusing on "Increase scientific knowledge, develop research capacity and transfer marine technology, taking into account the Intergovernmental Oceanographic Commission Criteria and Guidelines on the Transfer of Marine Technology, in order to improve ocean health and to enhance the contribution of marine biodiversity to the development of developing countries, in particular small island developing States and least developed countries".

This has however not proven easy as there still exists some challenges which include the challenge of accounting for the effect of seamanship (human factors), validation of the different methods, inclusion of the different phenomenon such as scaling laws for the formation of air cushions, compressibility effects of the fluid (air and water), hydroelastic response of the structure after impact as well as the volume fraction of air existing in the fluid mixture at an instantaneous time prior to the unlikely event of slamming (Kapsenberg, 2011).

1.1 Aim of The Study

The aim of this study is to understand the physics of the slamming event through numerical analysis of the effect of the fluid, the structure and the interaction between the fluid and the structure (FSI Analysis). In-depth knowledge and understanding of the physics of slamming could serve as a springboard to achieve the criteria that can be incorporated in the design stages to account for slamming and slamming-induced loads.

1.2 Objectives of the Study

The main objectives to achieve the specified aim of the study are outlined below:

I. To find out if there exists a relationship between the compressibility of the fluid (mixture of air and water) and the hull structure influencing the slamming event

II. To solve the transient compressible, two-phase, viscous problem of the fluid simultaneously as the transient, non-linear dynamic problem of the structure

1.3 Research Questions

I. How does the shape of the hull structure influence the slamming event?

II. How does the speed/velocity of motion of the hull structure in the fluid influence the slamming event?

III. How does the compressibility of air and water influence the slamming event?

IV. Is there a threshold velocity for slamming to occur?

V. How does the shape of the hull structure influence the threshold velocity for slamming?

1.4 Methodology

This study is based on a preliminary study for the ISSC Benchmark Study on Slamming loads carried out at Chalmers University of Technology (Janson, 2017).

The investigation was carried out numerically using STAR-CCM+ and ABAQUS with STAR-CCM+ as the main simulation software and ABAQUS as the co-simulation software. The present investigations were carried out using the same FE model of the plate as well as the same fluid domain as in (Janson, 2017); however, the only parameters in the set-up that were changed are the entry velocities of the block of water hitting the plate from below which serves as the wave for the study as well as the deadrise angles of the plate.

1.5 Scope and Limitations of the Study

The investigation is mainly focused on the stern and bow of the hull structure represented structurally as a flat stiffened plate. The fluid is considered a mixture of air and water accounting for compressibility and turbulence. The structure on the other hand is considered accounting for elasticity and plasticity.

1.6 Outline of Thesis

This thesis report is sectioned into six main chapters. Following the Introduction is Chapter Two which highlights the physical phenomenon of slamming and the different underlying theories for slamming analysis as well as the challenges and background information serving as the motivation and backbone of the continued research on slamming.

Chapter Three presents the methodology followed in realising the main objectives of this research study. It gives a general introduction to the software tools used for the study as well as a step by step approach into the model development highlighting governing equations and theories.

In Chapter Four the obtained results from the simulations ran are presented and discussed. Owing to the nature of the study, several plots and scenes are generated of which most can be found in the Appendix for further perusal so as not to bore the audience.

Finally, the conclusions drawn in this research study are presented in Chapter Five and in Chapter Six proposed future investigations and recommendations.

2. BACKGROUND & THEORY

This chapter presents the general background to the current study and the underlying theory inspiring the different investigations.

2.1 General overview of the physical phenomenon of hull slamming

Hull slamming in other words slamming is basically defined as water impact of the hull or a section of the hull as it re-enters water, it involves the interaction of the hull structure and the surrounding fluid that has a free surface (seawater/waves) (Abrate, 2013). Slamming could also be defined as an occurrence resulting from the entry of the hull or a structure or body into a fluid (with a free surface) with an existing relatively small angle between the free surface and the structural surface (Faltinsen, 2005; Hoque, 2014; Cheon *et al.*, 2016).

Slamming according to (Abrate, 2013) is categorized generally into four different types, namely; hull slamming, bow slamming, wet-deck slamming and green water slamming. In his submission, hull slamming is defined as the re-entry of the hull into water (fluid) after being fully or partially lifted from the free surface; bow slamming, wet-deck slamming and green water slamming refer to impact of water (waves) on marine vehicles/structures or part of the ship's hull structure (Abrate, 2013).

Slamming is physically characterized by an abrupt impact force of high magnitude occurring in a relatively short period of time (Kapsenberg, 2011). It has been proven that the magnitude of the impact force is as a result of the naturally occurring relative angle between the free surface and the structure; this is evident from the results of physical experiments and demonstrations by means of dropping wedges of different deadrise angles into a fluid with a free surface with the assumption that the wedge is a rigid body (Hayman, Haug and Valsgard, 1991; Faltinsen, 2005).

2.1.1 Physical Effects Occurring During Hull Slamming

When considering hydroelasticity, different physical effects do occur in the unlikely event of slamming. These include the effect of surface tensions and viscosity; the formation of an air cushion (trapped air); large impact loads and vibrations mostly giving rise to cavitation and ventilation (Faltinsen, 2005; Abrate, 2013).

If the local angle formed between the structural surface and the free surface of the fluid is relatively small at the impact position, it gives rise to the formation of an air cushion / trapped air which gradually leads to the formation of air bubbles when the air cushion collapses; also, large impact loads can be realised which cause local dynamic hydroelastic effects (Faltinsen, 2005; Abrate, 2013). The effect of viscosity and surface tension are negligible however in hull slamming analysis (Faltinsen, 2005; Abrate, 2013).

The different physical effects occurring during the slamming event have different time scales with the most important one being when local maximum stresses occur, from structural perspective (Faltinsen, 2005).

The flow of the fluid on the other hand is affected by the compressibility of air and water as well as the formation of air cushions (Faltinsen, 2005) which occur before the local maximum stresses occur.

2.1.2 Compressibility and Formation of Air Cushions

A compressible air pocket is formed when a structure with a flat bottom or small deadrise angle has impact with a free surface of a fluid (Abrate, 2013) . The air pocket formed has pressure (that deforms both the structure and the free surface) and cushioning effects that cannot be neglected (Chung *et al.*, 2007; Oh, Kwon and Chung, 2009). Not only does the shape of the structure (being flat or with some deadrise angle) result in the creation of an air pocket, but could also be created dependent on the shape of the free surface encountered (Abrate, 2013).

The compressibility of water in slamming analysis is also a noteworthy instance. Most slamming analysis conducted consider the fluid (water) as incompressible but then there are several cases analysed where the compressibility of the fluid (water) is credible. This has been investigated using acoustic effects in the events of water impact of blunt bodies (Korobkin, 1992; Alexander A. Korobkin and Iafrati, 2006). Other investigations also prove that for wedges or cylinders, the effect of water compressibility is negligible since the maximum impact force is realised in the incompressible phase as the cylindrical or wedge shaped body enters the free surface (Campana *et al.*, 2000).

2.2 Theories / Methods Used to Tackle the Problem of Slamming

This section highlights in general, the different theories and methods used by different authors / researchers in studying and understanding the slamming phenomenon.

2.2.1 Momentum theory

The momentum theory which expresses the conservation of linear momentum has been employed by a number of researchers and is the oldest theory used in the subject area of slamming (Kapsenberg, 2011; Abrate, 2013) first employed in the study of the estimation of applied forces on the floats of sea planes (Von Kármán, 1929; Pabst, 1930). This theory is based on the conservation of linear momentum during the entire phase of water entry of a body (Abrate, 2013). Von Kármán (Von Kármán, 1929) and Wagner (Wagner, 1932) are the well-known authors to have used this approach from different points of reference (Kapsenberg, 2011) and in turn, other authors based on their fundamental approaches have carried out further refined and improved investigations (Prohaska, 1947; Szebehely V.G, 1952; Leibowitz, 1962; Kapsenberg and Thornhill, 2010) .

Von Karman's study was based on the theory of added mass and is recorded as the first to have used this approach to estimate the force of impact on floats of landing seaplanes by using the added mass of a flat plate with a specified width to represent the added mass of the float (Von Kármán, 1929). In Von Karman's approach however, the force estimation was based only on the component of the vertical velocity (Von Kármán, 1929; Kapsenberg, 2011), this approach was employed and further improved in (Pabst, 1930) who included the forward velocity to estimate the change in impulse on the floats.

Though Von Karman was the first to use the approach of momentum theory, the study carried out by Wagner is well-known in this area of research (Kapsenberg, 2011). Wagner's approach follows the theory of potential flow focused on the combination of the concept of the float and flow around a wing at an incident angle, likening the model to that of a surface planing vessel (Wagner, 1932; Kapsenberg, 2011).

One main setback / limitation of the momentum theory in its application on ship hulls was the difficulty in the calculation of the added mass of each ship section requiring the use of computers as demonstrated in (Leibowitz, 1962; Kapsenberg, 2011). However, quite recently, (Kapsenberg and Thornhill, 2010) using a three-dimensional panel code, calculated the added mass at infinite frequency which was further implemented in the calculation of the impulsive force using the product of the added mass derivatives and the squared value of the reference relative velocities.

2.2.2 Numerical Methods

Several numerical methods that have been used to tackle the problem of slamming are discussed in this subsection

2.2.2.1 Boundary Element Method

Greenhow and Lin (Greenhow and Lin, 1985) were the first to employ the use of Boundary Element Method in the two-dimensional study of the water entry of wedges. Further research using this method have been carried out by several authors (Zhao and Faltinsen, 1993; Lu, He and Wu, 2000; Battistin and Iafrati, 2004; Sun and Faltinsen, 2006; Xu, Duan and Wu, 2011). Generally, Boundary Element Methods present credible solutions within the scope of assumptions made to offset the cost of computations (Kapsenberg, 2011). However, a numerical setback / limitation with the use of this method is centred on the existence of a discontinuity of the velocity component causing an infinite pressure on the body surface (Ogilvie, 1963; Kapsenberg, 2011). This setback, as proposed by Ogilvie (Ogilvie, 1963) will require the inclusion of the compressibility properties of the components of the fluid mixture (i.e. air and water). The Boundary Element Method has also been used for developing approximate approaches for three dimensional study of slamming predictions using the strip theory (Kvålsvold, Svensen and Hovem, 1996; Sames, Kapsenberg and Corrignan, 2001) which is till this day used in slamming analysis (Hermundstad and Moan, 2005; Tuitman, 2010).

2.2.2.2. SPH Method

The Smooth Particle Hydrodynamics Method was developed using a set of particles in place of the continuum in governing equations to obtain approximate numerical solutions (Gingold and Monaghan, 1977). This approach has been used in several research studies and simulations of the water entry of rigid bodies (Shao, 2009; Viviani, Brizzolara and Savio, 2009; Vandamme, Zou and Reeve, 2011; Veen and Gourlay, 2011, 2012) as well as flexible structures (elastic bodies) based on fluid-structure interaction (Oger *et al.*, 2009, 2010; Groenenboom and Cartwright, 2010; Grimaldi *et al.*, 2011).

2.2.2.3 Finite Element Method

Finite Element developed software including LS-DYNA and ANSYS have been used in recent times in analysis of water impact on elastic or rigid bodies entering a fluid with a free surface (Stenius, 2006; Stenius, Rosén and Stenius, 2007). This approach has also been adopted in the modelling of the fluid domain (Donguy *et al.*, 2001; Peseux, Gornet and Donguy, 2005) and also to model structures in case of studies involving structures or bodies that deform.

2.2.2.4 Fixed Grid Method

Fixed Grid Methods refer to finite difference and finite volume methods where the fluid (i.e. air and water) and the structure / body are interacting (Abrate, 2013). Three approaches following this method include the Level Set Method, Volume of Fluid Method and the Cubic Interpolated Pseudoparticle Method (Abrate, 2013). Each of these methods have been employed in several researches involving water impact on a fluid with free surface (Kleefsman *et al.*, 2005; Zhang *et al.*, 2010; Yang and Qiu, 2012).

2.2.2.5 Computational Fluid Dynamics

CFD methods are designed to analyse ship motions in waves without accounting for slamming and steep waves (Kapsenberg, 2011). Of course, there were setbacks encountered with the development of the CFD codes which included the requirement of a large computer memory space as well as implementation of the wave field in the computational domain (Kapsenberg, 2011). The Computational Fluid Dynamics approach has been utilized by a number of researchers to carry out simulations focused on the slamming of ship sections using Euler Solvers and the Volume of Fluid approach (Arai, Cheng and Inoue, 1995) as well as the strip theory (Sames, Kapsenberg and Corrignan, 2001; Sames *et al.*, 2008).

2.2.3 Statistical Methods

Statistical Methods are employed to study the probability of occurrence of slamming (Ochi, 1964; Kapsenberg, 2011). The well-known and commonly used method is that developed by Ochi (Ochi, 1964), which predicts the probability of bottom slamming. This method has proven useful in the comparison of different vessels operating in different sea states to ascertain the maximum sustainable operational speed with reference to a specified allowed probability of bottom slamming (Kapsenberg, 2011). It is easy to use, however a major setback of this method is that, the vessel or the section under study has to fully emerge from the free surface and then have impact on the fluid surface (free surface) horizontally (Kapsenberg, 2011).

2.2.4 Analytical Methods

These methods are mostly used for simplified impact or water entry cases (Scolan and Korobkin, 2001; Korobkin and Scolan, 2006) and present definite solutions to the specified problems (Kapsenberg, naval and 2010, no date; Kapsenberg, 2011). As such, analytical methods are used as a fundamental for other well-known methods and approximate approaches. A remarkable aspect of the analytical approach is that prediction of infinite pressure or an infinite pressure gradient on the structural surface is possible, however, this is limiting in other methods such as the Computational Fluid Dynamics approach (Kapsenberg, 2011).

2.2.5 Experimental Techniques

Though not an easy task, the experimental approach has been used in the study of slamming and water impact. Such experiments carried out include, drop tests using wedges (Lewis *et al.*, 2010) to ascertain the impact velocity or impact force, flat plates (Kvålsvold and Faltinsen, 1994). Limitations that relate to this approach include the requirements of rather sophisticated data measuring tools / system since mostly the duration of impact / water entry is extremely short, most especially in instances where local quantities such as the pressure on the structure or body surface is central focus (Kapsenberg, 2011).

2.2.6 Full Scale Experiments

The number of slamming analysis work carried out using full scale experimental approaches are rather few. Though geared towards a good course, the technicalities involved are rather challenging. Full scale experiments require sophisticated and sensitive measuring / control systems; a good prediction of rough or extremely bad weather which is rather speculative; and also each experiment could span over a number of years (Kapsenberg, 2011). Full scale experiments carried out in the subject area of slamming include full scale seakeeping trials on the Dutch Destroyers (Leibowitz, 1962), bottom slamming measurements on the SS Wolverine (Kapsenberg, 2011) as well as undisclosed research projects being carried out by research institutes such as the Maritime Research Institute in the Netherlands (Kapsenberg, 2011).

2.3 Water Entry of / Impact on Flat Plates

The concept of a flat plate is considered when the surface of the plate is parallel to the free surface (Abrate, 2013). Several research studies have been conducted using this concept; (Okada and Sumi, 2000) carried out analysis on the water entry of a flat plate using different deadrise angles, from their research study, it was realised that the effect of the air trapped at relatively low deadrise angles is noteworthy with the maximum pressures being recorded at the central position of the plate; (Faltinsen and Semenov, 2008) also carried out a similar analysis and postulated an analytical solution for a plate forming an angle with a free surface, in the event of entering the free surface either vertically or obliquely. Other research studies following

Von Karman's approach and Asymptotic Analysis using flat plates have also been conducted (Iafrati and Korobkin, 2004; A.A. Korobkin and Iafrati, 2006). In view of this, for the purpose of the already established limitations, the concept of a flat plate is employed.

3. METHODOLOGY

As already established, this study is a build-up of the a preliminary study for the ISSC Benchmark Study on Slamming loads carried out at Chalmers University of Technology (Janson, 2017); to study the slamming pressure on a semi-submersible platform using a Fluid-Structure-Interaction (FSI) approach. Similar studies have been carried out using different combinations of commercial fluid and structure analysis software (Camilleri, Taunton and Temarel, 2015; Cheon *et al.*, 2016). In (Janson, 2017) however, a combination of the CFD software STAR-CCM+ together with structure analysis software ABAQUS; both software programmes have an already existing coupling/link. The investigations were focused on the pressure, deformations and volume fraction of air on the semi-submerssible plate at different water impacts (water entry velocities) in comparison to a similar investigation carried out by Cheon et al (Cheon *et al.*, 2016) using LS-DYNA.

This current investigation was however focused on investgating further different water entry velocities (lower and higher than in (Janson, 2017)), the effect of the compressibility of air and water and the effect of deadrise angles.

3.1 NUMERICAL ANALYSIS USING STAR-CCM+ & ABAQUS

Based on the Finite Volume approach, STAR-CCM+ is designed to solve the governing Reynolds Averaged Navier Stokes, RANS or URANS for unsteady flow equations. ABAQUS is a FE solver for dynamic non-linear structure analysis.

To begin with, the domain of the model is divided into a finite number of control volumes and governing equations approximated for each control volume using the 2nd order approximation. The targeted time period for the simulation is also divided into a finite number of time steps. An implicit time-stepping option is selected as it enables a larger number of time steps and provides a better numerical stability. The time derivative is approximated using the first order Euler scheme. The free surface of the fluid domain is modelled using the Volume of Fluid approach. STAR-CCM+ uses the High-Resolution-Interface-Capturing to achieve a definitive interface and to ensure that results are realistic. A morphing motion model (multi-quadratic morphing model) serves to deform the fluid grid domain to allow for deformations on the structure.

An explicit scheme (ABAQUS Explicit Coupling) is used for coupling STAR-CCM+ to ABAQUS for the Co-Simulation phase ensuring that in each coupling time step there is one interaction between the software.

3.1.1 Modelling of the Stiffened Plate

The Finite Element model of the plate and stiffeners as an ODB file in ABAQUS is as in Figure 1. The plate model was provided as part of the requirements and description on the ISSC Benchmark Study for Slamming loads carried out in (Janson, 2017).

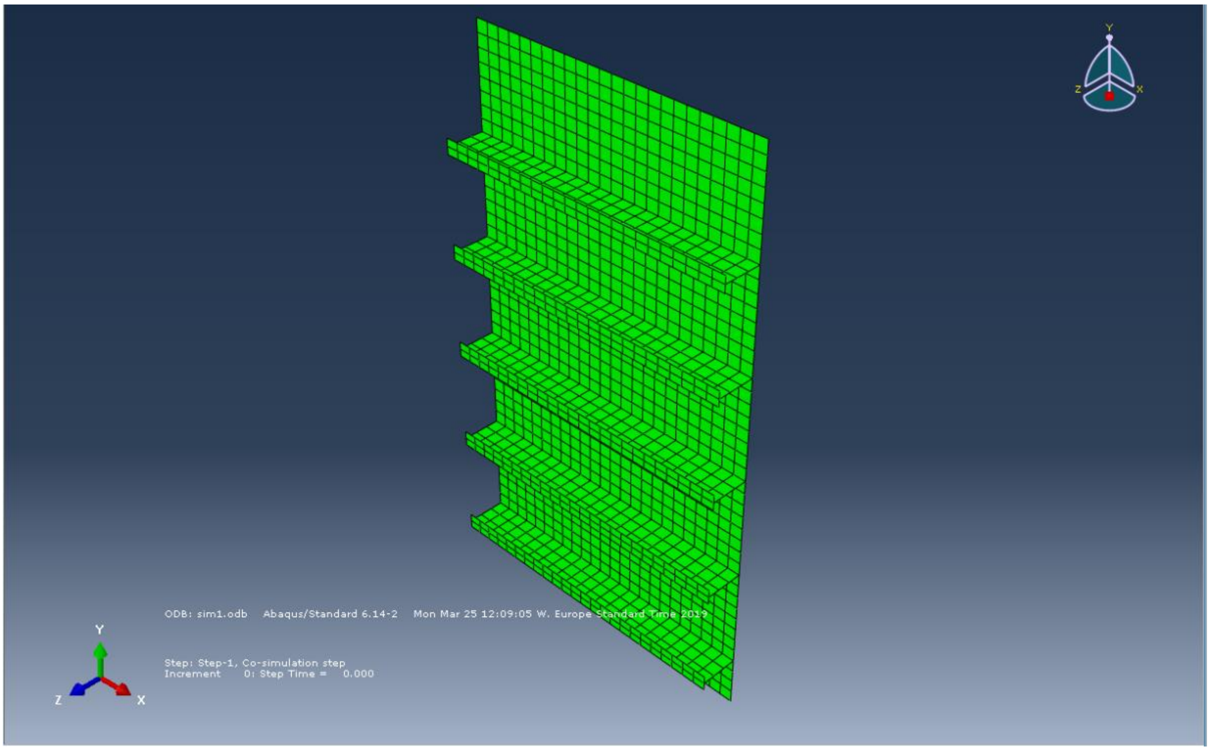

Figure 1: Finite Element Model of Stiffened Plate

3.1.2 Generating the Geometry and Mesh

The geometry of the fluid domain and plate were modelled in STAR-CCM+, being the control volumes for the intended simulations. The fluid domain had the dimensions 3.0 x 5.0 x 4.1 m and the plate had the dimensions 2.4 x 4.4 x 0.015 m respectively. The plate was positioned 3.6m from the bottom of the fluid domain and as such, in order to get the thickness of the plate, the input data for the plate was: 2.4 x 4.4 x 3.615 m.

To generate the control volumes of the fluid domain and the plate for no deadrise angle, the Boolean operation “Subtract” in STAR-CCM+ was performed on the plate and the fluid domain (block) to achieve this. However, to achieve the deadrise angles on the plate, after a tranformation of the plate (translation along the x-axis and y-axis and rotation about the y-axis) the Boolean operation "Intersect" was performed on the block and the plate, thereafter, the Boolean operation "Subtract" was performed on the block and the generated surfaces after the "Intersect" operation.

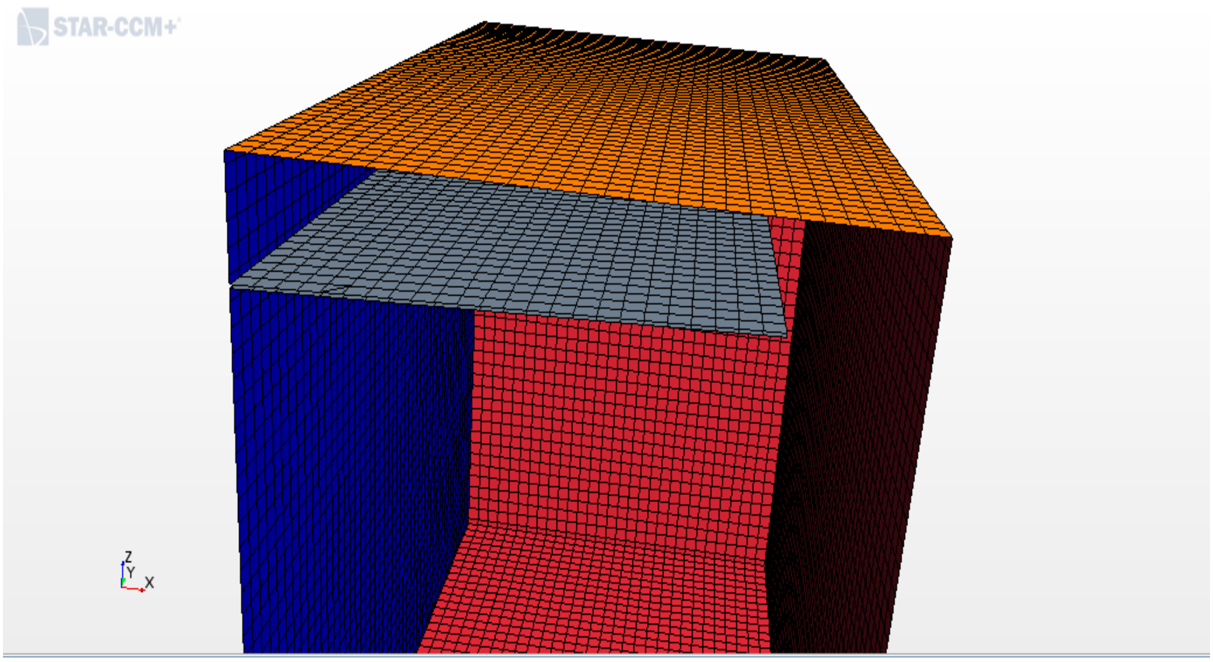

Figure 2: Mesh model of the Fluid Domain and Plate

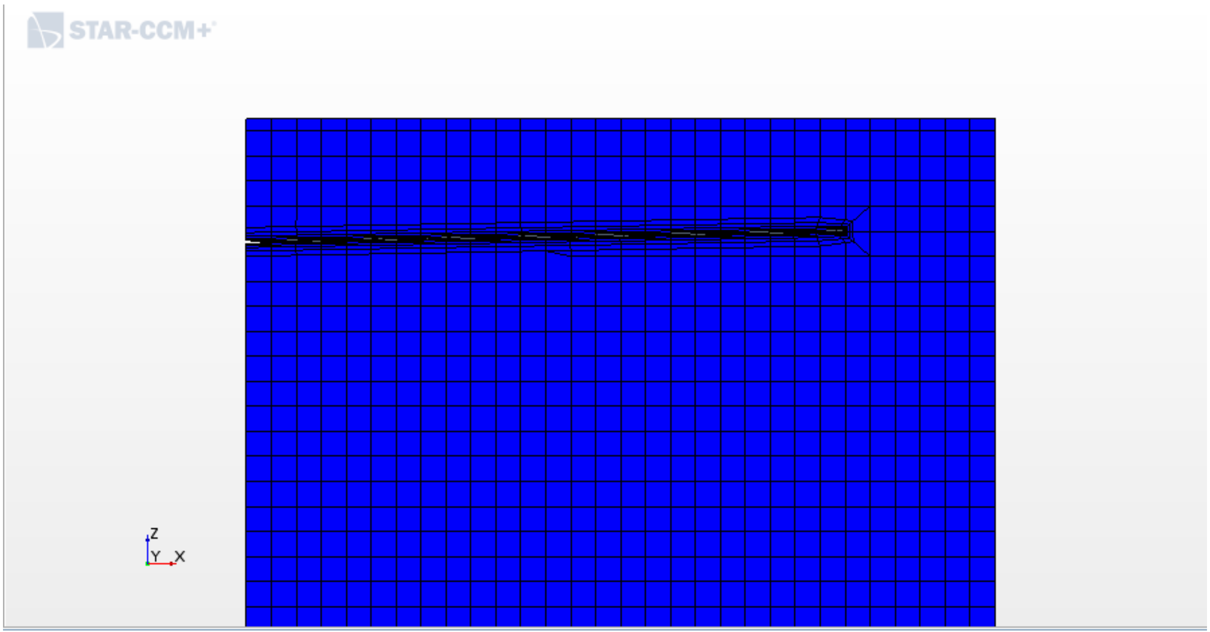

Figure 3: 1° Deadrise

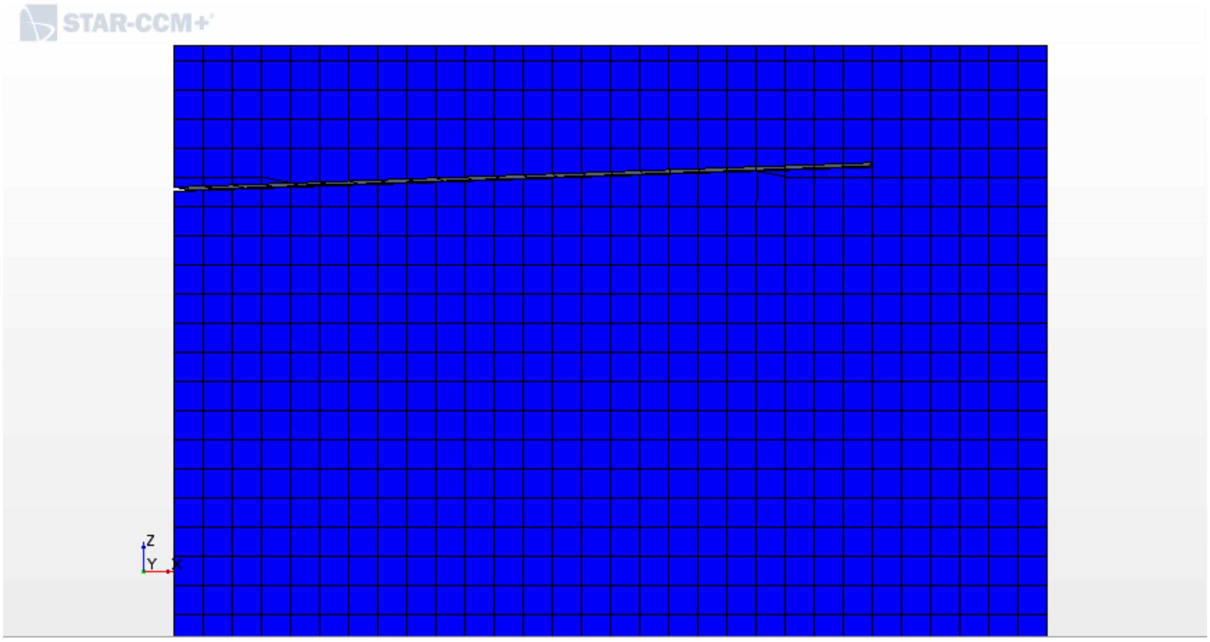

Figure 4: 2° Deadrise

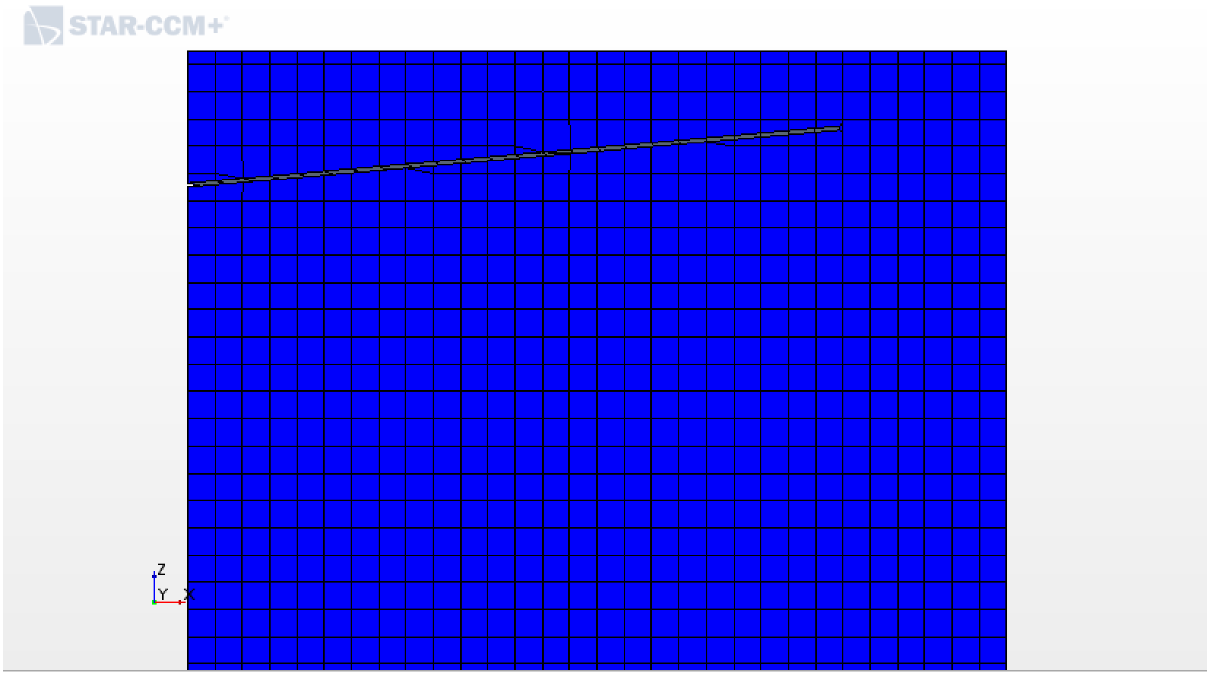

Figure 5: 5° Deadrise

With the assumption that the upper side of the fluid domain will have a negligible effect on the pressure solution on the lower side (on the plate), the stiffeners on the plate were not included in the geometry.

The dimension of the mesh size is 100 x 100 x 100 mm.

Figure 2 – 5 are images of the mesh scenes in the STAR-CCM+ workspace of the different deadrise angles on the flat plate used in investigating the effect of deadrise angles on slamming.

3.1.3 Modelling of the Fluid Domain

To model the transient, compressible, two-phase viscous problem, air and water are included in the fluid model using a Eulerian Multiphase to account for the desired properties of the fluid and the Volume of Fluid approach for the two-phase problem. The compressibility of air was accounted for by treating air as an ideal gas. However, to account for the compressibility of water, a user defined field function was employed following the mathematical relation proposed by Tait's.

$$\rho = \rho_o \left(\frac{p + B}{p_o + B}\right)^{\frac{1}{A}}$$

ρ_o is a reference density, p is the computed total pressure, p_o is a reference atmospheric pressure, A=7.15 and B=3.047e8.

To model the effect of viscosity, the Reynolds-Averaged-Navier-Stokes equations were solved using the K-Epsilon turbulence model and the Two-Layer All y+ Wall Treatment law in STAR-CCM+.

3.1.4 Initial and Boundary Conditions

For the purpose of the study, since the plate is set 0.06m above the initial set position of the block of water, the initial velocities were set to account for the effect of the force of gravity following Newton's third equation of motion:

$$v_f^{\,2} = v_i^{\,2} + 2as$$

Where v_f is the final velocity; v_i is the initial velocity; a is the acceleration due to gravity; s is the displacement of the body; in this case the displacement of the block of water.

Thus, the resulting respective set entry velocities for the block of water were: 3.574m/s, 3.971m/s, 4.558m/s, 8.705m/s, 9.632m/s and 10.572m/s for the investigated velocities: 1m/s, 2m/s, 3m/s, 8m/s, 9m/s and 10m/s.

Inlet boundary conditions and symmetry boundary conditions were set. At the inlet boundary, the volume fraction of air and water were set to 1.0 and 0.0 respectively with a small velocity of 0.01m/s in the z-direction for the incoming flow. Above the plate, a constant pressure outlet was employed as outlet boundary condition.

4. RESULTS & DISCUSSION

This chapter presents the results of the three main investigations carried out: the effect of the magnitude of different water entry velocities; the effect of the compressibility of air and water and the effect of deadrise angles.

4.1 Investigation of The Effect of the Magnitude of Different Entry Velocities

This investigation was carried out whilst keeping air and water as compressible at the investigated velocities: 1m/s, 2m/s, 3m/s, 8m/s, 9m/s and 10m/s.

It can be inferred from the plots in Figures 6, 8 and 10 that at lower entry velocities i.e. 1m/s, 2m/s and 3m/s several deformations occur before the maximum deformation occurs. At 1m/s (Figure 6) deformations occur at points ranging from 0.18mm to 0.45mm; the maximum deflection is at 1mm. The resulting permanent deformation is recorded around -0.6mm; this negative recording with an already existing air pocket (since the plate has no deadrise, parallel to the free surface) depicts that the impact on the plate started before it actually came into contact with the block of water and the maximum peak force is recorded whilst a rather thin layer of the air pocket still remains beneath the plate. Similar findings were made by (Ng and Kot, 1992). Same can be said at 2m/s and 3m/s (Figures 8 and 10) where several deformations occur before the maximum deformation and permanent deformation approaches relatively low negative recorded figures.

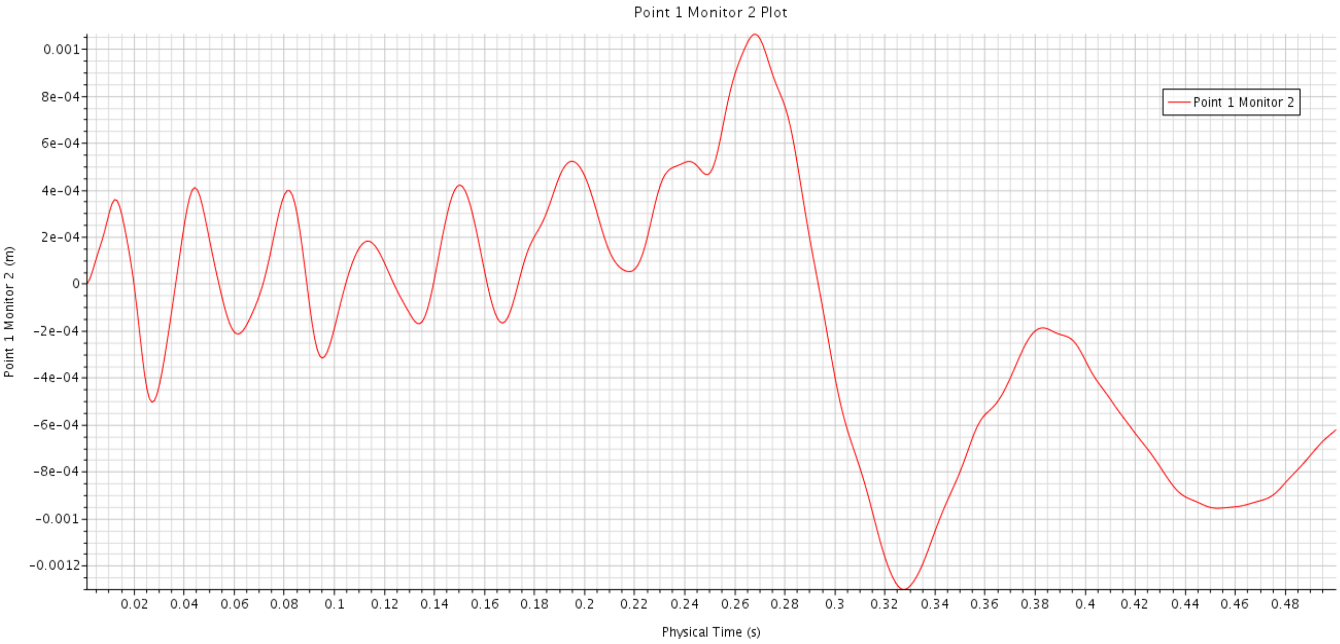

Figure 6: Point Monitor Plot at 1m/s (3.574 m/s)

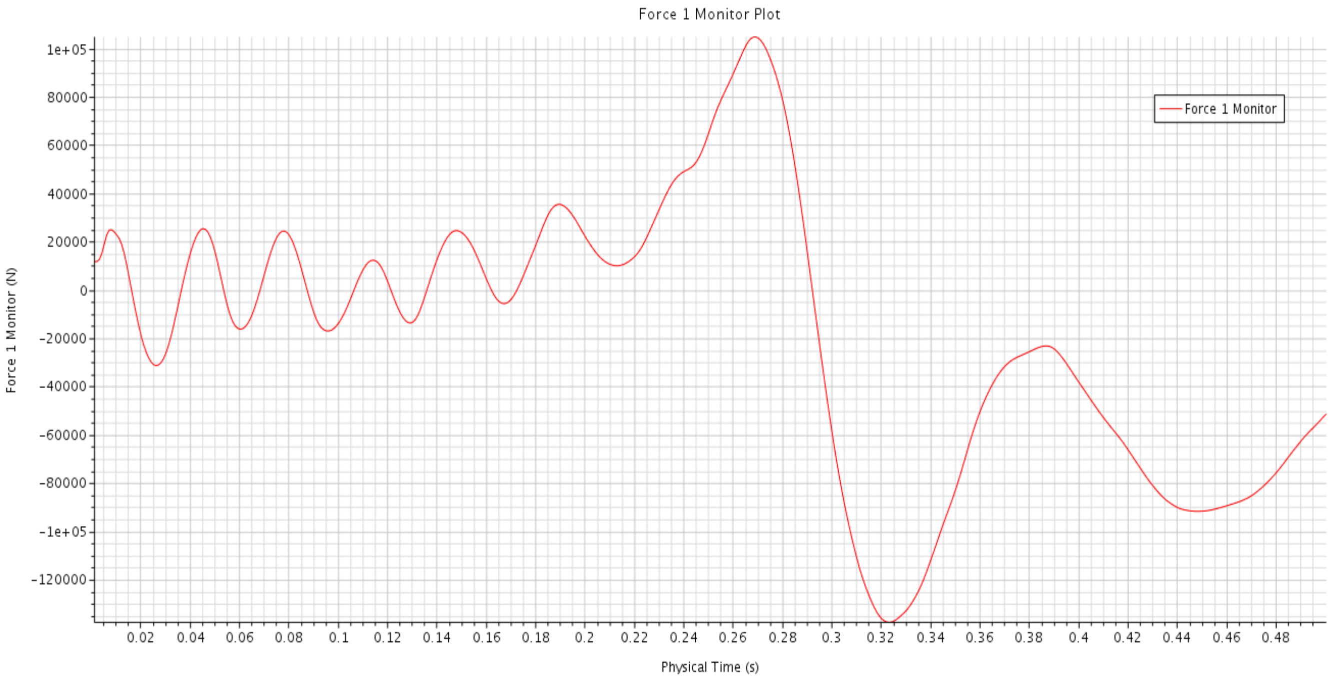

Figure 7: Force Monitor Plot at 1m/s (3.574 m/s)

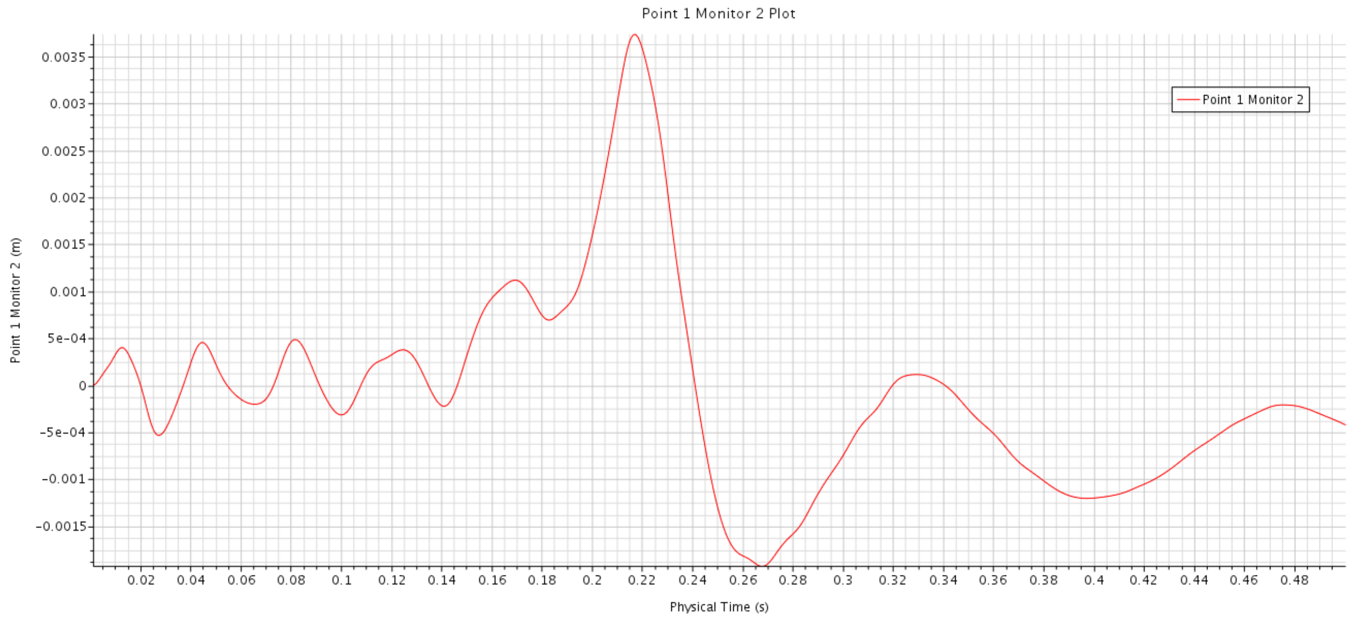

Figure 8: Point Monitor Plot at 2 m/s (3.971 m/s)

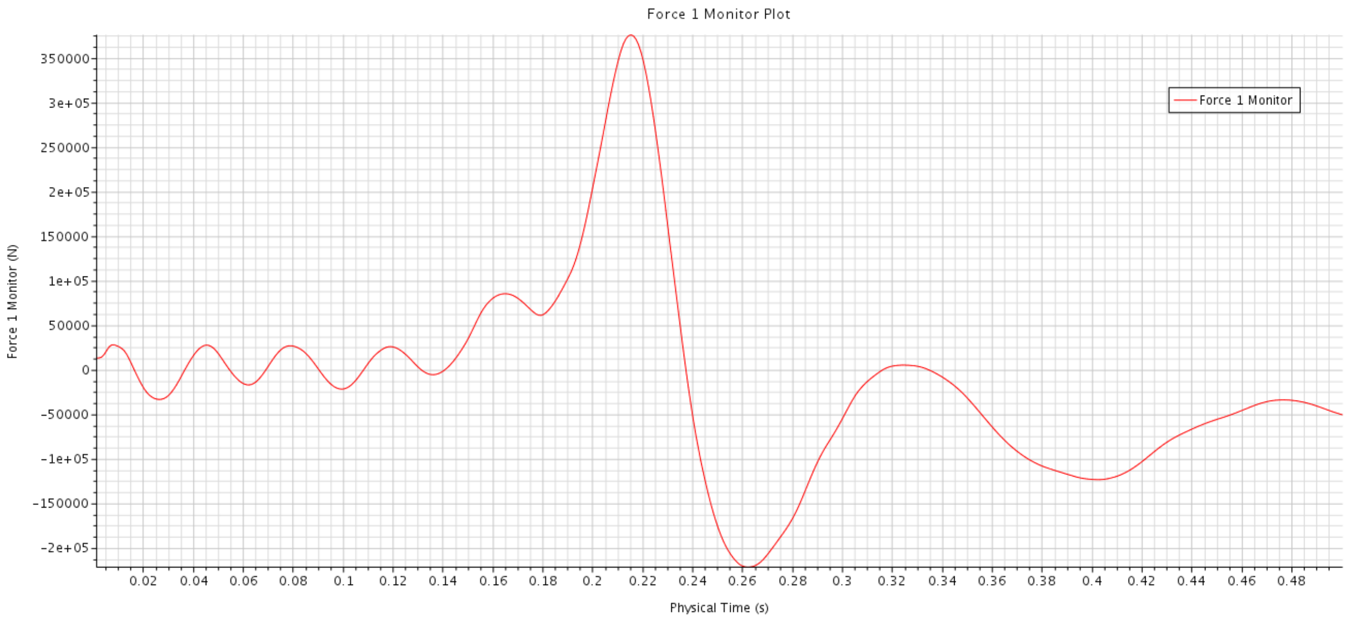

Figure 9: Force Monitor Plot at 2 m/s (3.971 m/s)

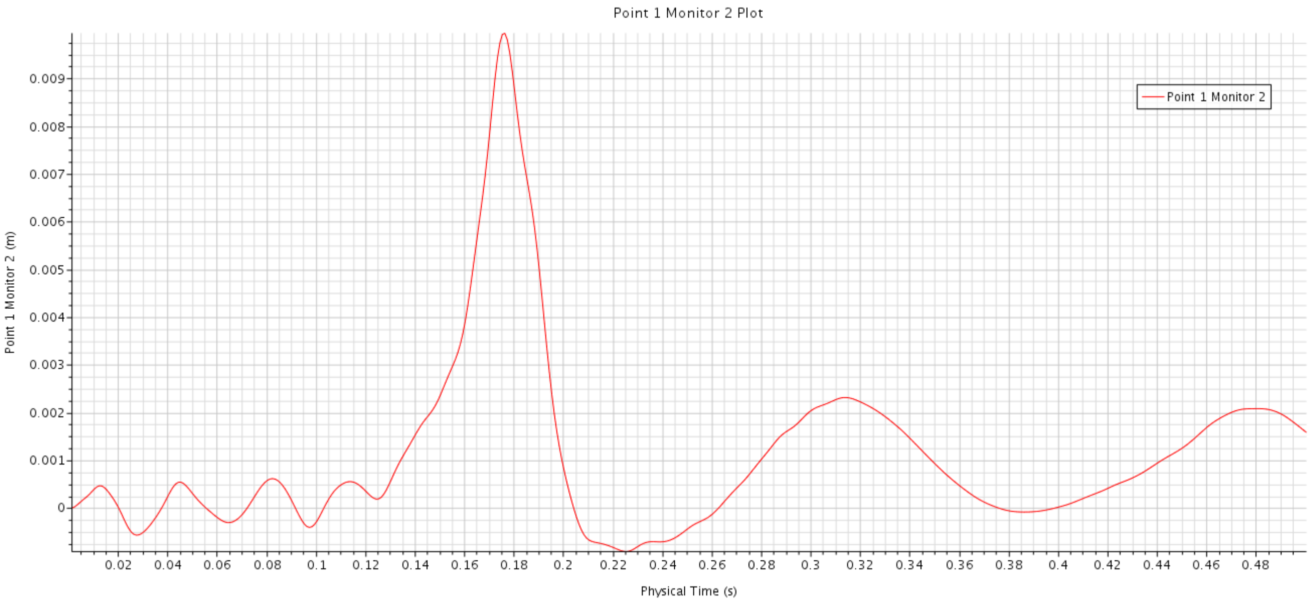

Figure 10: Point Monitor Plot at 3 m/s (4.558 m/s)

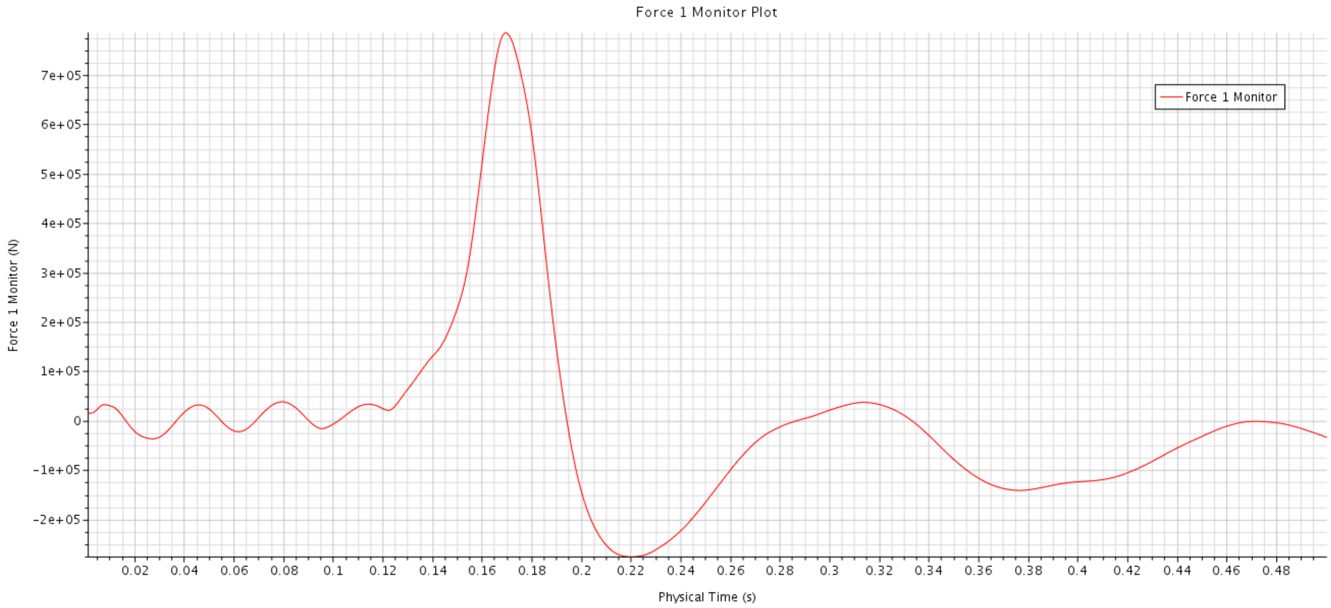

Figure 11: Force Monitor Plot at 3 m/s (4.558 m/s)

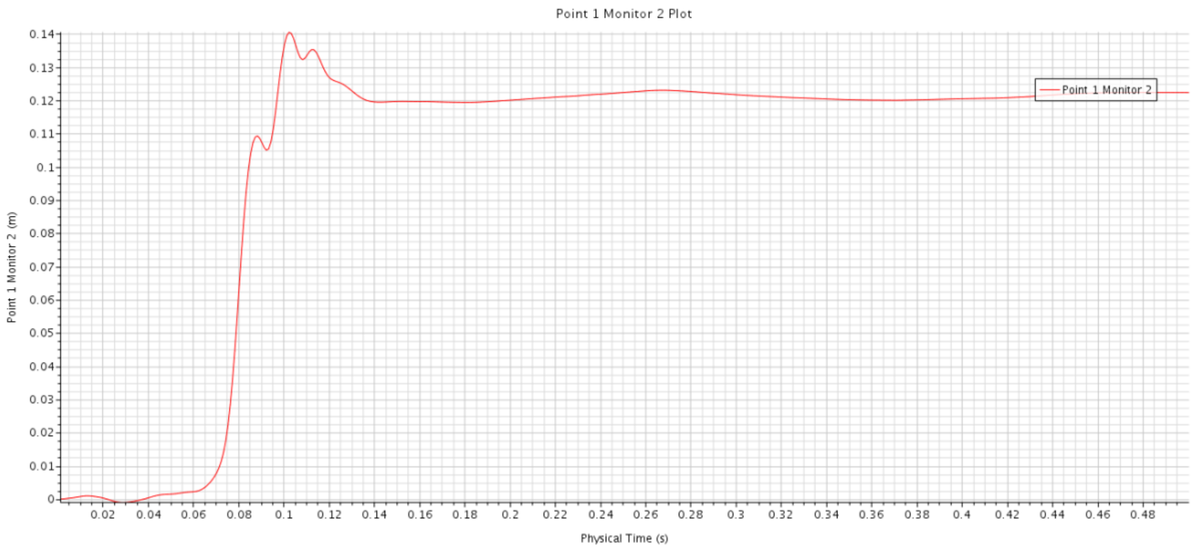

Figure 12: Point Monitor Plot at 8 m/s (8.705 m/s)

However, as the entry velocities increase i.e. 8m/s, 9m/s and 10m/s, there isn't the visualisation of several deformations before the maximum deformation. Then again, the permanent deformations are recorded around 120mm, 140mm and 190mm for 8m/s, 9m/s and 10m/s respectively. Also, the maximum deformations have values that are relatively larger than at the lower velocities. This could reflect the fact that the magnitude of the impact velocity is significant in the slamming event.

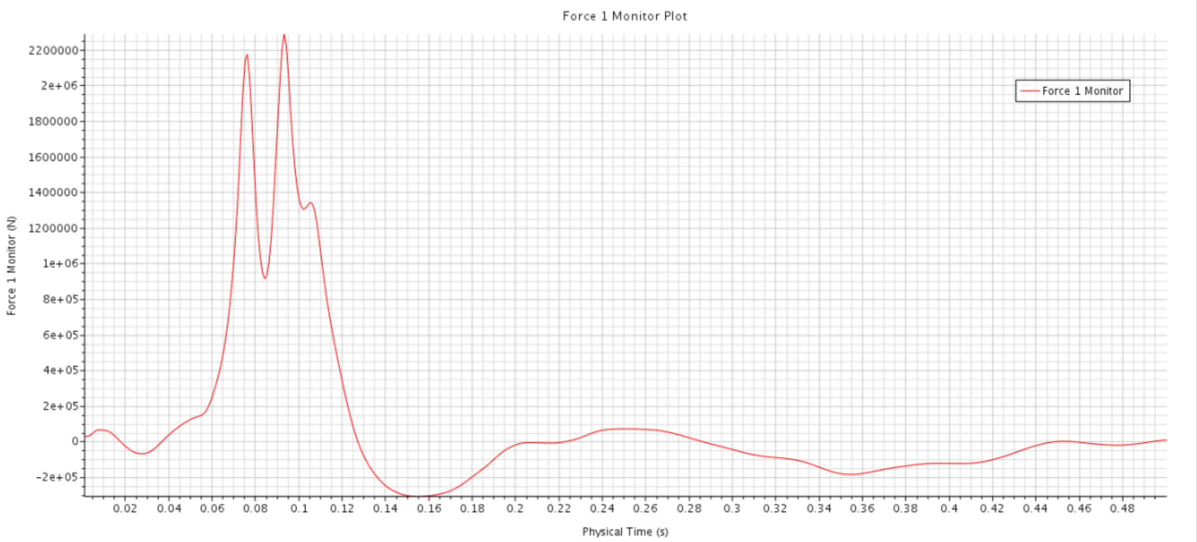

Figure 13: Force Monitor Plot at 8 m/s (8.705 m/s)

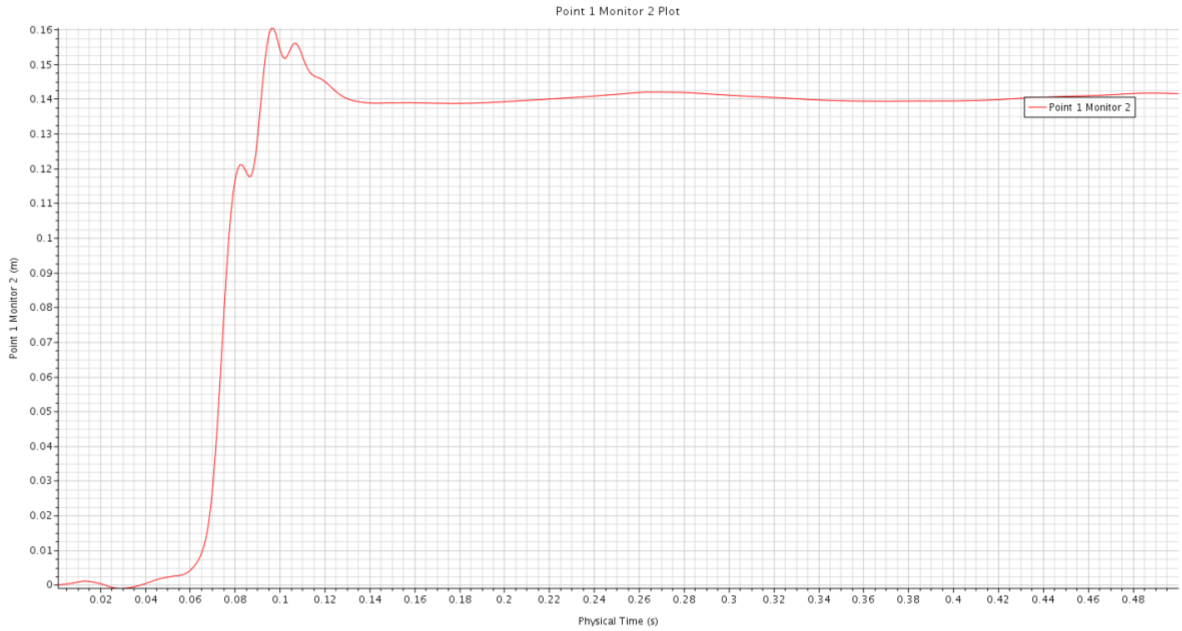

Figure 14: Point Monitor Plot at 9 m/s (9.632 m/s)

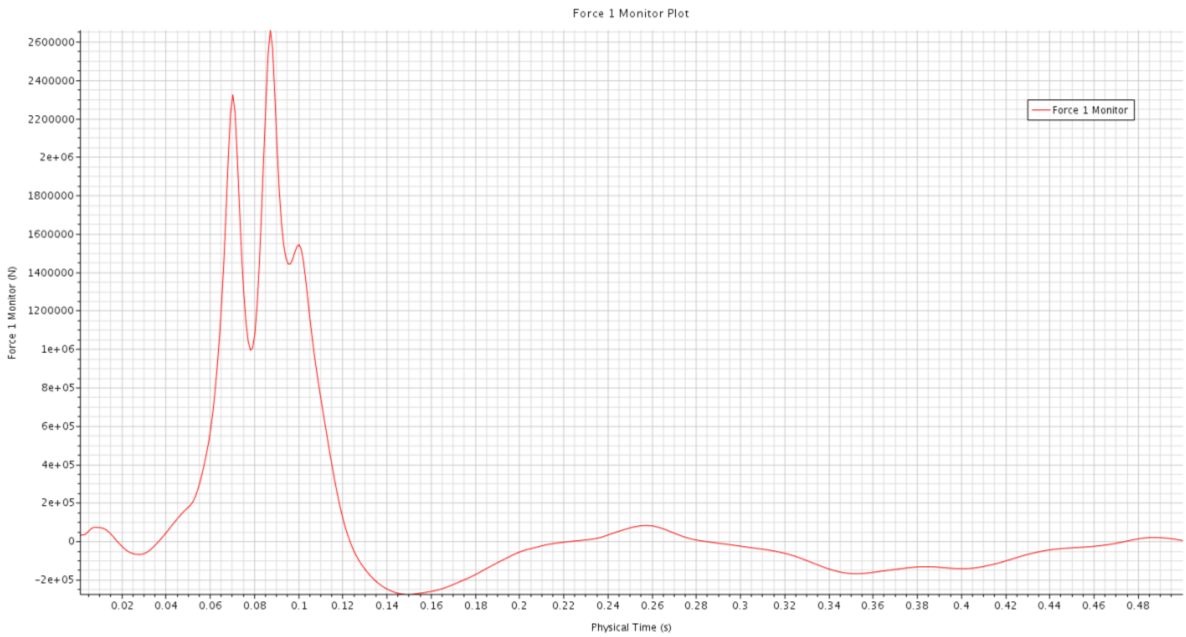

Figure 15: Force Monitor Plot at 9 m/s (9.632 m/s)

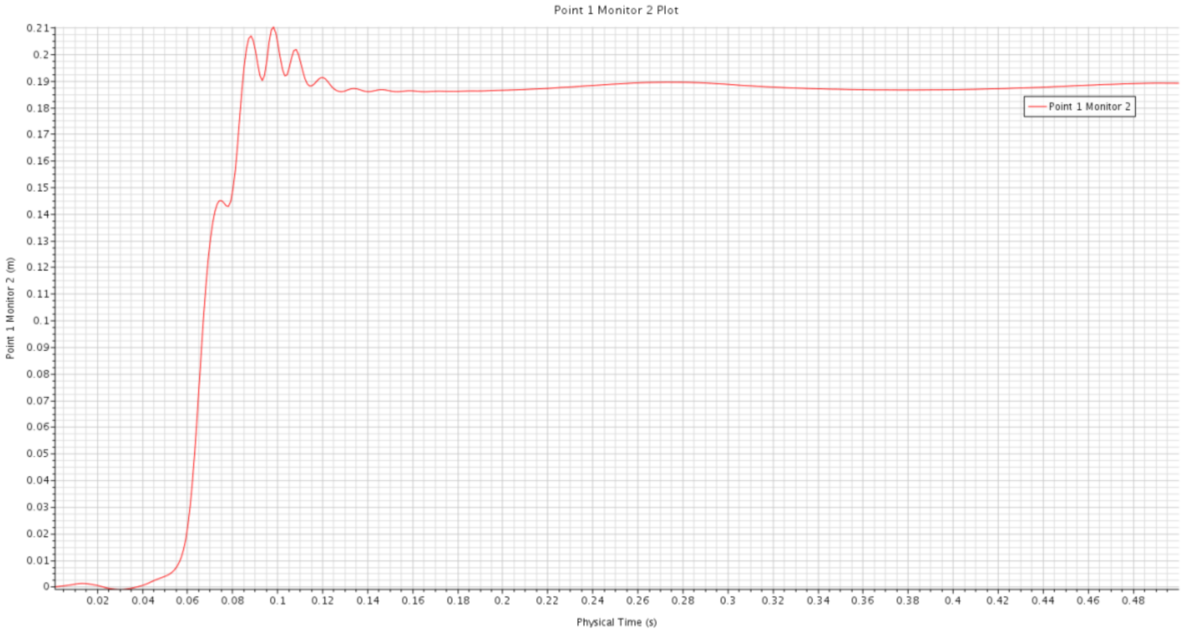

Figure 16: Point Monitor Plot at 10 m/s (10.572 m/s)

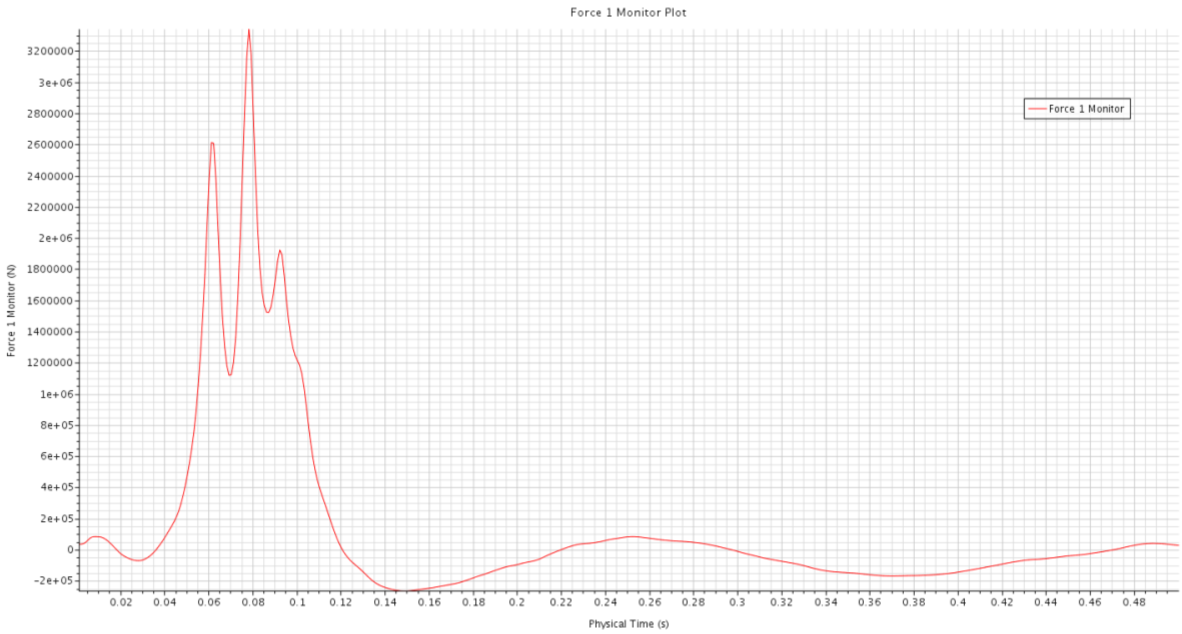

Figure 17: Force Monitor Plot at 10 m/s (10.572 m/s)

Generally, it can be observed that at relatively low block water entry velocities (wave velocities), there are several small deformations and probability of the progressive formation of bubbles beneath the plate surface before maximum and permanent deformations; also recorded at rather relatively lower points. On the other hand, at increasing values of entry velocities, maximum deformations occur sharply and permanent deformation after a shorter period which are recorded at relatively higher points compared to lower velocities.

The force peaks have an increasing magnitude with increasing velocity values. Also, the number of force peaks is observed to decrease relatively with increasing velocities but with higher magnitude of forces.

4.2 Investigation of The Effect of the Compressibility of Air and Water

In investigating the effect on the compressibility of the flow, simulations were carried out by interchangeably keeping constant the densities of air and water i.e.:

i. Setting air as incompressible and water compressible
ii. Setting air as compressible and water compressible
iii. Setting air as compressible and water incompressible
iv. Setting air as incompressible and water incompressible

These investigations were carried at one low velocity (1 m/s), one intermediate velocity (4 m/s) and one high velocity (8 m/s).

From the results, as seen in the appendix, it can be observed that for the combinations: **air incompressible, water compressible** and **air incompressible, water incompressible** have the same force and point monitor plots; on the other hand, the combination: **air compressible, water compressible** and **air compressible, water incompressible** also have the same force and point monitor plots. From this, the question arises, does the compressibility of water affect the slamming event since alternating the state of its compressibility does not affect the solution? This occurrence probably needs to be investigated further since water can be compressed in its natural/physical state by applying an extremely large magnitude of pressure, though only a relatively low compressive effect may be realized.

On the other hand, it is evident that the compressibility of air does affect the solution. With reference to the force monitor plots in the cases where air was set as incompressible, it is observed that there is a bandwidth of peaks whose magnitude and size increase with increasing velocity. These peaks physically represent vibrations on the plate with reference to the point on the plate being observed (set close to the middle of the plate: [0.1, 0.1, 3.6 m]).

This occurrence may be likened to the Asymptotic Theory of (Faltinsen, 1997). The water and air cushion pressures balance the inertia of the plate since a relative amount of time needs to be elapsed before elastic deformations start to occur on the plate. The plate progressively experiences an impact force of higher magnitude in a short time period same as the highest natural period for the plate vibrations. This causes the space averaged elastic vibration velocity to be equal to the rigid body water entry velocity. The plate then experiences a free vibration phase as the plate begins to vibrate (as seen in the different force monitor plots in the figures), during this free vibration phase, maximum strains occur.

Also presented in the results, the Volume Fraction of Air, Volume Fraction of Water, the Pressure distribution in the domain, the Vector plot of the velocity of the fluid and the ABAQUS solution on the plate.

From the Volume Fraction of air and water scenes, it can be observed that at velocities 4m/s and 8m/s for all sets of simulations, there is a fraction of fluid that "escapes" and lines up along the corners close to the boundaries of the plate. It is important that the cause of this be further investigated. On the other hand, from the vector plots of the combinations **air compressible, water compressible** and **air compressible, water incompressible**, what appears to be vortex flow of the fluid is visible for each of the investigated velocities, i.e. 1m/s, 4m/s and 8m/s. However, the size of this vortex flow appears to grow with the increasing magnitude of the velocity. The scenes of the pressure distribution show a range of negative to positive pressure variations. There exists a large range of negative pressures (magnitude) for combinations where air is compressible. However, it is of great concern to investigate the cause of this, more importantly the physics behind it; and to identify if these negative pressures do quantify cavitation or ventilation or progressive formation of air bubbles on the plate surface with respect to the fluid or if it quantifies the deformations on the plate.

In all sets of the simulations, it is observed that the plate starts to buckle/bend at the velocity of 8m/s which could imply that at high impact wave velocities, there are structural deformations on the plate. Each simulation took a total running time of 0.5seconds.

4.3 Investigation of The Effect of Deadrise Angles (1°, 2°, 5°)

The investigations on the effect of the deadrise angles on the slamming event were simulated at a constant velocity of 7m/s i.e. 7.796m/s entry velocity. As already established in theory, the magnitude of impact of the slamming loads are sensitive to the size of the naturally occurring angle between the plate / structural surface and the free surface, in other words, the deadrise angle (Faltinsen, 1997, 2005; Abrate, 2013). At relatively small deadrise angles, very high pressure impact forces may be recorded and the force of impact is expected in theory to be of lower magnitude as the deadrise angle increases (Faltinsen, 1997; Okada and Sumi, 2000; Kapsenberg, 2011; Abrate, 2013).

The results from the simulation ran are however in contrast to what is established in theory. Comparing the force monitor plots for 1°, 2°, 5° deadrise angles when water is incompressible and air compressible, the magnitude of peak impact force decreases with increasing size of the deadrise angle. These obtained results could be stemming from the fact that the plate is modelled fixed lengthwise on one edge of the plate making the plate stiff and restricting translations and rotations in the respective y-axis affecting the solution. Further investigation into this is highly motivated.

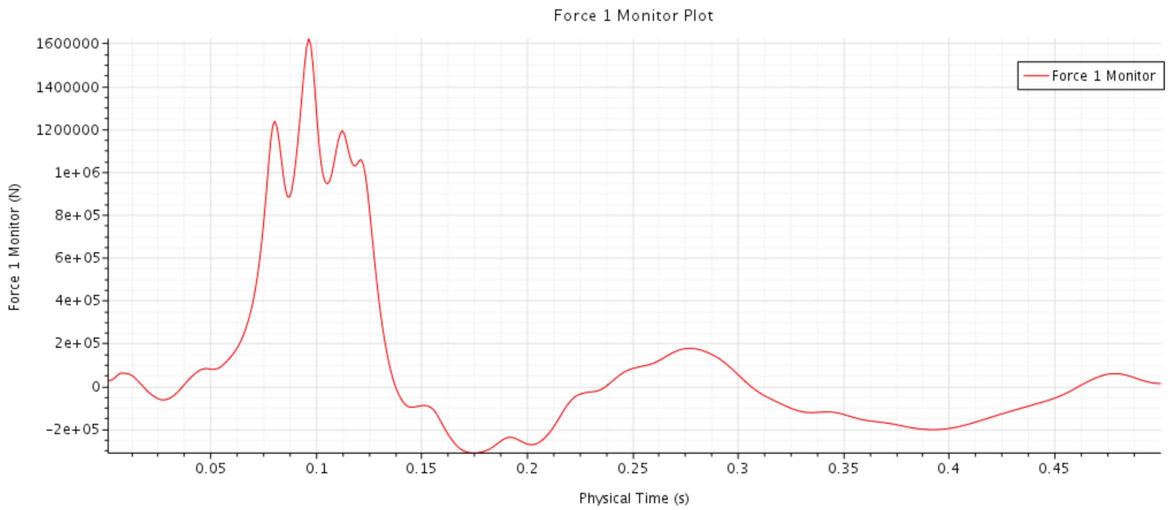

Figure 18: Force Monitor Plot 1° deadrise (water incompressible, air compressible)

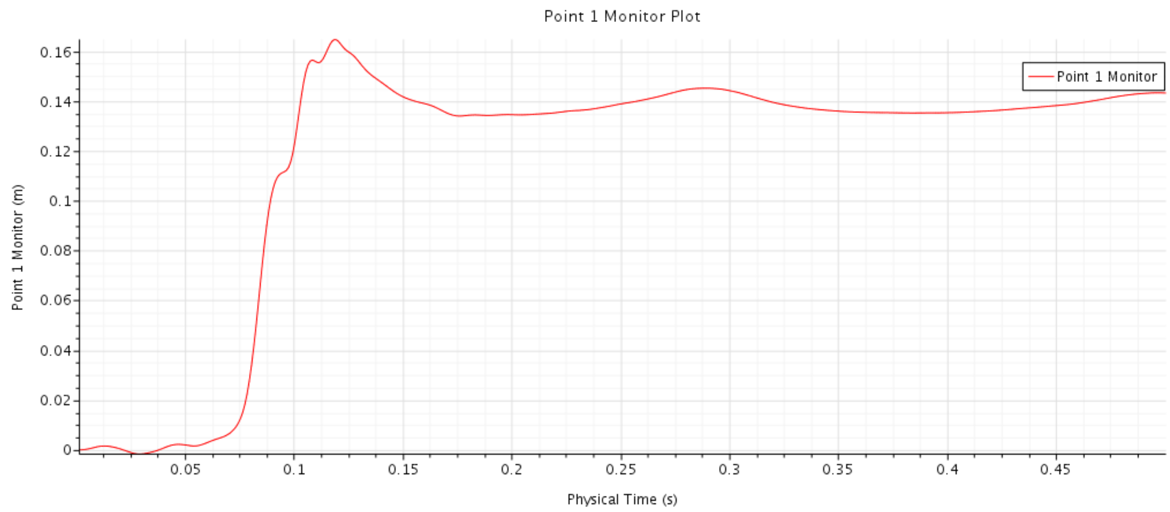

Figure 19: Point Monitor Plot 1° deadrise (water incompressible, air compressible)

At 2° deadrise angle, simulations for the different combinations of the compressibility of air and the compressibility of water was executed. As can be seen from the plots in Figures 20 – 25 below, the results of the different combinations of the compressibility of air and water return the same values; as already stated in the earlier submission where the compressibility of air and water were investigated, further investigations are required to ascertain if the physical quantities representing the compressibility of water were properly modelled.

From the results, the maximum force peak in each of the force monitor plots is recorded at 1.7MN with maximum deformation occurring around 0.185m. Comparing these results with the plate at a 0° deadrise angle (parallel to the free surface of the entry of the block of water) with water entry velocity set at 7.796m/s in (Janson, 2017), the maximum force peak for 0° deadrise angle is 1.8MN with maximum deformation occurring around 0.112m. From this it can be inferred that indeed at lower or no deadrise angles, the force magnitude of the force of impact is high and deformations occur abruptly as postulated in theory. This could be due to the presence of an already existing air pocket beneath the plate when it is flat (0° deadrise compared to a 2° deadrise where an appreciable amount of the air could escape before impact (Okada and Sumi, 2000; Faltinsen and Semenov, 2008).

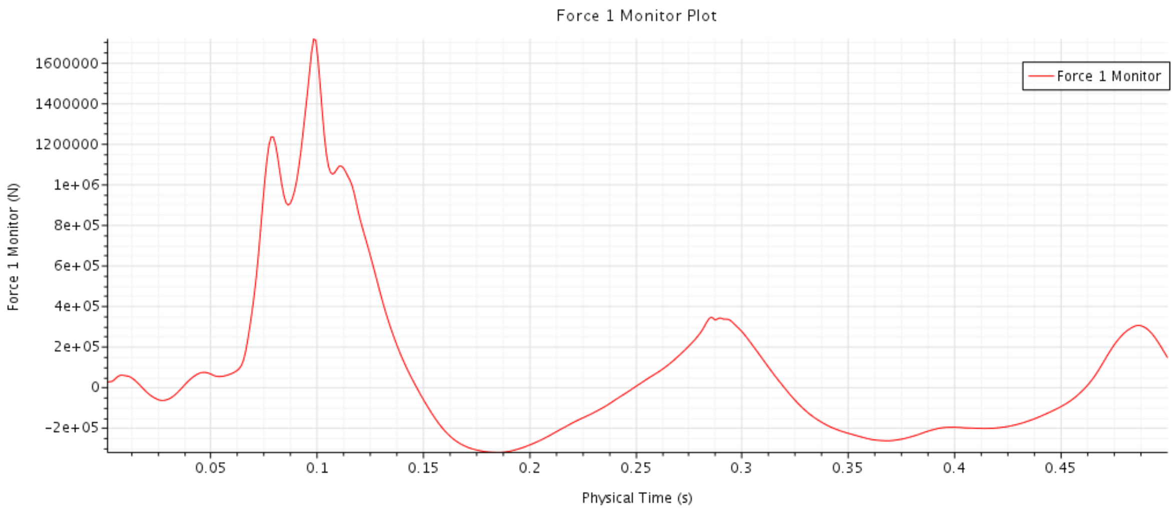

Figure 20: Force Monitor Plot 2° deadrise (water compressible, air compressible)

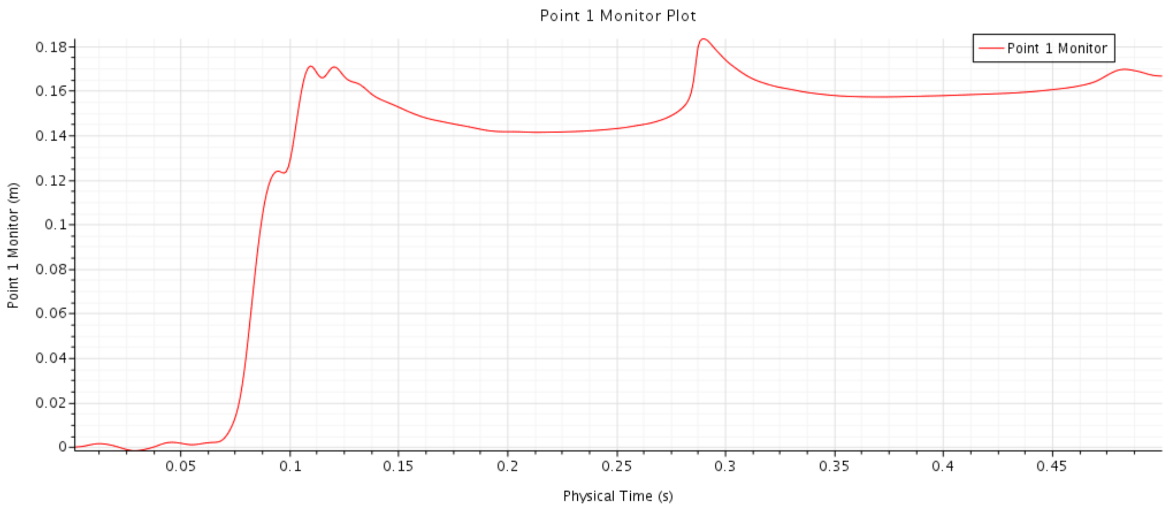

Figure 21: Point Monitor Plot 2° deadrise (water compressible, air compressible)

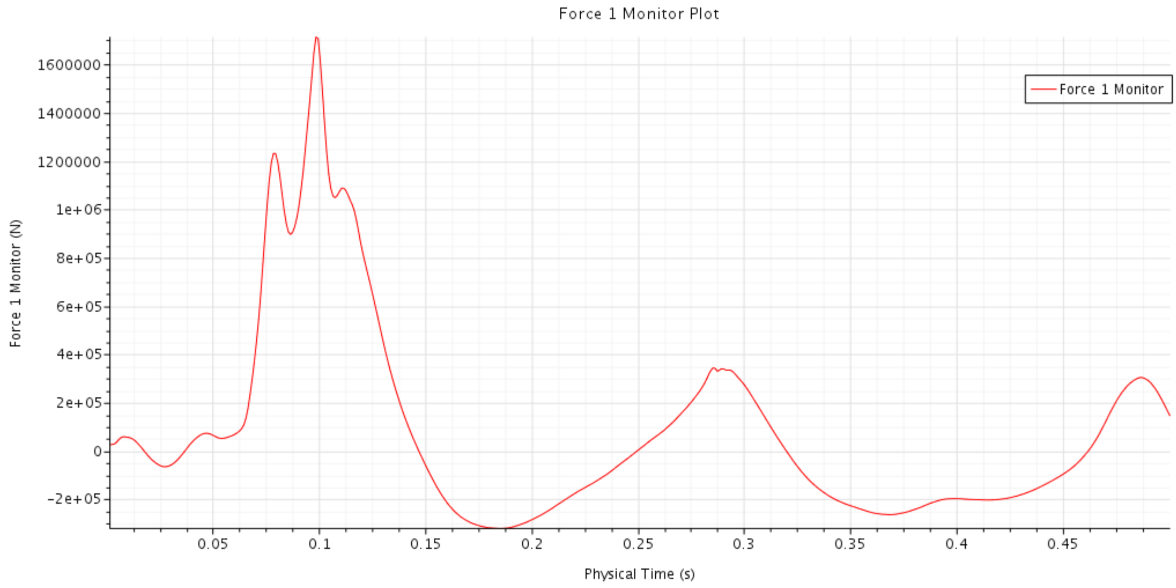

Figure 22: Force Monitor Plot 2° deadrise (water compressible, air incompressible)

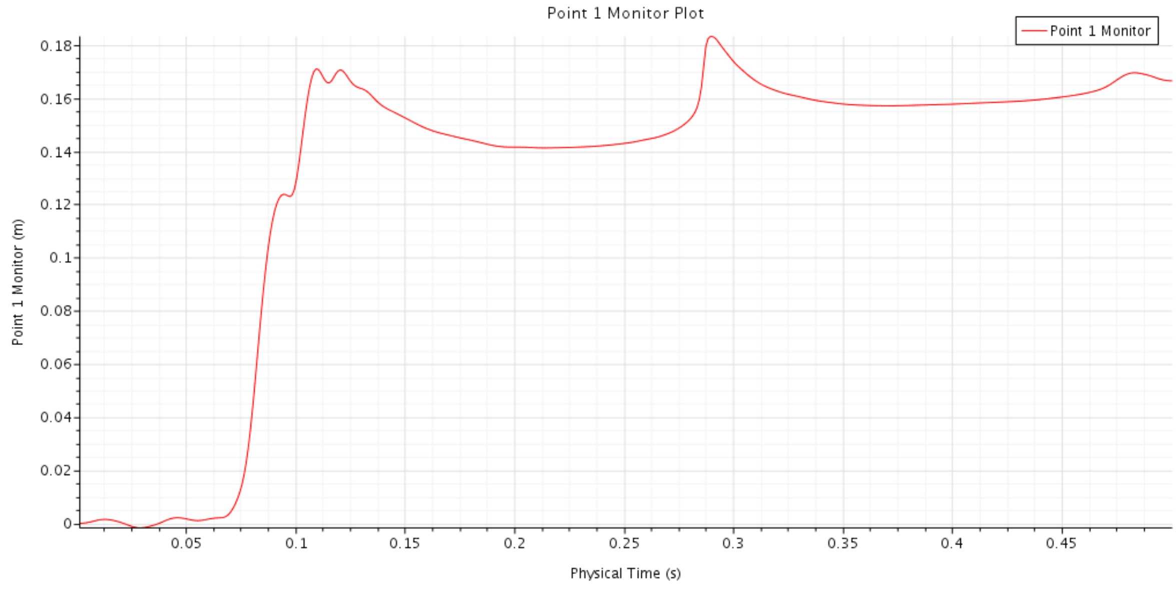

Figure 23: Point Monitor Plot 2° deadrise (water compressible, air incompressible)

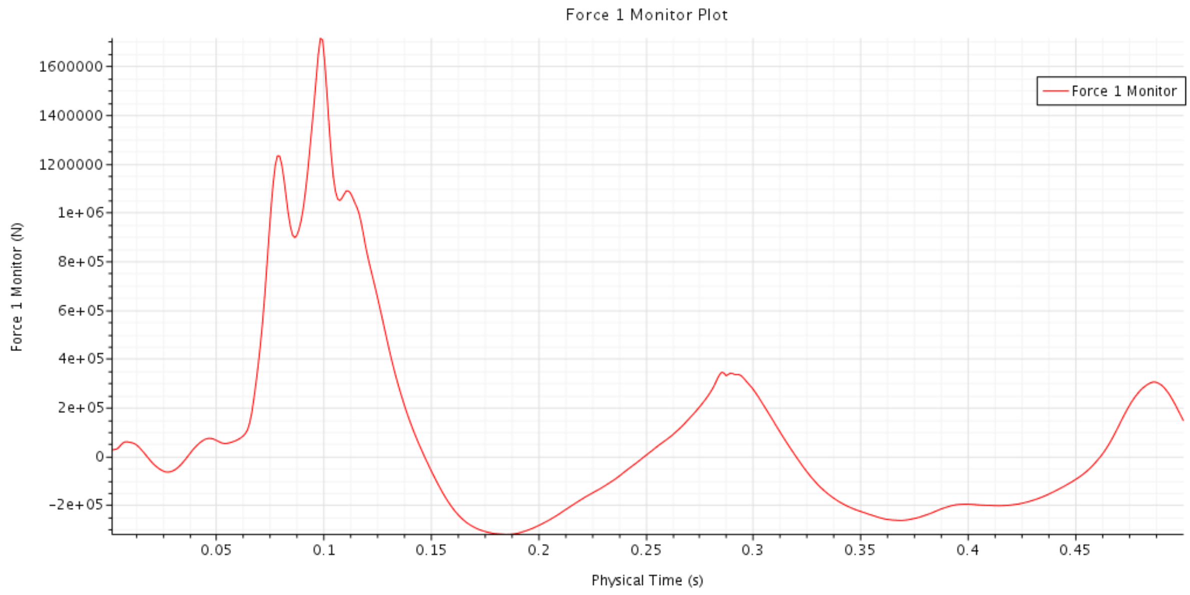

Figure 24: Force Monitor Plot 2° deadrise (water incompressible, air compressible)

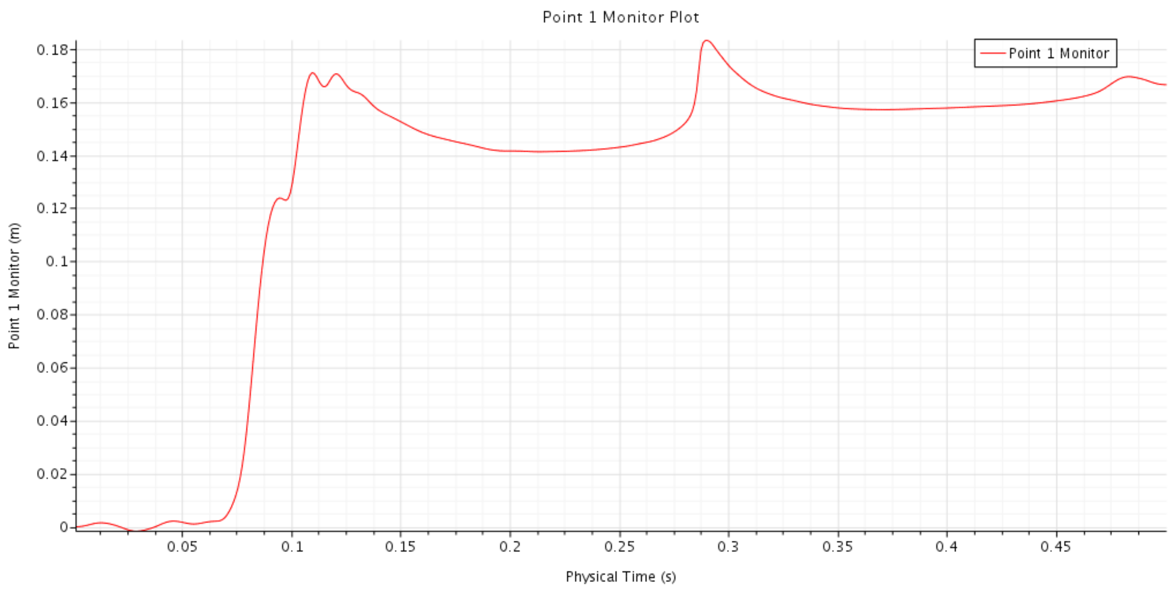

Figure 25: Point Monitor Plot 2° deadrise (water incompressible, air compressible)

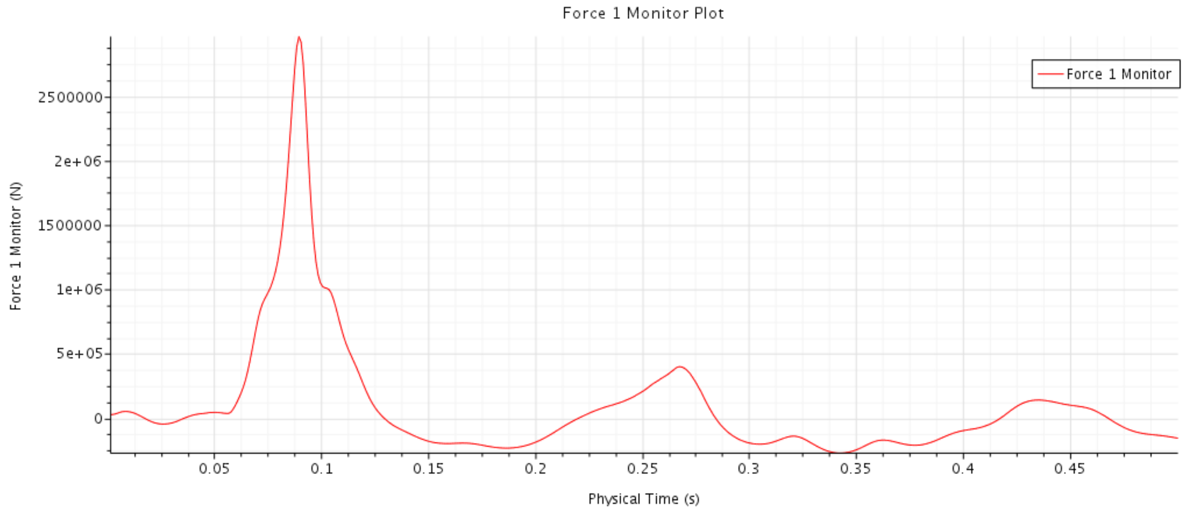

Figure 26: Force Monitor Plot 5° deadrise (water incompressible, air compressible)

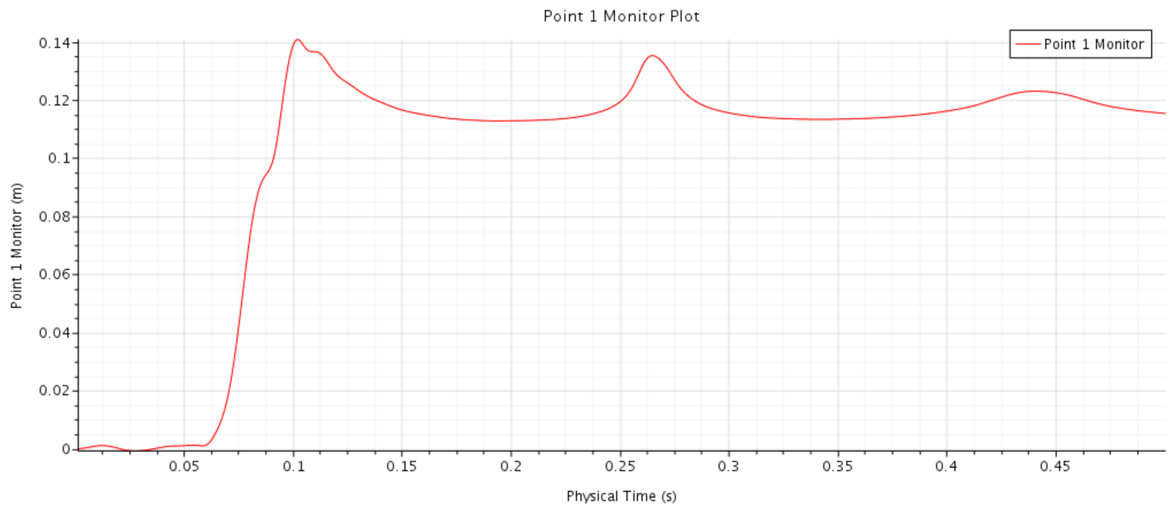

Figure 27: Point Monitor Plot 5° deadrise (water incompressible, air compressible)

Generally, from the investigation of the effect of deadrise angles, it can be observed from the force monitor plots that with increasing size of the deadrise angles, the number of force peaks decrease. There also exists a discrepancy when comparing the points at which maximum deformations occur. Maximum deformation at 1°, 2° and 5° deadrise angles occur at 0.165m, 0.185m and 0.14m respectively. The expected pattern here is that, at increasing deadrise angles, maximum deformations be recorded at higher points at constant water entry velocities. More investigations in this regard with the right modelling of the physical quantities involved will give more understanding into this occurrence. Also, as can be seen from the Volume Fraction of Air scenes in the Appendix, with increasing deadrise angles, the Volume Fraction of air increases; these scenes are recorded at the end of each simulation i.e. at 0.55s.

5. CONCLUSIONS

Continuous and extensive research work has been conducted over a century in the subject area of hull slamming in the attempt to understand the rather complicated phenomenon and help curb the accidents and effects it has on the structural integrity of hulls.

Different approaches, methods and theories have been used to study the problem with much more emphasis placed on the practical application of the postulated theories related to the slamming phenomenon mostly through experiments. It is undeniable that though full scale experiments involve a lot of technicalities and could be long-term, it may be the only way to understand the complexity of this naturally occurring probabilistic event of slamming. In spite of the rather long time the full scale experiment approach may require, the final solution in recent times is to adopt the CFD approach by properly modelling all the physical quantities related to the slamming event. Some challenges in relation to this could be modelling and scaling of the formation of bubbles, air pockets.

The current research work was carried out using STAR-CCM+ a CFD software and ABAQUS a FE software to investigate mainly the effect of deadrise angles, compressibility of the fluid (mixture of air and water) and the magnitude of water entry velocities on the slamming phenomenon. Though positive, the results obtained suggest that much more focused research is required in each, be it the effect of the deadrise angles, compressibility and magnitude of the water entry velocities; and thereafter a combination of the effects. However, inferring from the results, it is credible that the slamming event is of course sensitive to the compressibility of the fluid, the deadrise angle of the structure and the magnitude of the water entry velocity. The sensitivity to low deadrise angles is however much more complicated as this is where impact forces are deemed to be the highest at the same time accounting for the effect of the air cushions / pockets.

The use of both STAR-CCM+ and ABAQUS made it possible to carry out the investigations as FSI analyses as well as accounting for hydroelasticity.

6. FUTURE WORK & RECOMMENDATIONS

Based on the experience from the current study, it is recommended that the development of the model be revisited and ensured that the different physical parameters related to the study are carefully and properly modelled in order to produce much credible results in-line with theory. Thereafter much more focused study in each of the three investigations carried out in this current study be conducted for a much better realized understanding of this complicated phenomenon. Then again, in modelling the plate and the domain, it could be investigated as to whether fixing the plate lengthwise on one edge to the fluid domain compared to detaching it has an influence on the obtained results.

Moving forward, it will be an improvement to use instead of a plate a wedge-shape in the current study since a wedge is an approximate shape of a ship's section.

Generally, Classification Rules are in recent years seeing a shift from being rule-based to risk-based design. Risk in context here is mathematically defined as the product of the probability of failure and the consequences resulting from the failure. In view of this, it is recommended that research or analysis in slamming be conducted based on the concept of risk-based design. The main challenge that may be faced here is defining the probability for the slamming event to occur as in effect it is rather difficult and complicated to define a threshold impact velocity or water entry velocity for slamming to occur (Faltinsen, 2005).

Understanding the slamming from a risk-based approach will serve as a springboard to design and incorporate criteria to be adopted in the early design stages to account for the perils and effects of the unlikely event of slamming.

REFERENCE

Abrate, S. (2013) 'Hull Slamming', *Applied Mechanics Reviews*, 64(6), p. 060803.

Arai, M., Cheng, L.-Y. and Inoue, Y. (1995) 'A Computing Method for the Analysis of Water Impact of Arbitrary Shaped Bodies (2nd Report)', *Journal of the Society of Naval Architects of Japan*, (177), pp. 91–99.

Battistin, D. and Iafrati, A. (2004) 'A numerical model for the jet flow generated by water impact', *Journal of Engineering Mathematics*. Kluwer Academic Publishers, 48(3/4), pp. 353–374.

Camilleri, J., Taunton, D. J. and Temarel, P. (2015) 'Two-dimentional Numerical Modelling of Slamming Impact Loads on High-speed Craft', *Hyel-2015*, (2012), pp. 73–81.

Campana, E. F. *et al.* (2000) 'Some insights into slamming forces: Compressible and incompressible phases', *Proceedings of the Institution of Mechanical Engineers, Part C: Journal of Mechanical Engineering Science*. SAGE PublicationsSage UK: London, England, 214(6), pp. 881–888.

Cheon, J. S. *et al.* (2016) 'A study on slamming pressure on a flat stiffened plate considering fluid–structure interaction', *Journal of Marine Science and Technology (Japan)*. Springer Japan, 21(2), pp. 309–324.

Chung, J. Y. *et al.* (2007) 'A novel experimental technique in slamming', in *22nd IWWWFB*. Zelenogorsk, Russia, pp. 41–44. Available at: https://www.fsb.unizg.hr/iwwwfb22/papers/W22-CHUNG-NAHM-KANG-KWON.pdf (Accessed: 9 July 2019).

Donguy, B. *et al.* (2001) 'Three-Dimensional Hydroelastic Water Entry: Preliminary Results'. International Society of Offshore and Polar Engineers. Available at: https://www.onepetro.org/conference-paper/ISOPE-I-01-392 (Accessed: 30 May 2019).

Faltinsen, O. M. (1997) 'The effect of hydroelasticity on ship slamming', *Philosophical Transactions of the Royal Society of London. Series A: Mathematical, Physical and Engineering Sciences*. Edited by S. D. Howison et al., 355(1724), pp. 575–591.

Faltinsen, O. M. (2001) 'Hydroelastic slamming', *Journal of Marine Science and Technology*. Springer-Verlag, 5(2), pp. 49–65.

Faltinsen, O. M. (2005a) *Hydrodynamics of High-Speed Marine Vehicles*. Norwegian University of Science and Technology: Cambridge University Press.

Faltinsen, O. M. (2005b) *Hydrodynamics of High Speed Marine Vehicles*. Norwegian University of Science and Technology: Cambridge University Press.

Faltinsen, O. M., Landrini, M. and Greco, M. (2004) 'Slamming in marine applications', *Journal of Engineering Mathematics*. Kluwer Academic Publishers, 48(3/4), pp. 187–217.

Faltinsen, O. M. and Semenov, Y. A. (2008) 'Nonlinear problem of flat-plate entry into an incompressible liquid', *Journal of Fluid Mechanics*. Cambridge University Press, 611, pp. 151–173.

Gingold, R. A. and Monaghan, J. J. (1977) 'Smoothed particle hydrodynamics: theory and application to non-spherical stars', *Monthly Notices of the Royal Astronomical Society*. Narnia, 181(3), pp. 375–389.

Greenhow, M. and Lin, W.-H. (1985) 'Numerical simulation of non linear free surface flows generated by wedge entry and wavemaker motions', in *International Conference on Numerical Ship Hydrodynamics, 4th*.

Grimaldi, A. *et al.* (2011) 'Steel Structure Impacting onto Water: Coupled Finite Element-Smoothed-Particle-Hydrodynamics Numerical Modeling', *Journal of Aircraft*, 48(4), pp. 1299–1308.

Groenenboom, P. H. L. and Cartwright, B. K. (2010) 'Hydrodynamics and fluid-structure interaction by coupled SPH-FE method', *Journal of Hydraulic Research*, 48(sup1), pp. 61–73.

Hayman, B., Haug, T. and Valsgard, S. (1991) 'Response of Fast Craft Hull Structures to Slamming Loads', in *NTNF Fast Craft Programme*, pp. 381–398.

Hermundstad, O. A. and Moan, T. (2005) 'Numerical and experimental analysis of bow flare slamming on a Ro–Ro vessel in regular oblique waves', *Journal of Marine Science and Technology*. Springer-Verlag, 10(3), pp. 105–122.

Hirdaris, S. E. and Temarel, P. (2009) 'Hydroelasticity of ships: Recent advances and future trends', *Proceedings of the Institution of Mechanical Engineers, Part M: Journal of Engineering for the Maritime Environment*, 223(3), pp. 305–330.

Hoque, M. (2014) 'Dynamic Response of Ship Hull due to Slamming', (June). Available at: http://www.diva-portal.org/smash/record.jsf?pid=diva2:733872 (Accessed: 29 May 2019).

Iafrati, A. and Korobkin, A. A. (2004) 'Initial stage of flat plate impact onto liquid free surface', *Physics of Fluids*. American Institute of Physics, 16(7), pp. 2214–2227.

Janson, C. (2017) 'ISSC Benchmark study on slamming loads'.

Kapsenberg, G. K. (2011) 'Slamming of ships: Where are we now?', *Philosophical Transactions of the Royal Society A: Mathematical, Physical and Engineering Sciences*, 369(1947), pp. 2892–2919.

Kapsenberg, G. K. and Thornhill, E. T. (2010) 'A practical approach to ship slamming in waves', in *28th Symposium on Naval Hydrodynamics*, p. 14.

Kapsenberg, G., naval, E. T.-28th symposium on and 2010, undefined (no date) 'A practical approach to ship slamming in waves', *Pasadena California*. Available at: https://scholar.google.se/scholar?hl=en&as_sdt=2005&sciodt=0%2C5&cites=10380472912740516653&scipsc=&q=Kapsenberg+and+Thornhill+2010&btnG= (Accessed: 29 May 2019).

Von Kármán, T. (1929) 'The impact on seaplane floats during landing', *National Advisory Committee for Aeronautics Technical Notes*. National Advisory Committee on Aeronautics, 321.

Kleefsman, K. M. T. *et al.* (2005) 'A Volume-of-Fluid based simulation method for wave impact problems', *Journal of Computational Physics*. Academic Press, 206(1), pp. 363–393.

Korobkin, A. (1992) 'Blunt-body impact on a compressible liquid surface', *Journal of Fluid Mechanics*. Cambridge University Press, 244(1), p. 437.

Korobkin, A.A. and Iafrati, A. (2006) 'Hydrodynamic loads on flat plate entering water.' Available at: https://ueaeprints.uea.ac.uk/20671/ (Accessed: 9 July 2019).

Korobkin, Alexander A. and Iafrati, A. (2006) 'Numerical study of jet flow generated by impact on weakly compressible liquid', *Physics of Fluids*. American Institute of Physics, 18(3), p. 032108.

Korobkin, A. A. and Scolan, Y.-M. (2006) 'Three-dimensional theory of water impact. Part 2. Linearized Wagner problem', *Journal of Fluid Mechanics*, 549(1), p. 343.

Kvålsvold, J. and Faltinsen, O. M. (1994) 'Slamming loads on Wetdecks of Multihull Vessels', in *International Conference on Hydroelasticity in Marine Technology*, pp. 205–222.

Kvålsvold, J., Svensen, T. and Hovem, L. (1996) 'Bow Impact Loads on RO-RO Vessels', *RINA Transactions*.

Leibowitz, R. C. (1962) 'Comparison Of Theory and Experiment for Slamming Of A Dutch Destroyer'. David Taylor Model Basin Report 1511.

Lewis, S. G. *et al.* (2010) 'Impact of a free-falling wedge with water: synchronized visualization, pressure and acceleration measurements', *Fluid Dynamics Research*, 42(3), p. 035509.

Lu, C. H., He, Y. S. and Wu, G. X. (2000) 'Coupled Analysis of Nonlinear Interaction Between Fluid and Structure During Impact', *Journal of Fluids and Structures*. Academic Press, 14(1), pp. 127–146.

Marine Accident Investigation Branch (2008) 'Napoli Report No 9/2008', (9).

Ng, C. O. and Kot, S. C. (1992) 'Computations of water impact on a two-dimensional flat-bottomed body with a volume-of-fluid method', *Ocean Engineering*. Pergamon, 19(4), pp. 377–393.

Ochi, M. K. (1964) 'Prediction of Occurrence and Severity of Ship Slamming at Sea', in *Proceedings of 5th Symposium on Naval Hydrodynamics*, pp. 545–596. Available at: https://ci.nii.ac.jp/naid/20000328486/ (Accessed: 30 May 2019).

Oger, G. *et al.* (2009) 'Simulations of Hydro-elastic Impacts Using a Parallel SPH Model'. International Society of Offshore and Polar Engineers.

Oger, G. *et al.* (2010) 'Simulations of hydro-elastic impacts using a parallel SPH model', *International Journal of Offshore and Polar Engineering*, 20(3), pp. 181–189. Available at: https://www.onepetro.org/conference-paper/ISOPE-I-09-038 (Accessed: 29 May 2019).

Ogilvie, T. F. (1963) 'Compressibility Effects in Ship Slamming', *Schiffstechnik*, Bd, 10, pp. 147–154.

Oh, S. H., Kwon, S. H. and Chung, J. Y. (2009) 'A close look at air pocket evolution in flat impact', in *Proceedings of the 24th Int. Workshop on Water Waves and Floating Bodies, Zelenogorsk, Russia*. Available at: http://www.iwwwfb.org/Abstracts/iwwwfb24/iwwwfb24_42.pdf (Accessed: 9 July 2019).

Okada, S. and Sumi, Y. (2000) 'On the water impact and elastic response of a flat plate at small impact angles', *Journal of Marine Science and Technology*. Springer-Verlag, 5(1), pp. 31–39.

Pabst, W. (1930) 'Theory of the landing impact of seaplanes', *N.A.C.A. Tech. Memo.*, 580.

Peseux, B., Gornet, L. and Donguy, B. (2005) 'Hydrodynamic impact: Numerical and experimental investigations', *Journal of Fluids and Structures*. Academic Press, 21(3), pp. 277–303.

Prohaska, C. W. (1947) 'THE VERTICAL VIBRATION OF SHIPS', *Shipbuilding and Marine Engineering International*, (46), pp. 171–215.

Sames, P. C. *et al.* (2008) 'Application of a Two-Fluid Finite Volume Method to Ship Slamming', *Journal of Offshore Mechanics and Arctic Engineering*, 121(1), p. 47.

Sames, P., Kapsenberg, G. K. and Corrignan, P. (2001) 'Prediction of bow door loads in extreme wave conditions', in *In RiINA Conference Design and operations for anormal conditions II*.

Scolan, Y.-M. and Korobkin, A. A. (2001) 'Three-dimensional theory of water impact. Part 1. Inverse Wagner problem', *Journal of Fluid Mechanics*. Cambridge University Press, 440, pp. 293–326.

Shao, S. (2009) 'Incompressible SPH simulation of water entry of a free-falling object', *International Journal for Numerical Methods in Fluids*. John Wiley & Sons, Ltd, 59(1), pp. 91–115.

Stenius, I. (2006) *Finite Element Modelling of Hydroelasticity in Hull-Water Impacts*. Stockholm, Sweden.

Stenius, I., Rosén, A. and Stenius, I. (2007) 'FE-Modelling of hydrodynamic hull-water impact loads', in *6th European LS-DYNA Users' Conference*, pp. 173–182.

Sun, H. and Faltinsen, O. M. (2006) 'Water impact of horizontal circular cylinders and cylindrical shells', *Applied Ocean Research*. Elsevier, 28(5), pp. 299–311.

Szebehely V.G (1952) *Hydrodynamics of slamming of ships*. David Taylor Model Basin Report 823, NS 715-084.

Tuitman, J. T. (2010) 'Hydro-elastic response of ship structures to slamming induced whipping'. Available at: https://repository.tudelft.nl/islandora/object/uuid:f9aa0204-650d-493f-b1e9-43e91c0f4993 (Accessed: 29 May 2019).

Vandamme, J., Zou, Q. and Reeve, D. E. (2011) 'Modeling Floating Object Entry and Exit Using Smoothed Particle Hydrodynamics', *Journal of Waterway, Port, Coastal, and Ocean Engineering*, 137(5), pp. 213–224.

Veen, D. and Gourlay, T. (2012) 'A combined strip theory and Smoothed Particle Hydrodynamics approach for estimating slamming loads on a ship in head seas', *Ocean Engineering*. Pergamon, 43, pp. 64–71.

Veen, D. J. and Gourlay, T. P. (2011) 'High Speed Marine Vessels', *Proceedings*. Available at: https://pdfs.semanticscholar.org/d9a9/eeb86d8e39cbdb4d21222101cc365d35e0e0.pdf (Accessed: 29 May 2019).

Viviani, M., Brizzolara, S. and Savio, L. (2009) 'Evaluation of slamming loads using smoothed particle hydrodynamics and Reynolds-averaged Navier—Stokes methods', *Proceedings of the Institution of Mechanical Engineers, Part M: Journal of Engineering for the Maritime Environment*. SAGE PublicationsSage UK: London, England, 223(1), pp. 17–32.

Wagner, H. (1932) 'Über Stoß- und Gleitvorgänge an der Oberfläche von Flüssigkeiten', *ZAMM - Zeitschrift für Angewandte Mathematik und Mechanik*. John Wiley & Sons, Ltd, 12(4), pp. 193–215.

Xu, G. D., Duan, W. Y. and Wu, G. X. (2011) 'Numerical Simulation of Water Entry of A Cone in Free-Fall Motion', *The Quarterly Journal of Mechanics and Applied Mathematics*. Narnia, 64(3), pp. 265–285.

Yang, Q. and Qiu, W. (2012) 'Numerical simulation of water impact for 2D and 3D bodies', *Ocean Engineering*, 43, pp. 82–89.

Zhang, Y. *et al.* (2010) 'A level set immersed boundary method for water entry and exit', *Communications in Computational Physics*, 8(2), pp. 265–288.

Zhao, R. and Faltinsen, O. (1993) 'Water entry of two-dimensional bodies', *Journal of Fluid Mechanics*. Cambridge University Press, 246(1), p. 593.

APPENDICES

APPENDIX I: SETTING AIR AS INCOMPRESSIBLE & WATER AS COMPRESSIBLE (Force Monitor Plot)

1 m/s	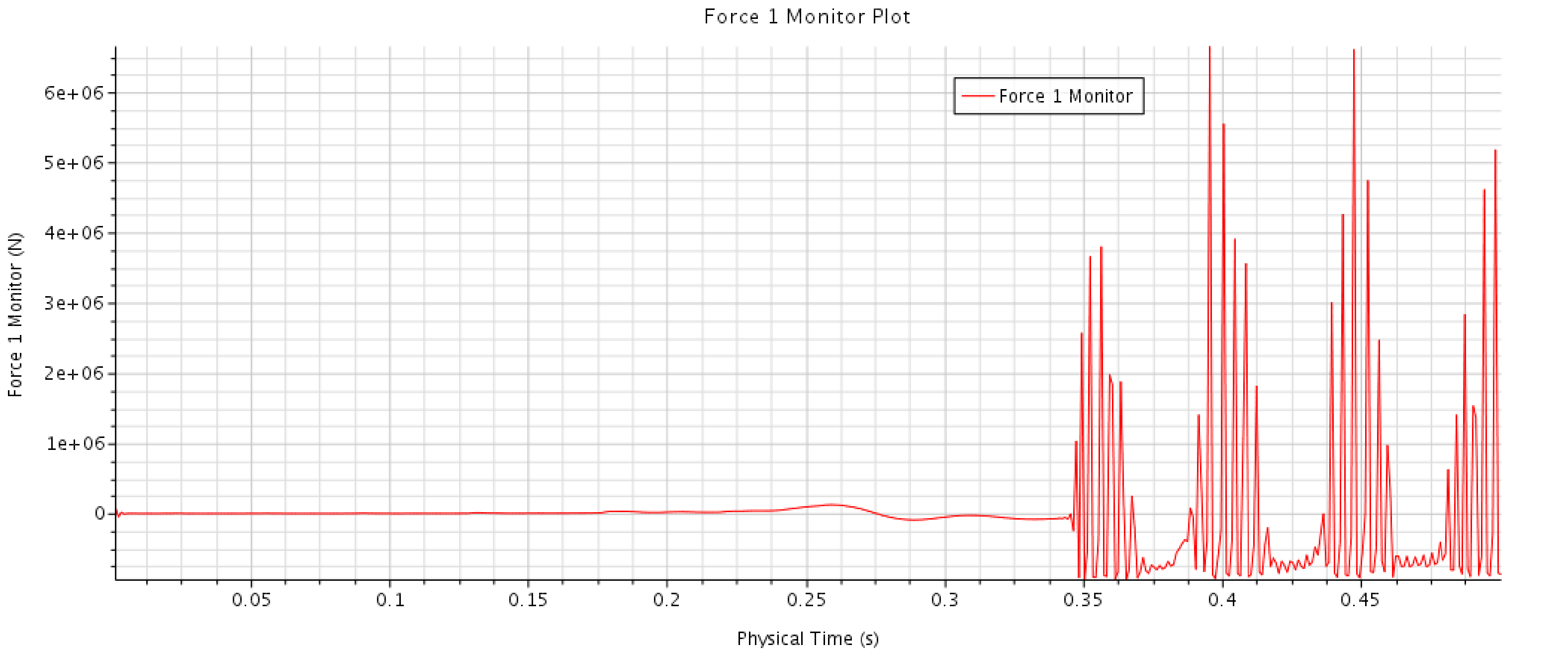

4 m/s	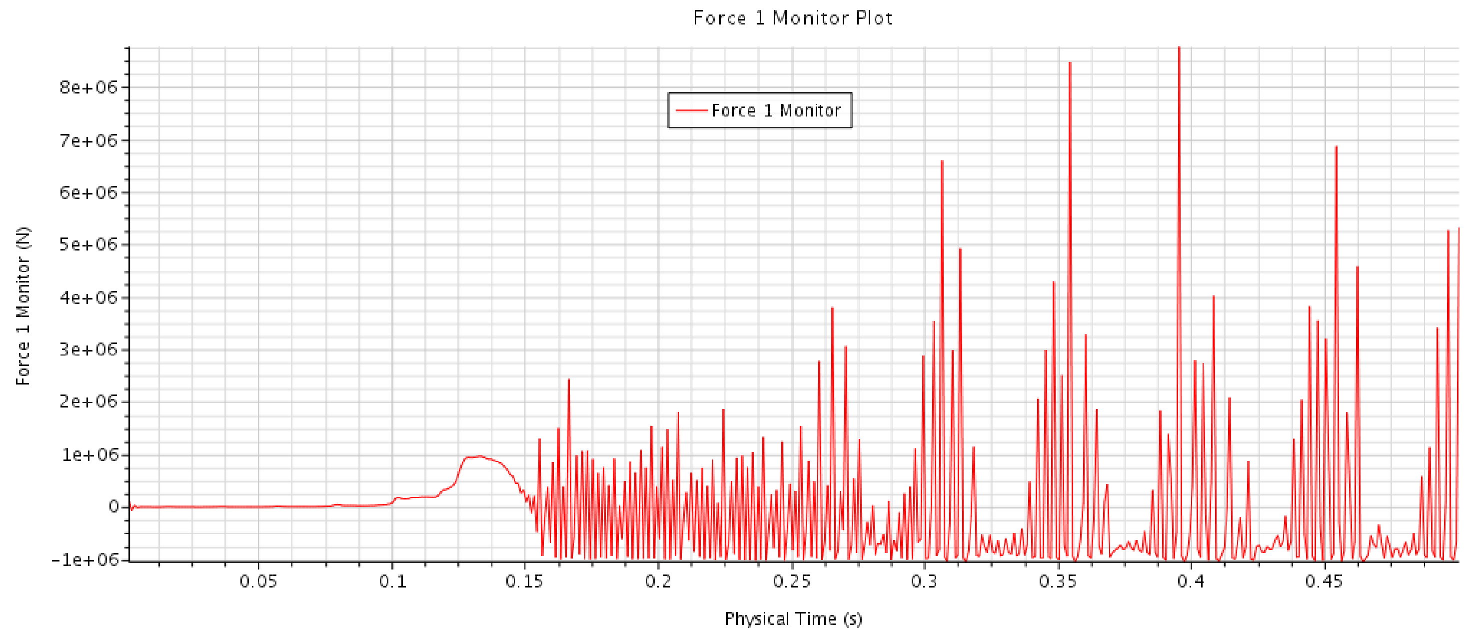 Force 1 Monitor Plot Force 1 Monitor Force 1 Monitor (N) 8e+06 7e+06 6e+06 5e+06 4e+06 3e+06 2e+06 1e+06 0 -1e+06 0.05 0.1 0.15 0.2 0.25 0.3 0.35 0.4 0.45 Physical Time (s)

8 m/s	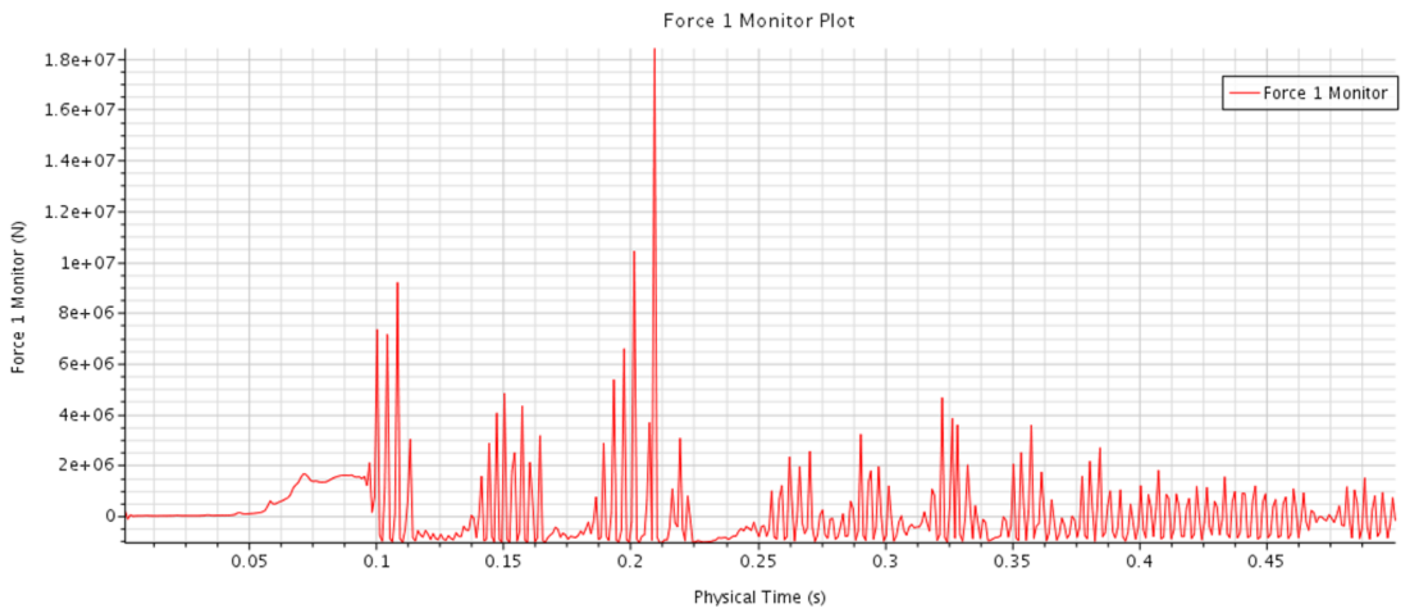

Force 1 Monitor Plot
Force 1 Monitor
Force 1 Monitor (N)
1.8e+07
1.6e+07
1.4e+07
1.2e+07
1e+07
8e+06
6e+06
4e+06
2e+06
0
0.05
0.1
0.15
0.2
0.25
0.3
0.35
0.4
0.45
Physical Time (s)

APPENDIX II: SETTING AIR AS INCOMPRESSIBLE & WATER AS COMPRESSIBLE (Point Monitor Plot)

1 m/s	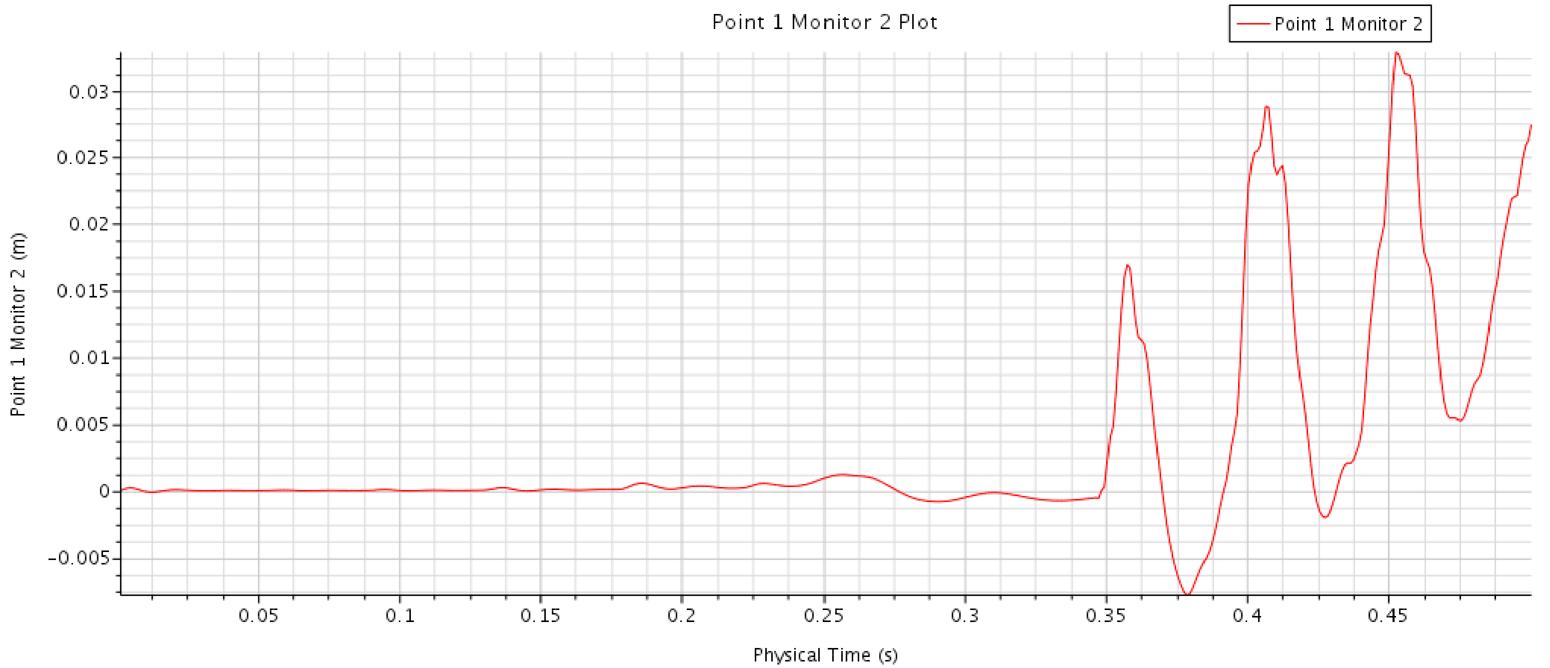

4 m/s	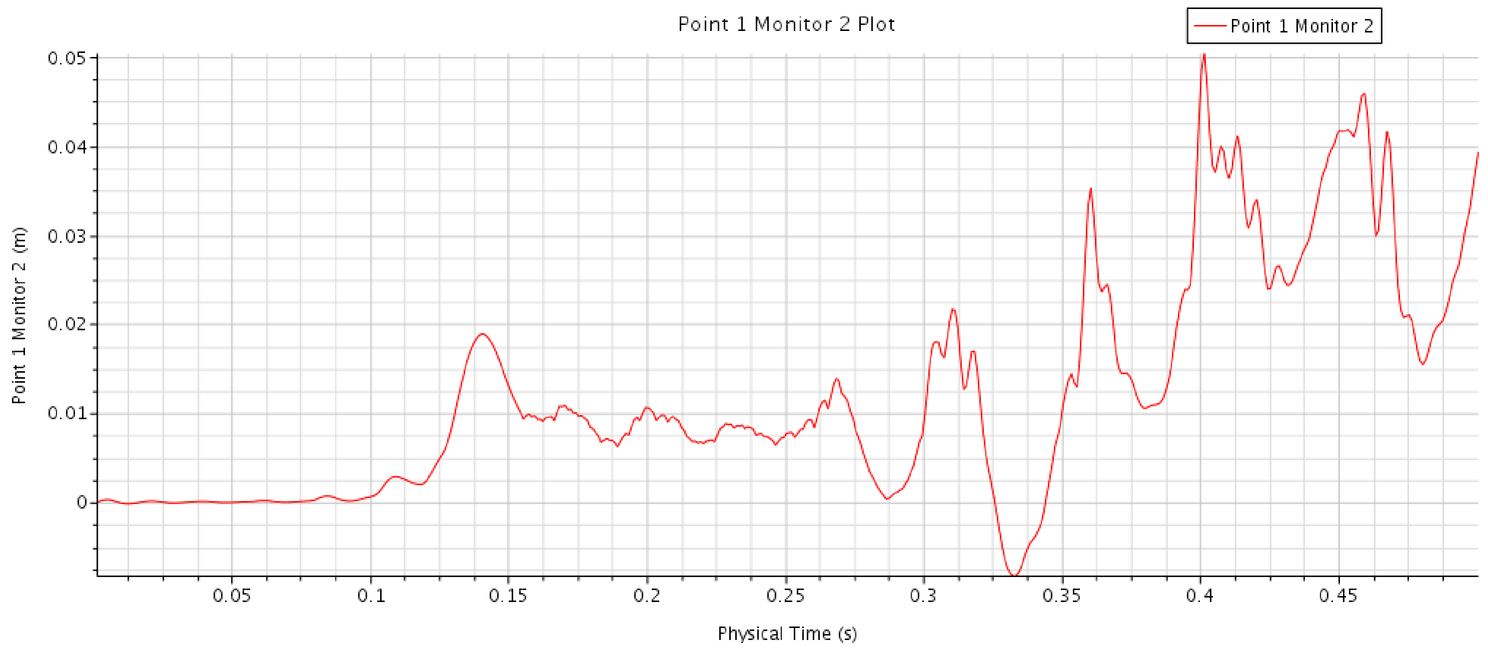Point 1 Monitor 2 Plot
Point 1 Monitor 2
0.05
0.04
0.03
0.02
0.01
0
Point 1 Monitor 2 (m)
0.05
0.1
0.15
0.2
0.25
0.3
0.35
0.4
0.45
Physical Time (s)

8 m/s	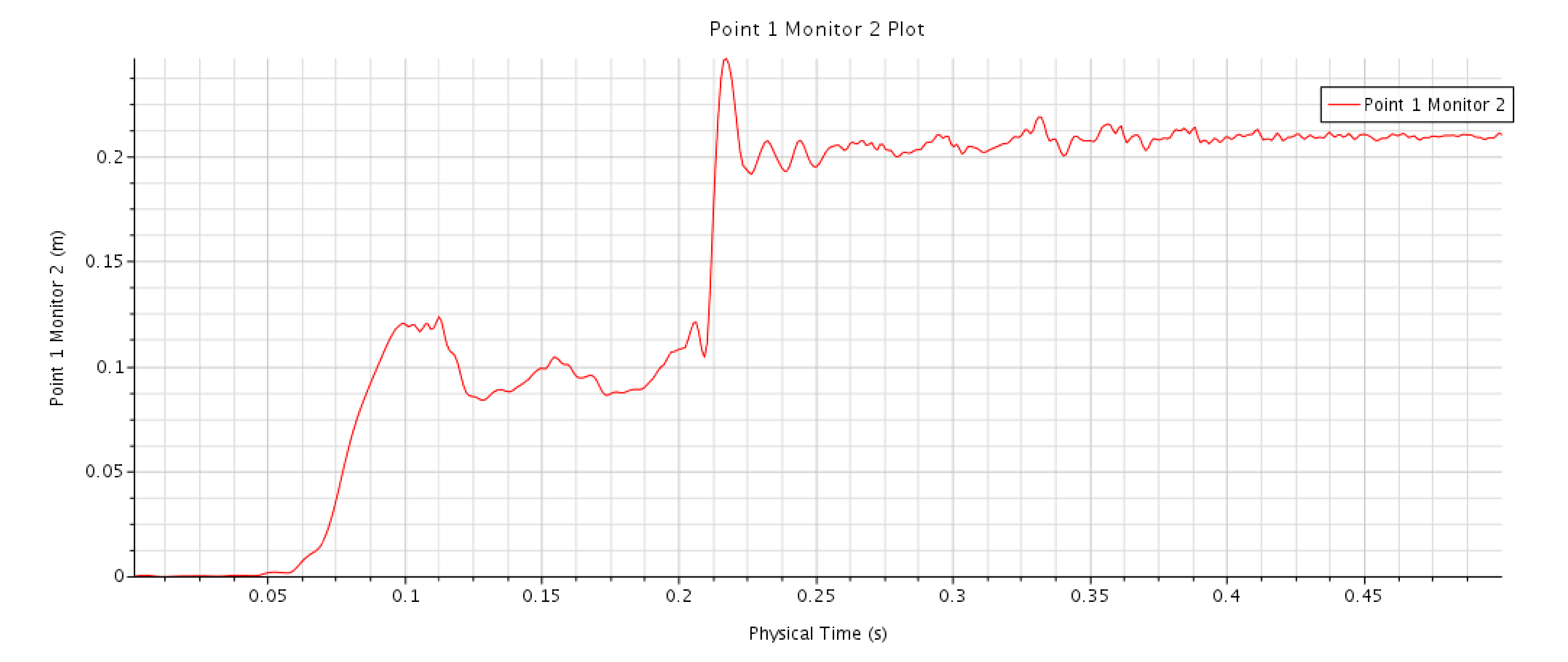

Point 1 Monitor 2 Plot
Point 1 Monitor 2
Point 1 Monitor 2 (m)
0.2
0.15
0.1
0.05
0
0.05
0.1
0.15
0.2
0.25
0.3
0.35
0.4
0.45
Physical Time (s)

APPENDIX III: SETTING AIR AS INCOMPRESSIBLE & WATER AS COMPRESSIBLE (Vector Plot)

1 m/s	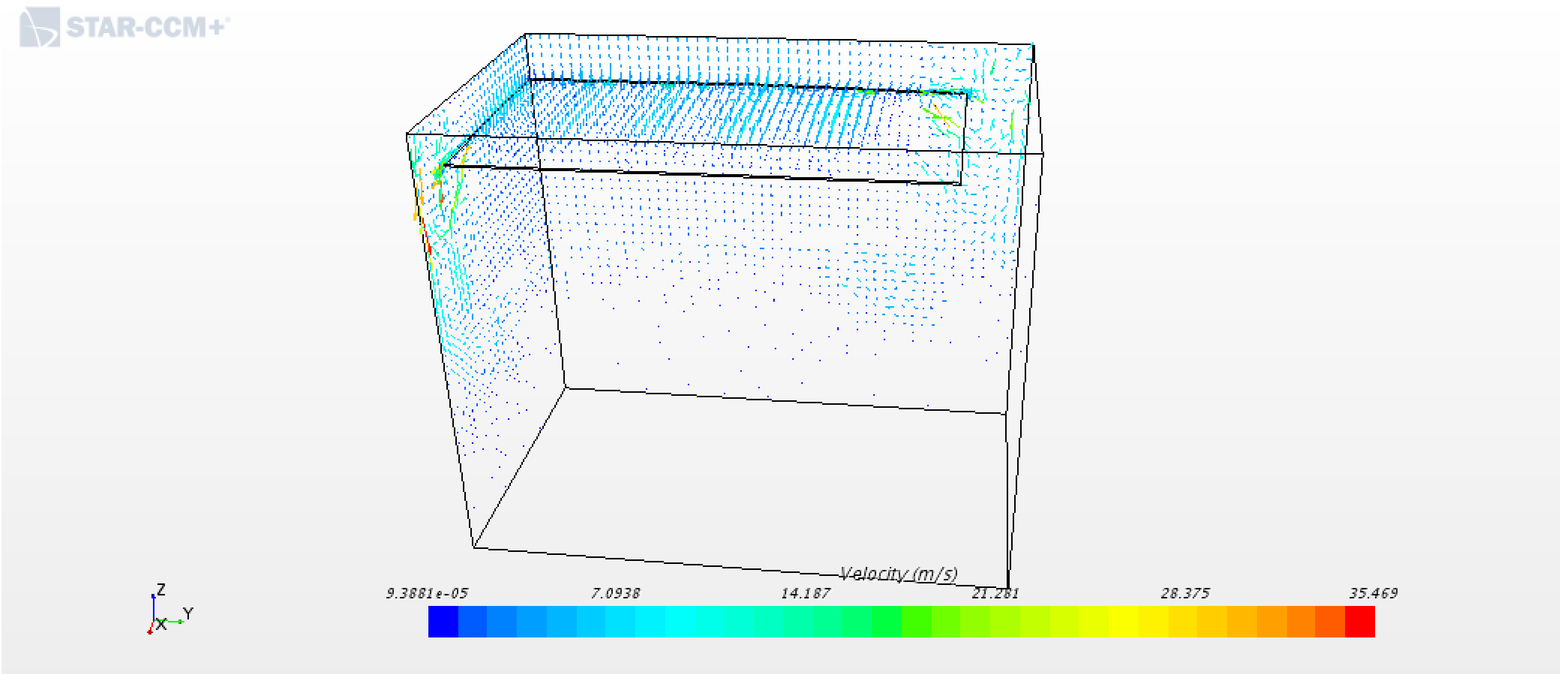

4 m/s	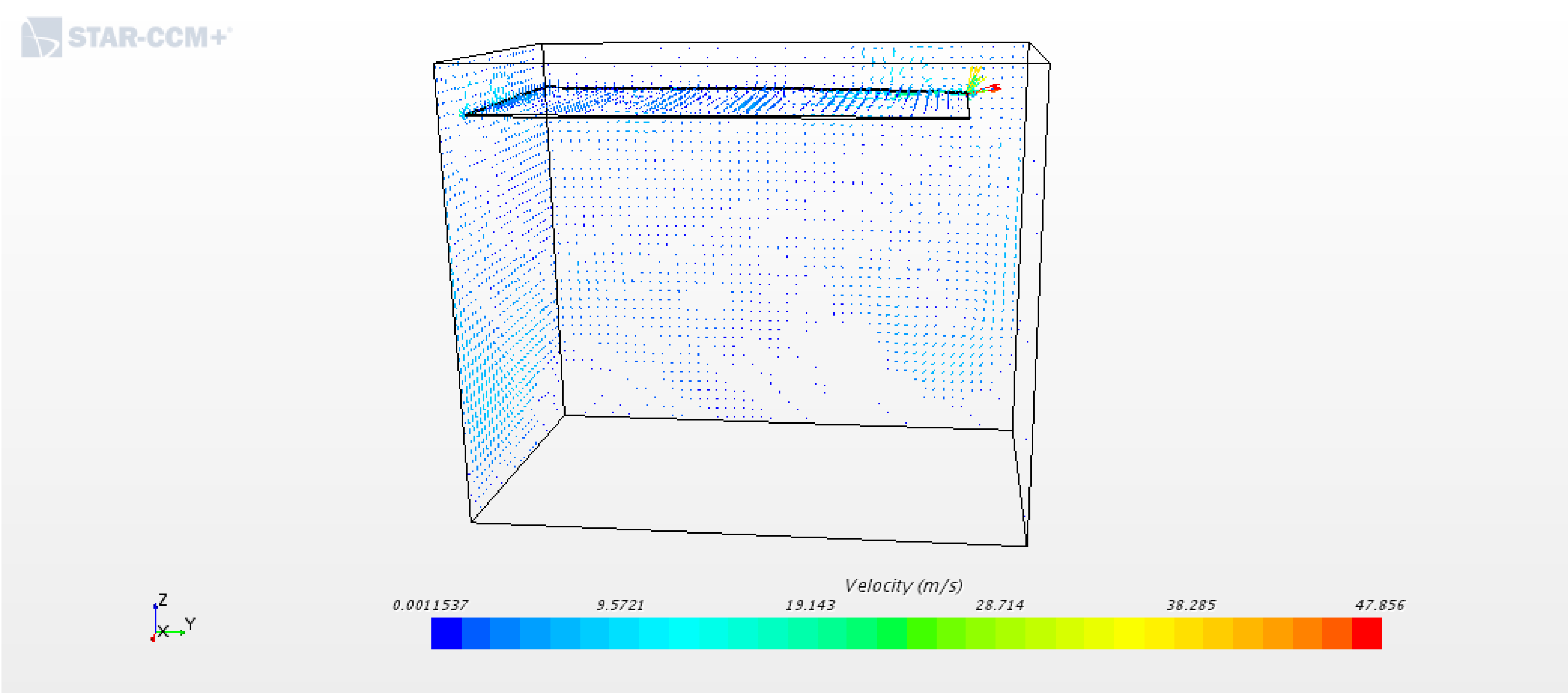STAR-CCM+
Velocity (m/s)
0.0011537
9.5721
19.143
28.714
38.285
47.856
Z
X
Y

8 m/s	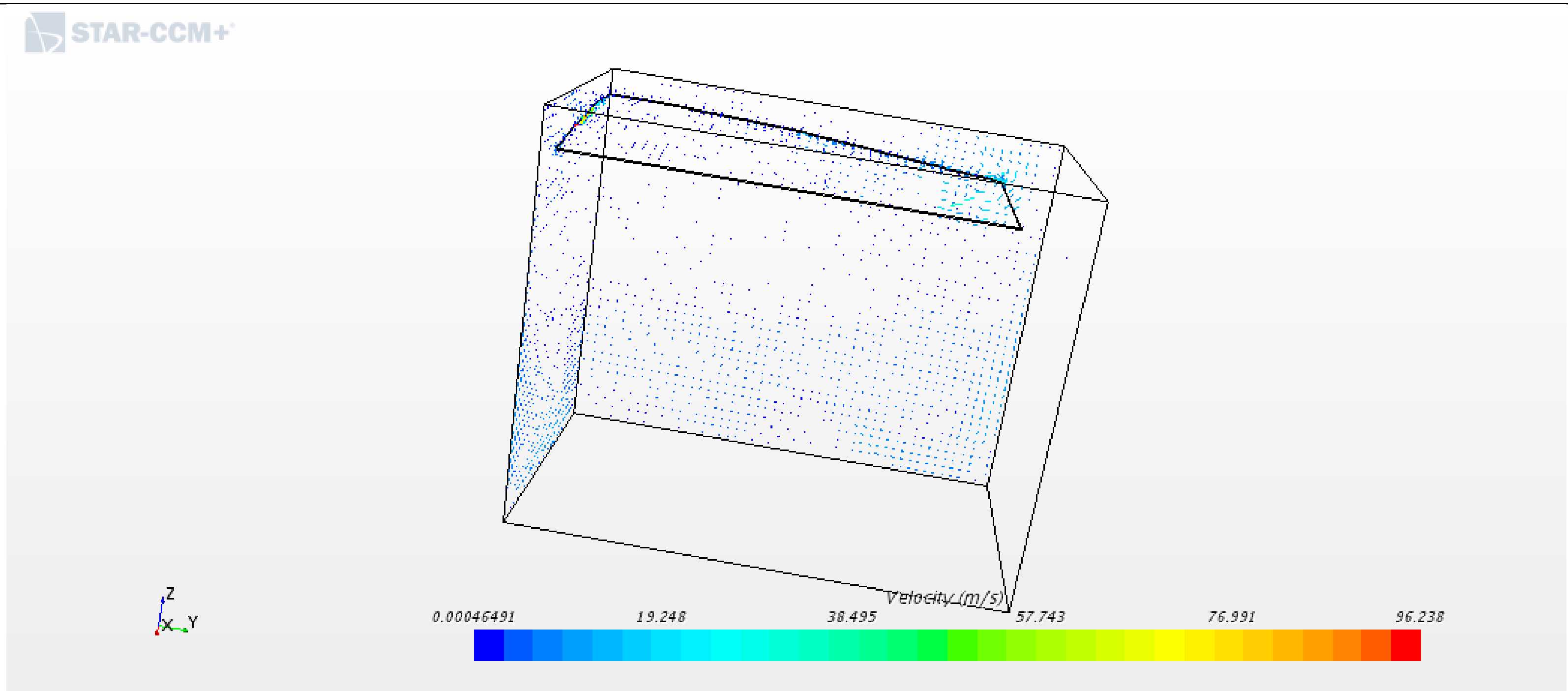STAR-CCM+ Z X Y Velocity (m/s) 0.00046491 19.248 38.495 57.743 76.991 96.238

APPENDIX IV: SETTING AIR AS INCOMPRESSIBLE & WATER AS COMPRESSIBLE (Volume Fraction of Air)

1 m/s	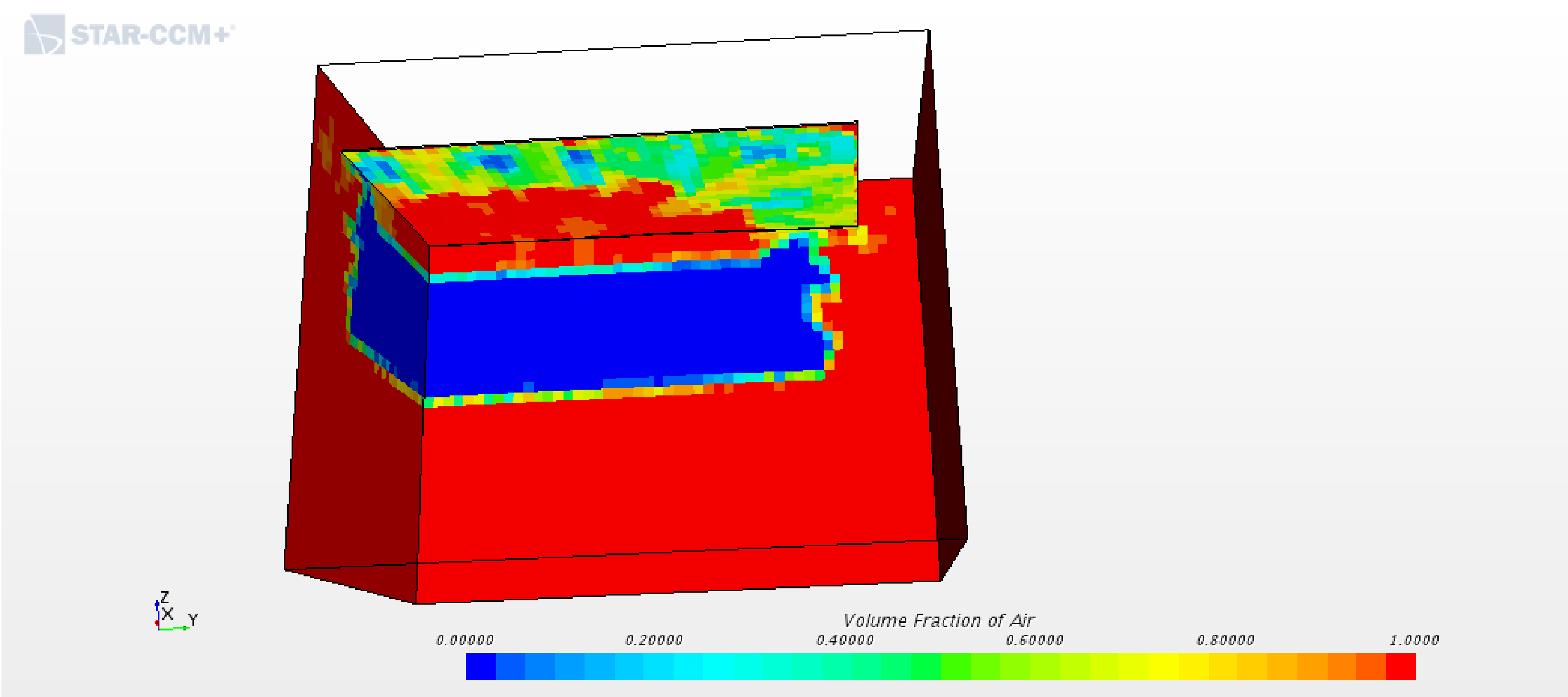

4 m/s	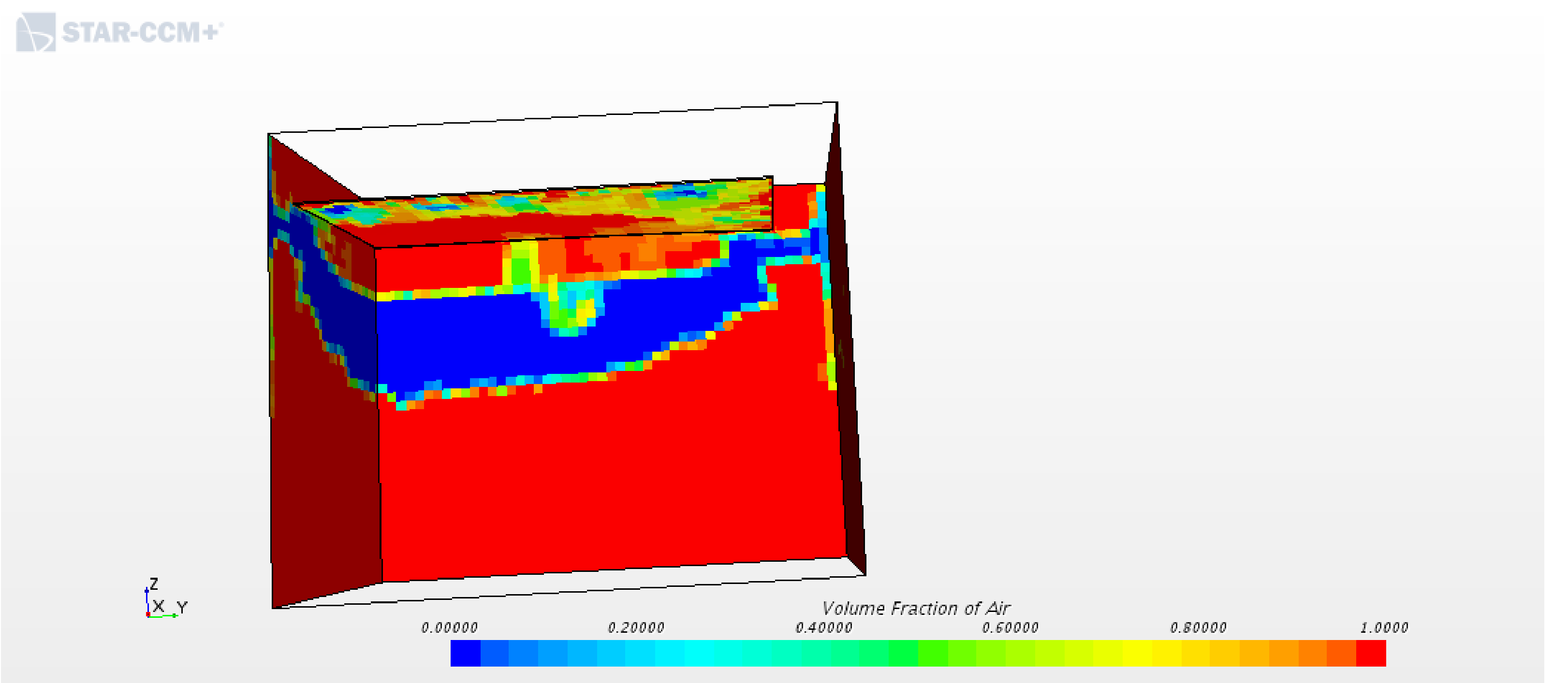STAR-CCM+ Z X Y Volume Fraction of Air 0.00000 0.20000 0.40000 0.60000 0.80000 1.0000

8 m/s	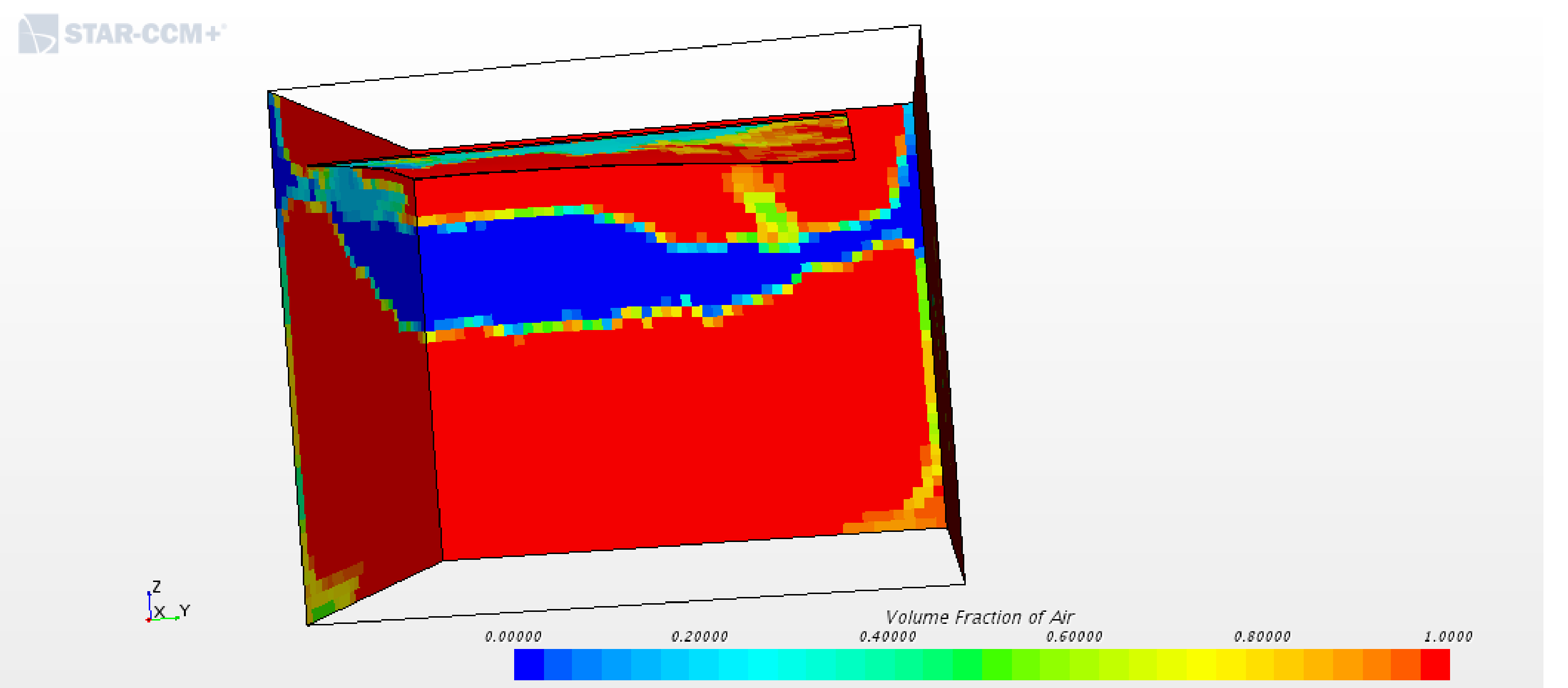STAR-CCM+ Volume Fraction of Air 0.00000 0.20000 0.40000 0.60000 0.80000 1.0000 Z X Y

APPENDIX V: SETTING AIR AS INCOMPRESSIBLE & WATER AS COMPRESSIBLE (Volume Fraction of Water)

1 m/s	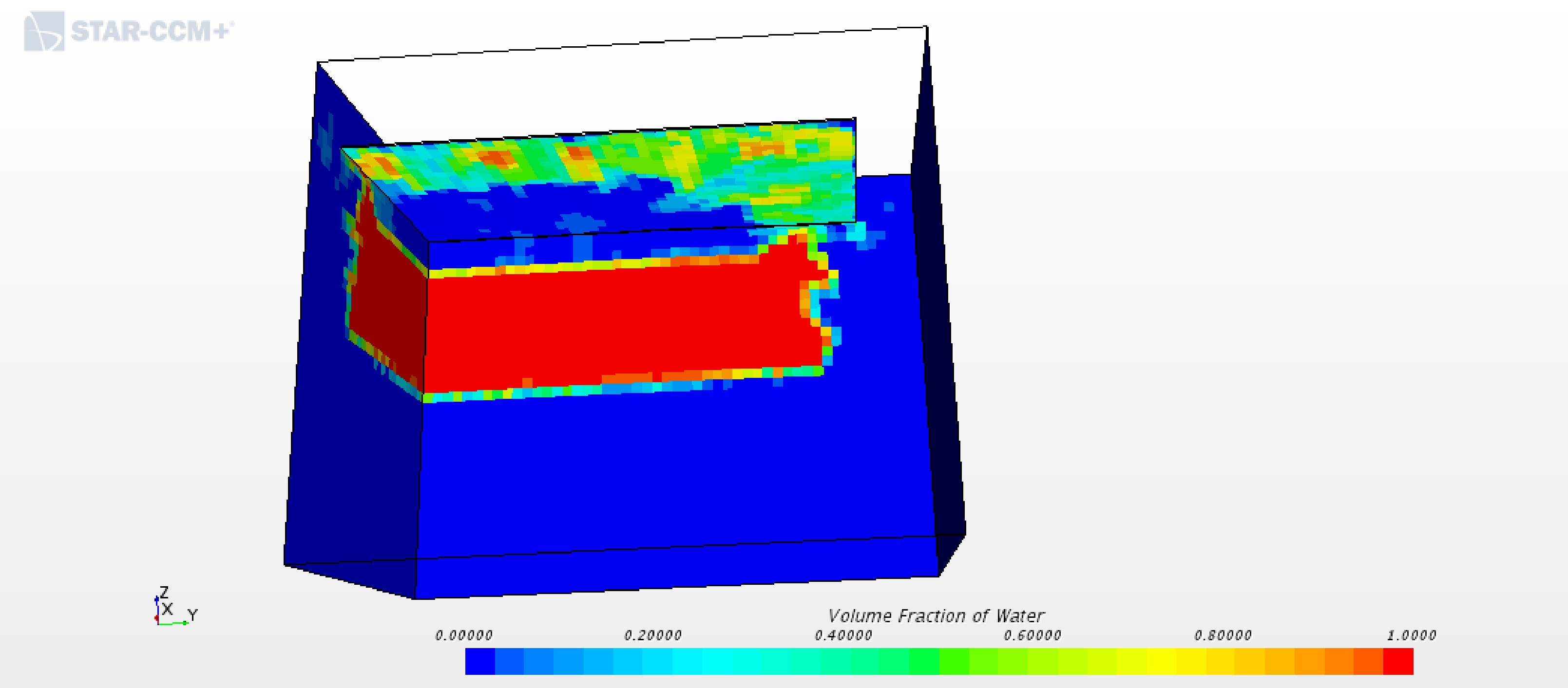

4 m/s	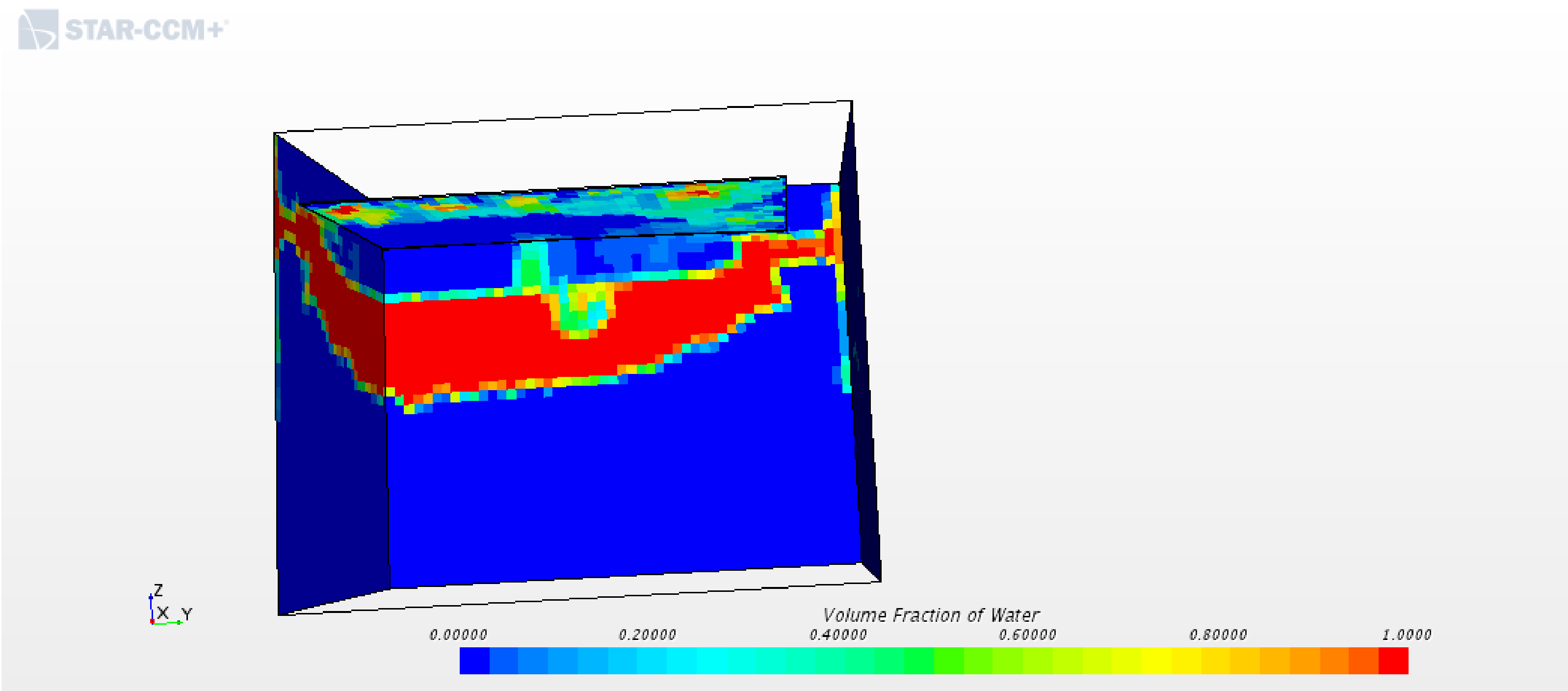 STAR-CCM+ Volume Fraction of Water 0.00000 0.20000 0.40000 0.60000 0.80000 1.0000 Z X Y

8 m/s	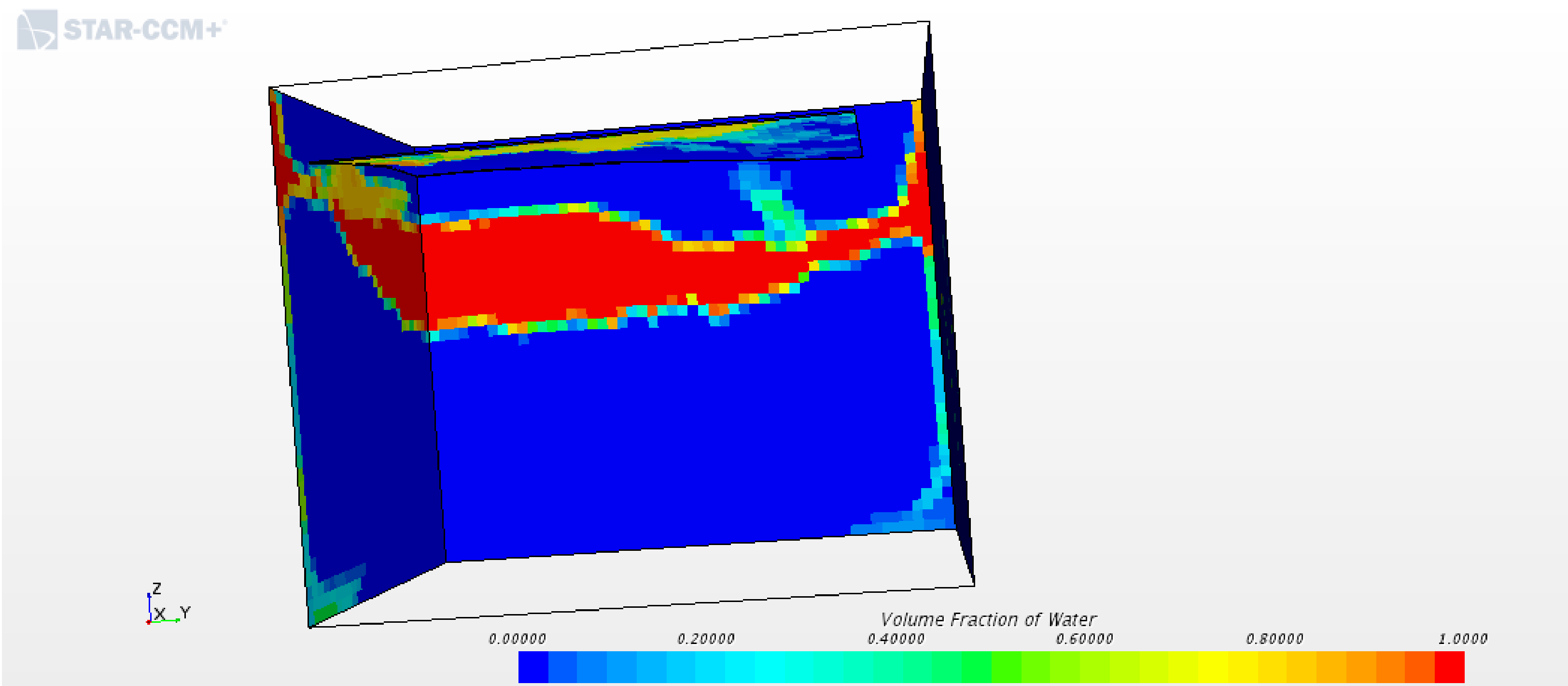

STAR-CCM+
Volume Fraction of Water
0.00000
0.20000
0.40000
0.60000
0.80000
1.0000
Z
X
Y

APPENDIX VI: SETTING AIR AS INCOMPRESSIBLE & WATER AS COMPRESSIBLE (Pressure Distribution)

1 m/s	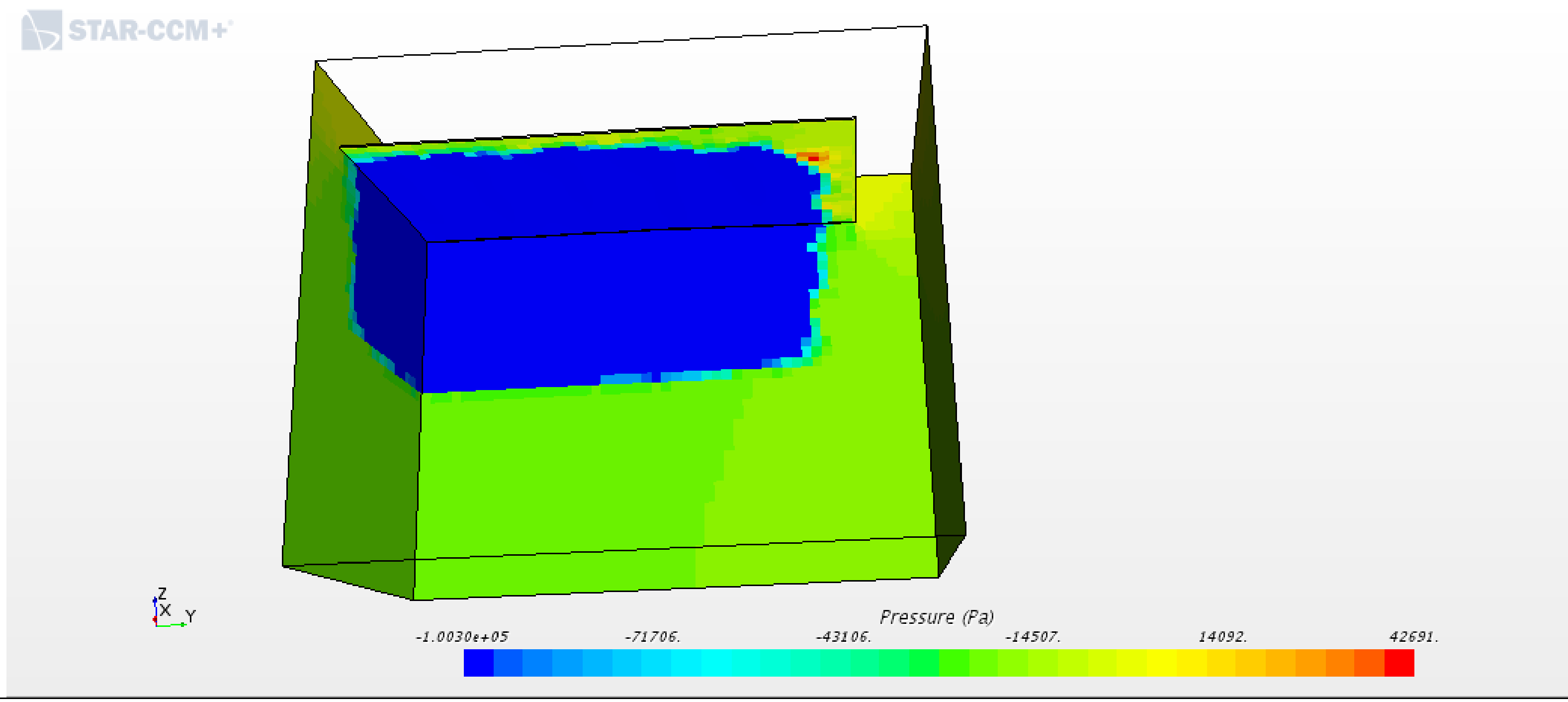

4 m/s	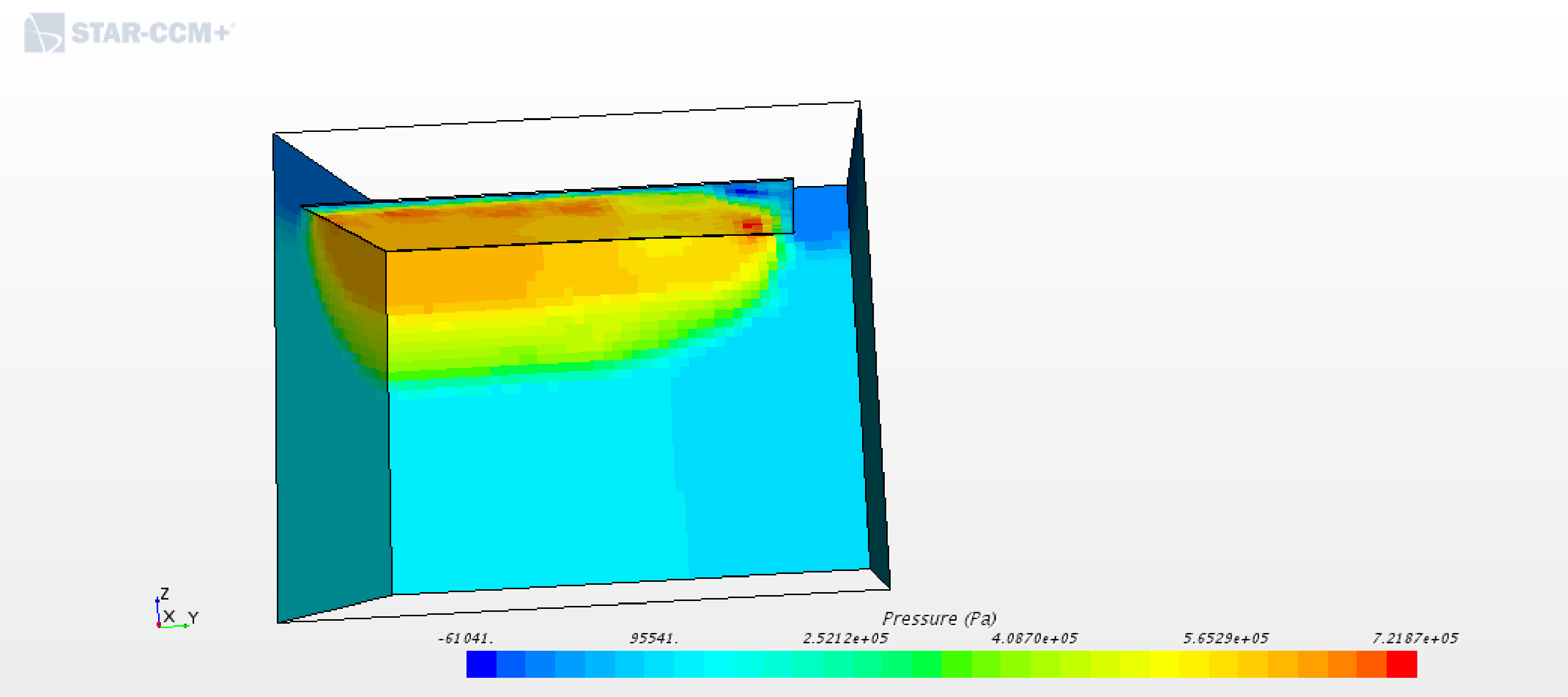 STAR-CCM+ Z X Y Pressure (Pa) -61041. 95541. 2.5212e+05 4.0870e+05 5.6529e+05 7.2187e+05

8 m/s	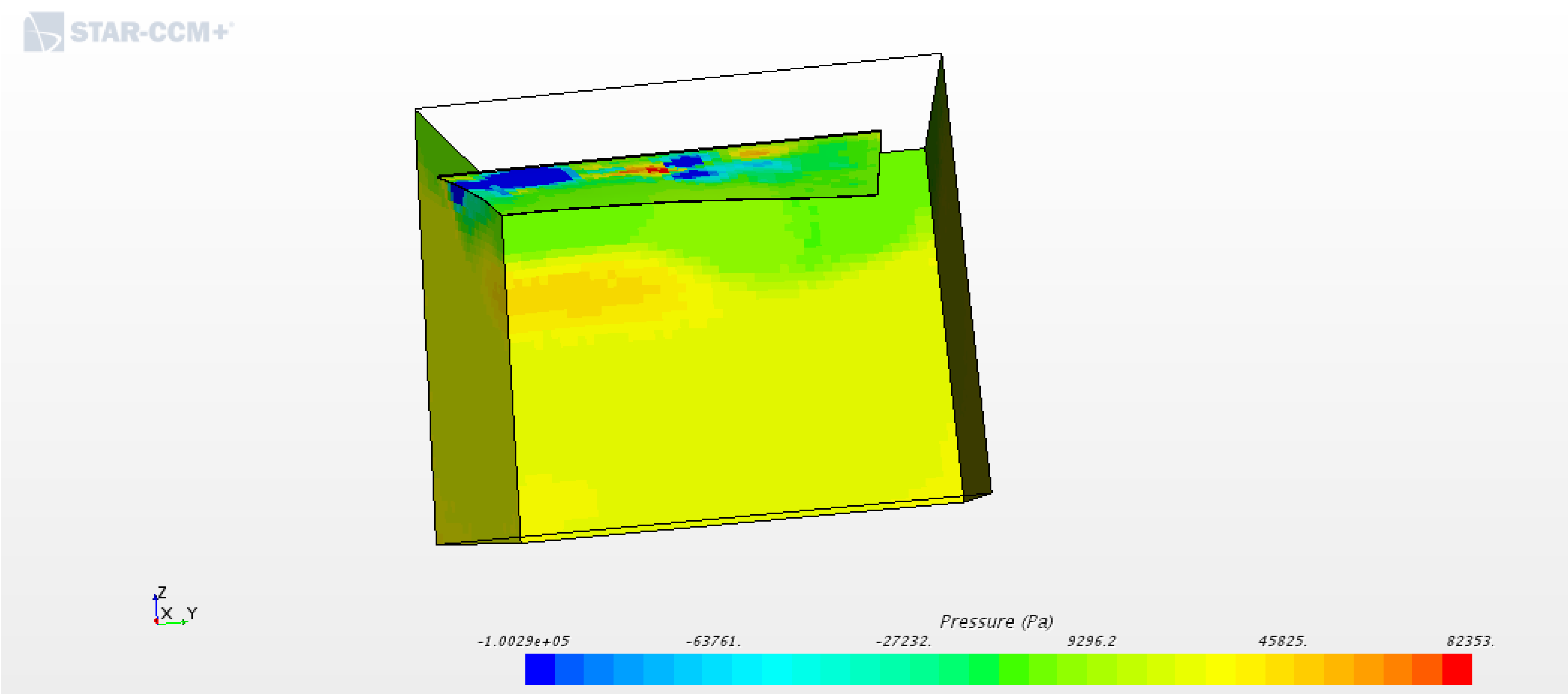STAR-CCM+ Z X Y Pressure (Pa) -1.0029e+05 -63761. -27232. 9296.2 45825. 82353.

APPENDIX VII: SETTING AIR AS INCOMPRESSIBLE & WATER AS COMPRESSIBLE (ABAQUS Solution on Plate)

1 m/s	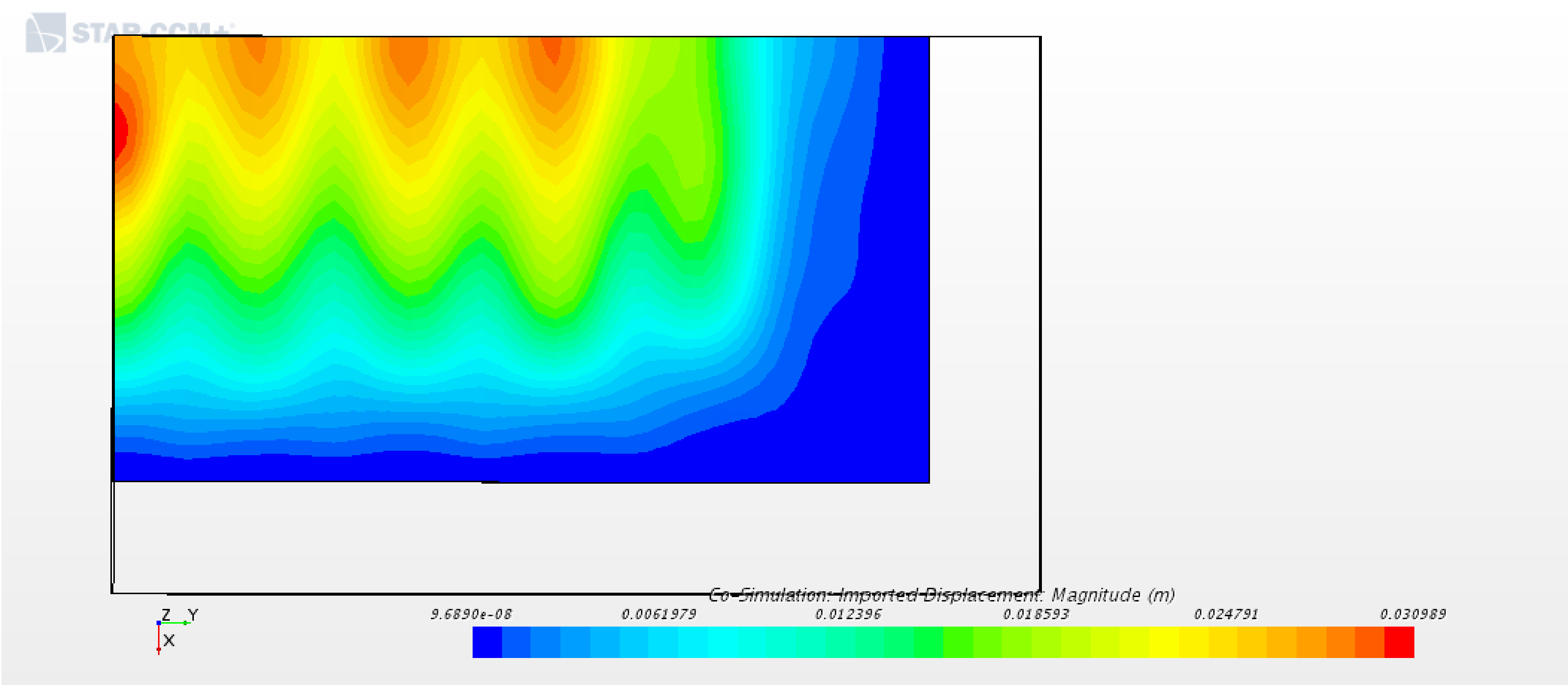

4 m/s	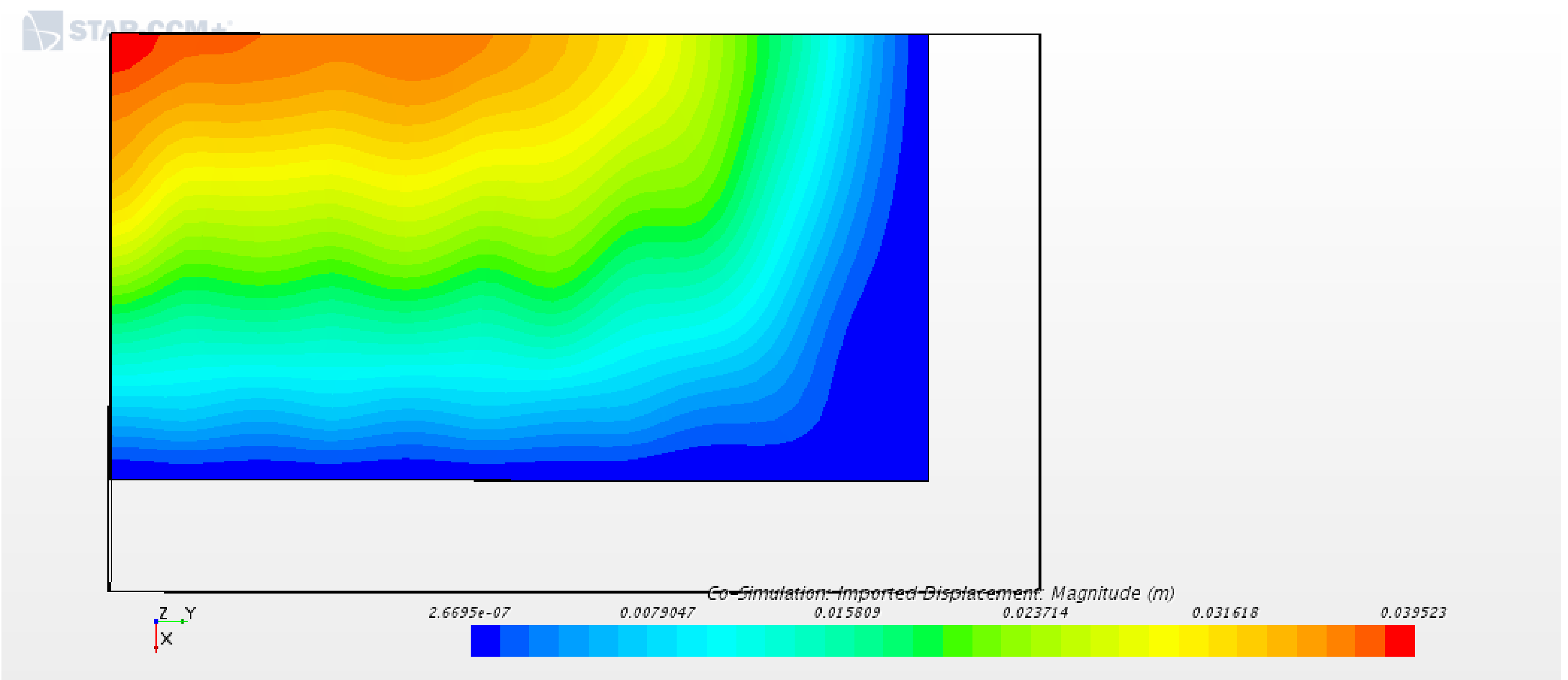STAR-CCM+ Co-Simulation: Imported Displacement: Magnitude (m) 2.6695e-07 0.0079047 0.015809 0.023714 0.031618 0.039523 Z Y X

8 m/s	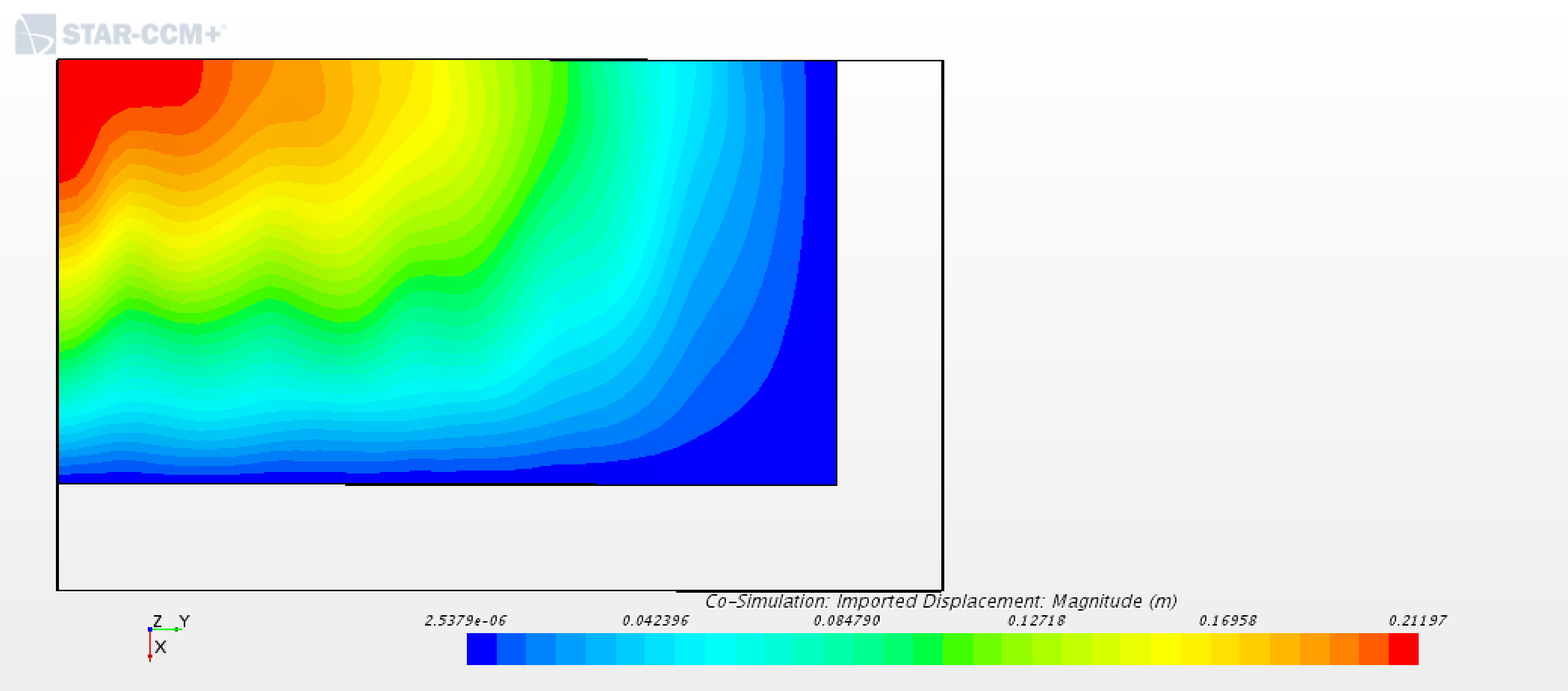STAR-CCM+ Co-Simulation: Imported Displacement: Magnitude (m) 2.5379e-06 0.042396 0.084790 0.12718 0.16958 0.21197 Z Y X

APPENDIX VIII: SETTING AIR AS COMPRESSIBLE & WATER AS COMPRESSIBLE (Force Monitor Plot)

1 m/s	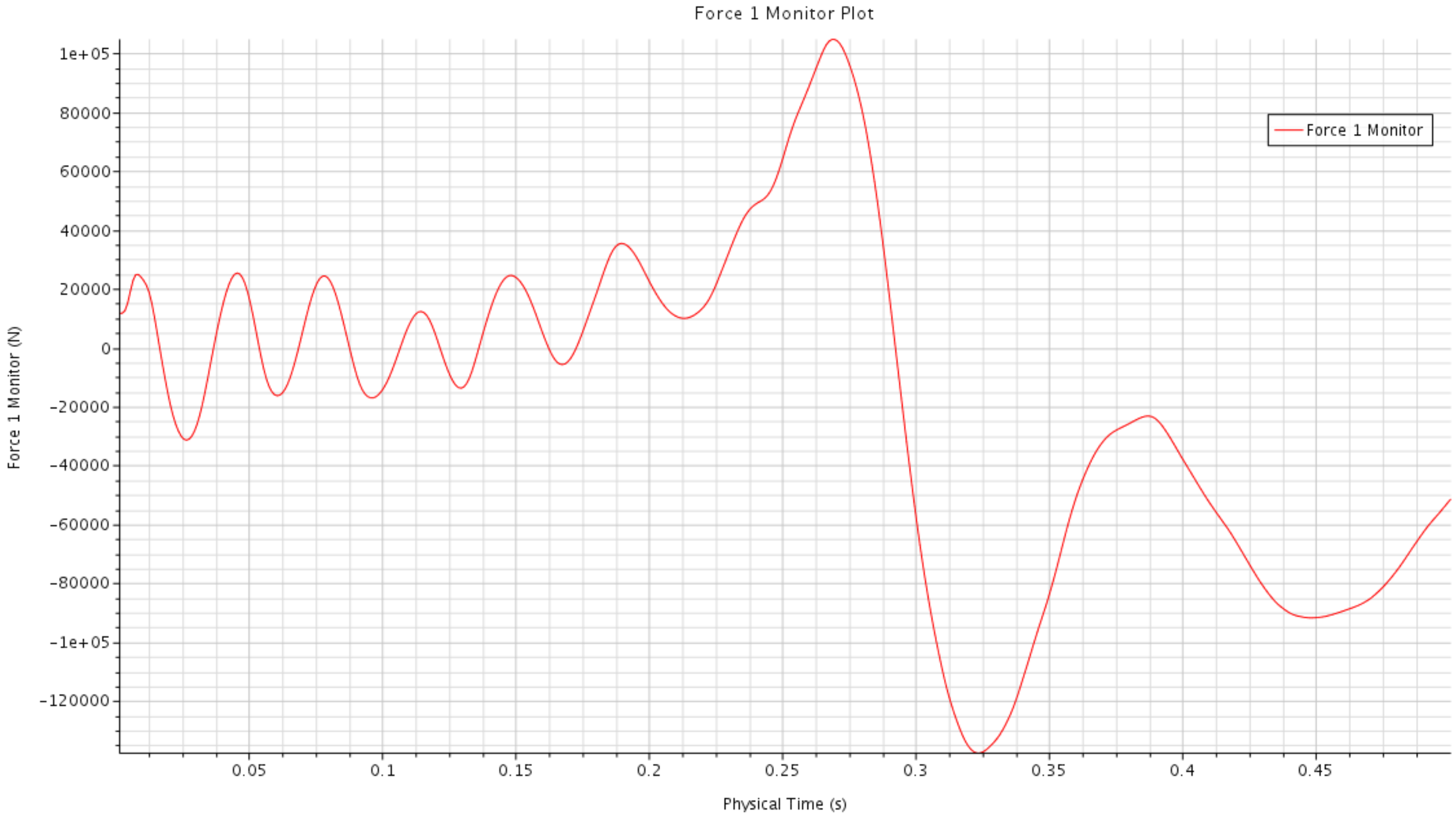

| **4 m/s** | 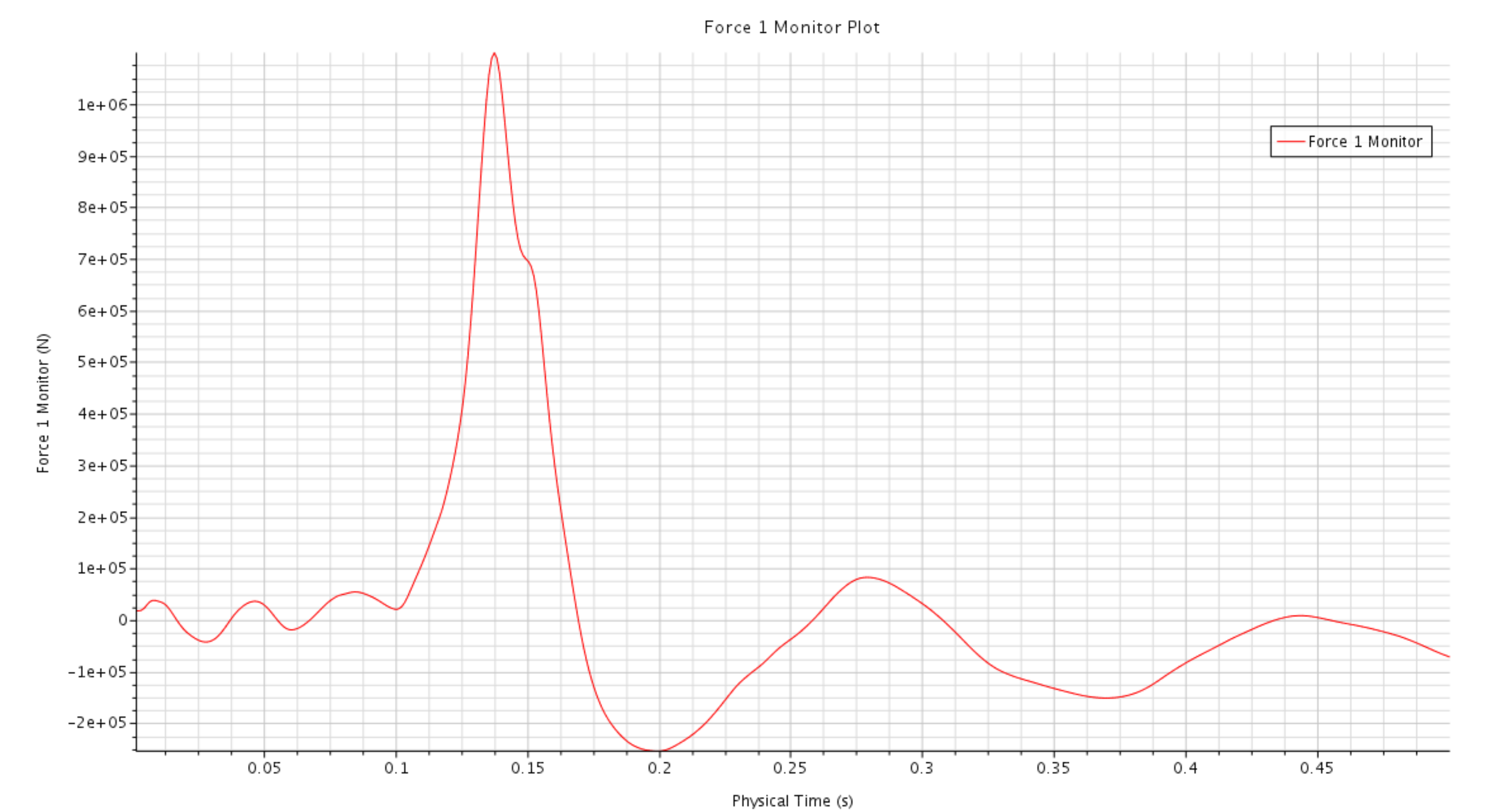Force 1 Monitor Plot
Force 1 Monitor
1e+06
9e+05
8e+05
7e+05
6e+05
5e+05
4e+05
3e+05
2e+05
1e+05
0
-1e+05
-2e+05
Force 1 Monitor (N)
0.05
0.1
0.15
0.2
0.25
0.3
0.35
0.4
0.45
Physical Time (s) |
|---|---|

8 m/s	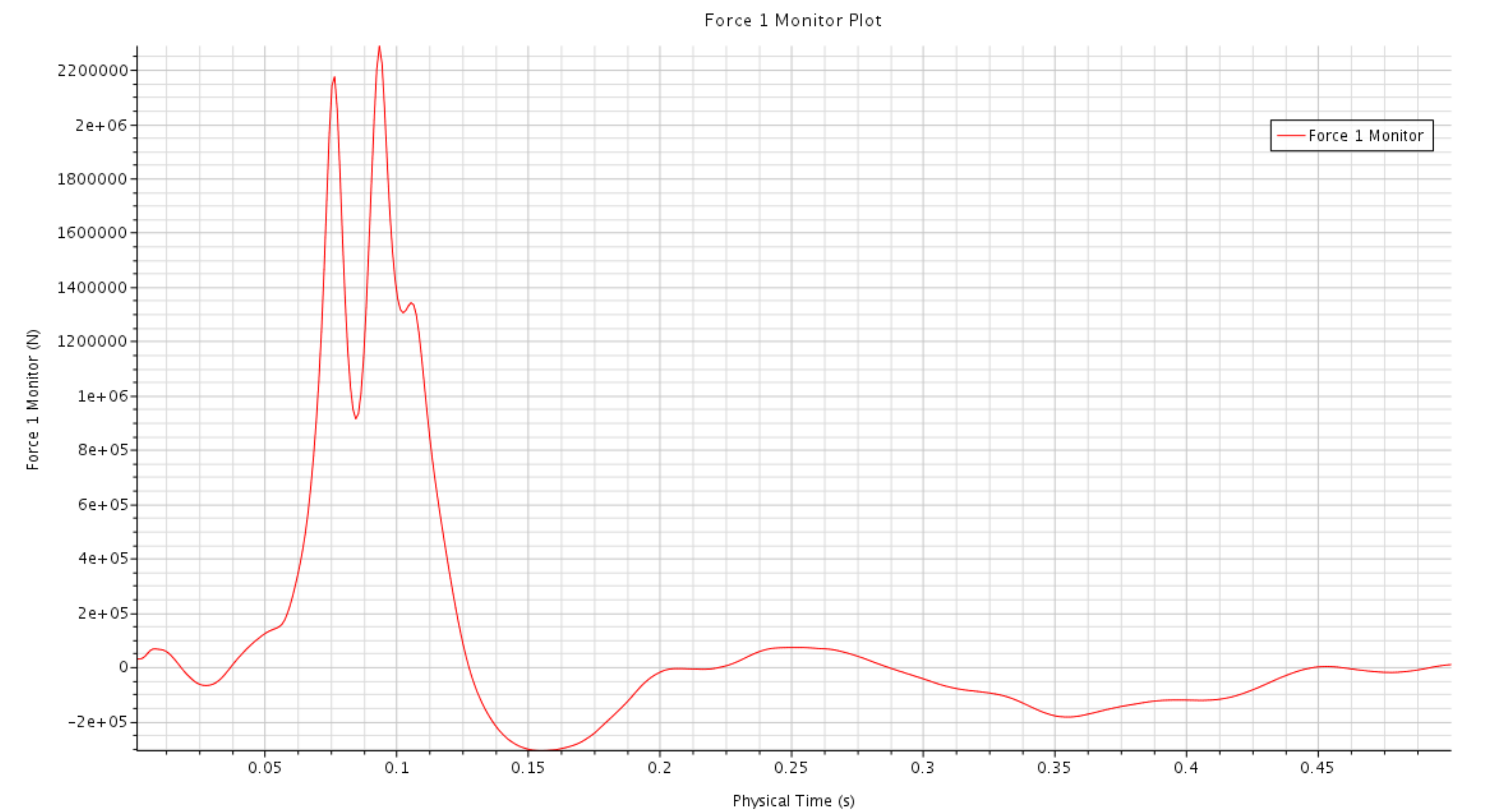

Force 1 Monitor Plot
Force 1 Monitor
Force 1 Monitor (N)
2200000
2e+06
1800000
1600000
1400000
1200000
1e+06
8e+05
6e+05
4e+05
2e+05
0
-2e+05
0.05
0.1
0.15
0.2
0.25
0.3
0.35
0.4
0.45
Physical Time (s)

APPENDIX IX: SETTING AIR AS COMPRESSIBLE & WATER AS COMPRESSIBLE (Point Monitor Plot)

1 m/s	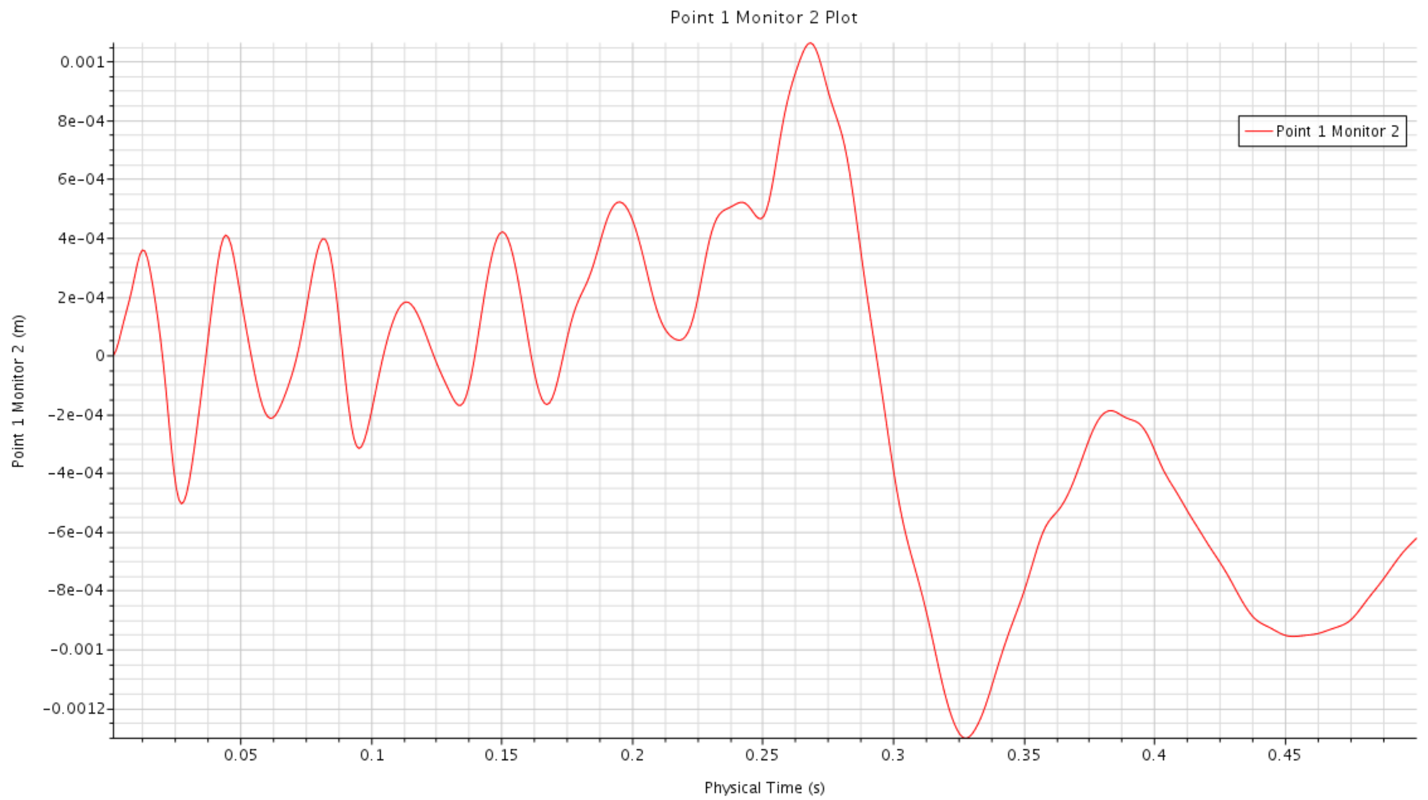

4 m/s

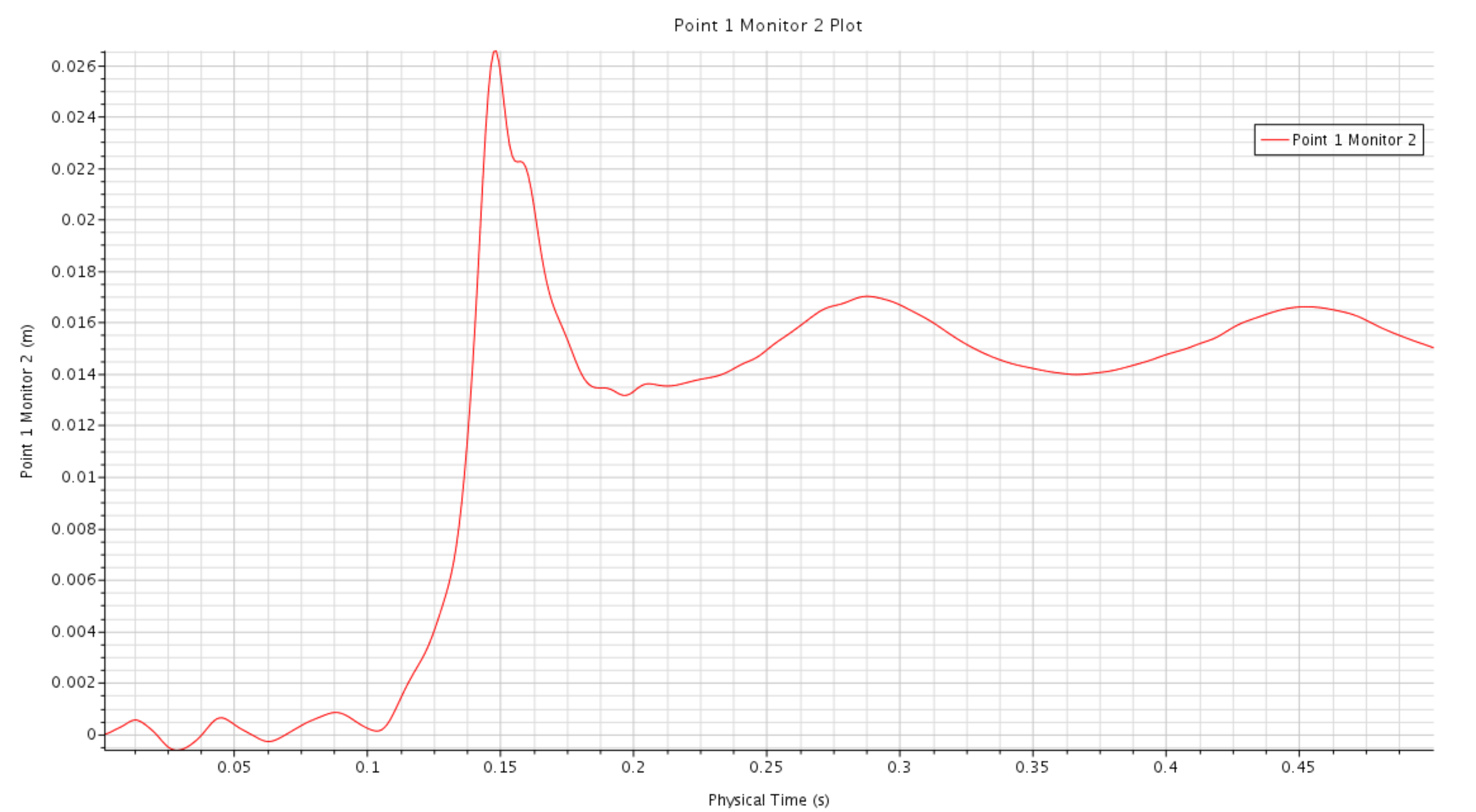

Point 1 Monitor 2 Plot
Point 1 Monitor 2
Point 1 Monitor 2 (m)
0.026
0.024
0.022
0.02
0.018
0.016
0.014
0.012
0.01
0.008
0.006
0.004
0.002
0
0.05
0.1
0.15
0.2
0.25
0.3
0.35
0.4
0.45
Physical Time (s)

8 m/s	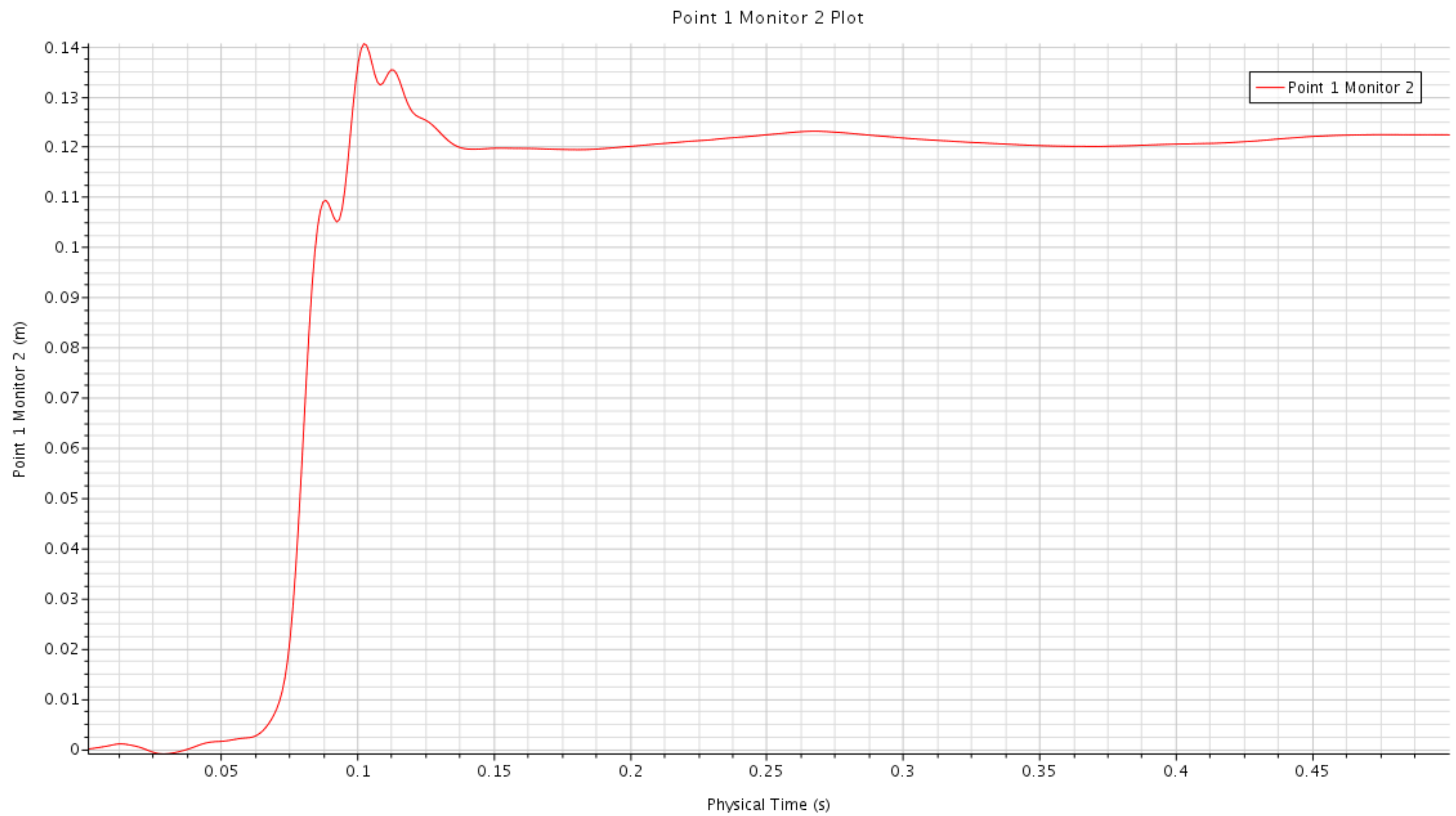 Point 1 Monitor 2 Plot Point 1 Monitor 2 Point 1 Monitor 2 (m) Physical Time (s) 0.14 0.13 0.12 0.11 0.1 0.09 0.08 0.07 0.06 0.05 0.04 0.03 0.02 0.01 0 0.05 0.1 0.15 0.2 0.25 0.3 0.35 0.4 0.45

APPENDIX X: SETTING AIR AS COMPRESSIBLE & WATER AS COMPRESSIBLE (Vector Plot)

1 m/s	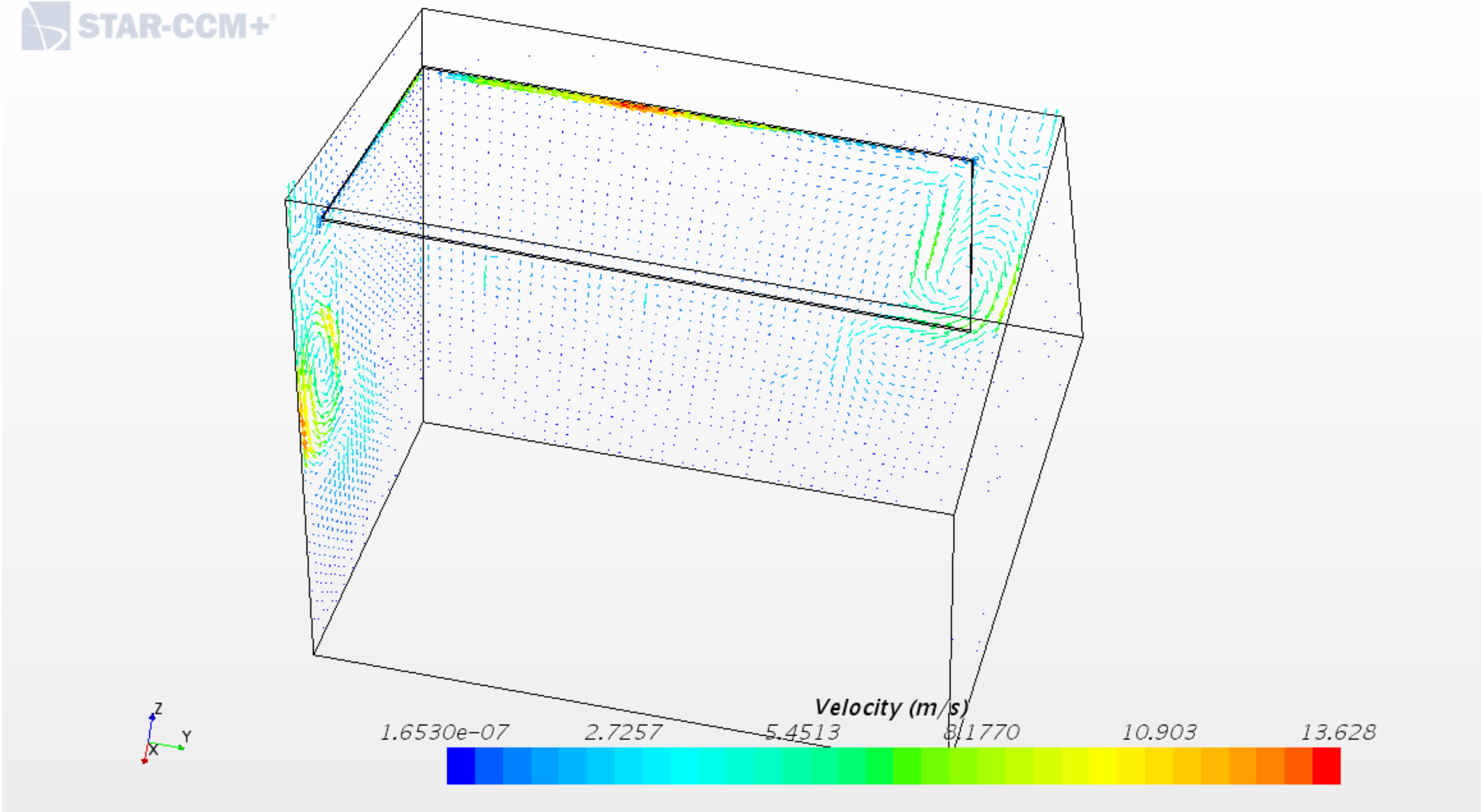

4 m/s	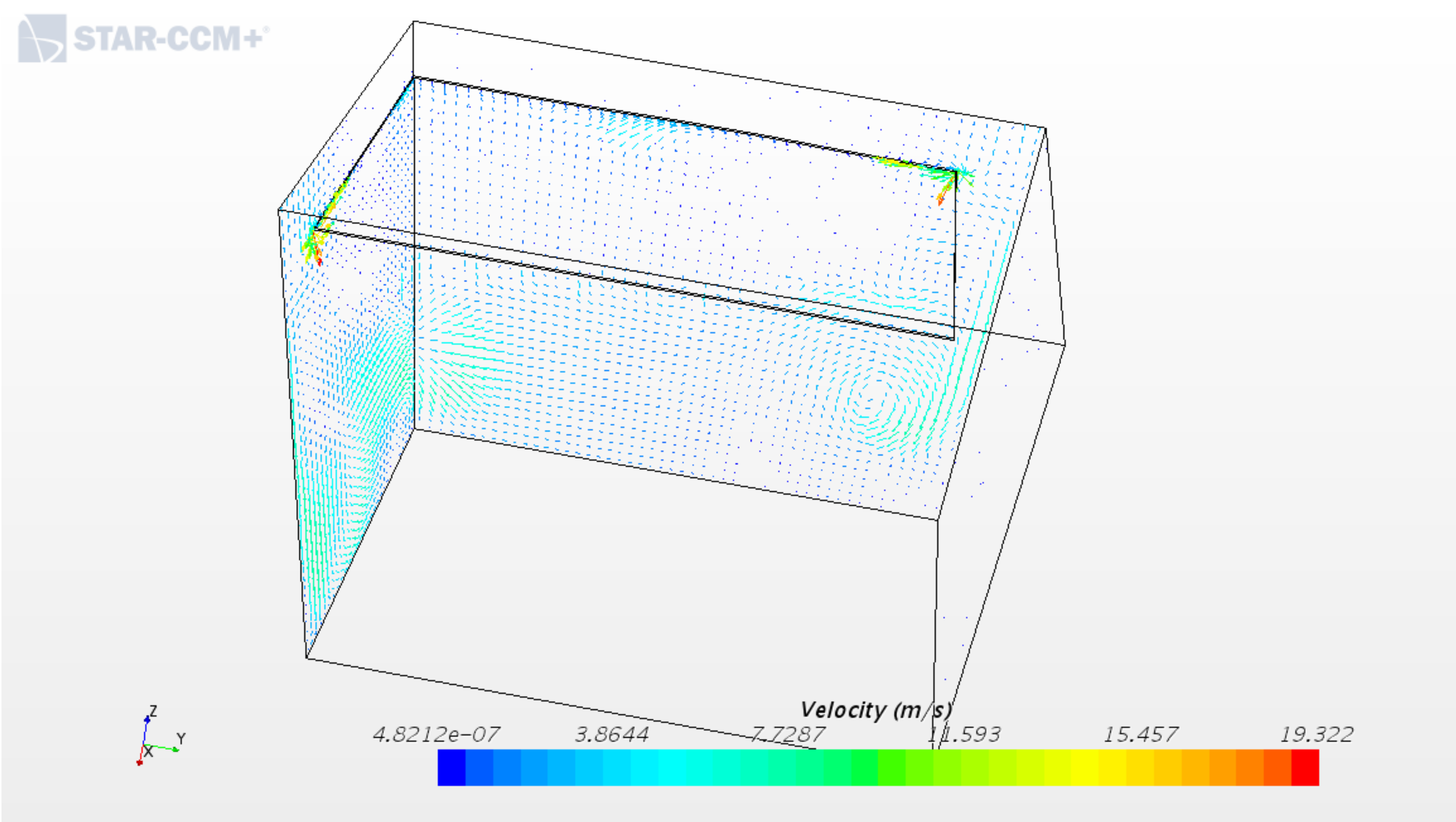STAR-CCM+ Velocity (m/s) 4.8212e-07 3.8644 7.7287 11.593 15.457 19.322 Z Y X

8 m/s	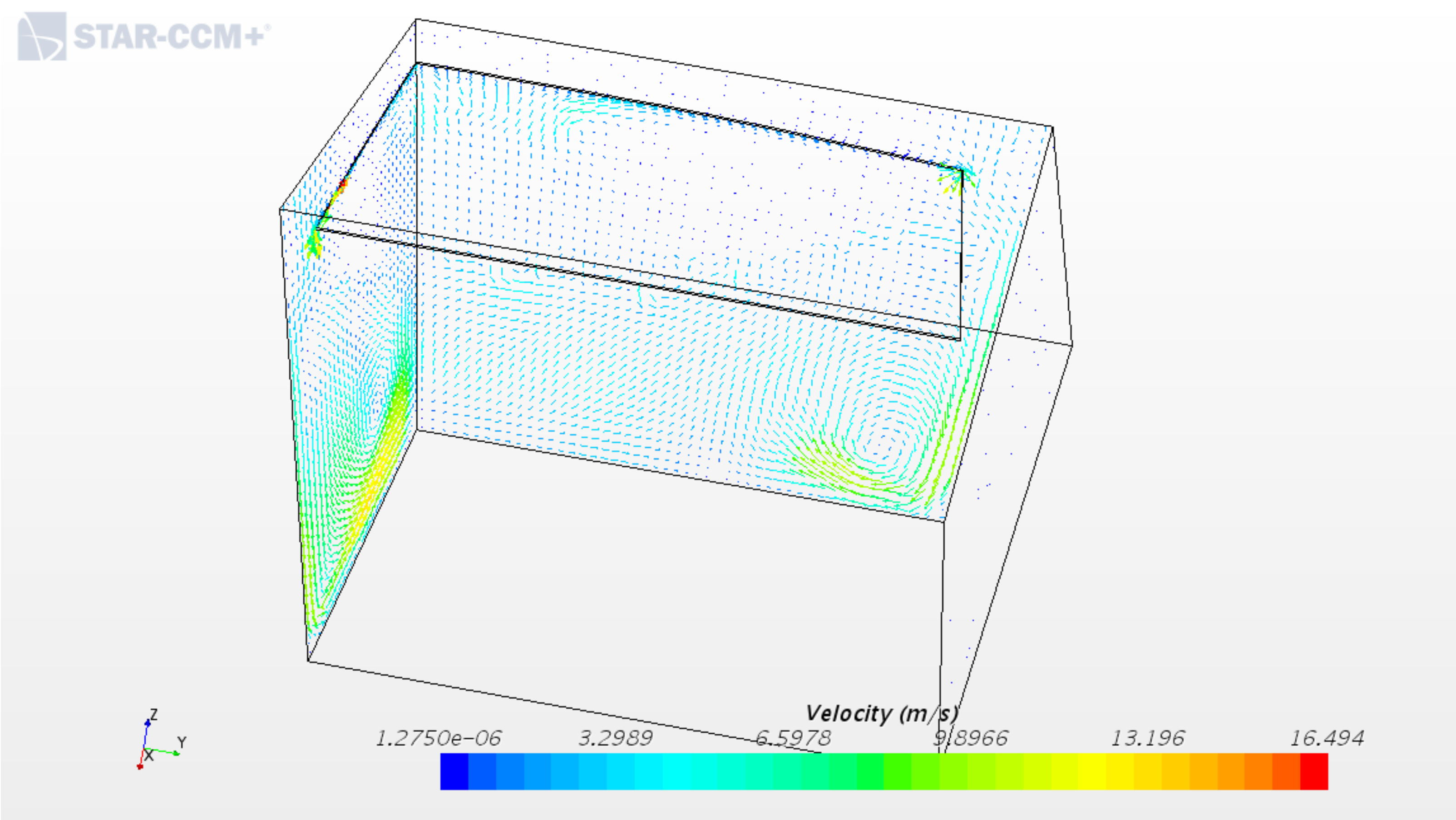STAR-CCM+ Velocity (m/s) 1.2750e-06 3.2989 6.5978 9.8966 13.196 16.494 Z Y X

APPENDIX XI: SETTING AIR AS COMPRESSIBLE & WATER AS COMPRESSIBLE (Volume Fraction of Air)

1 m/s	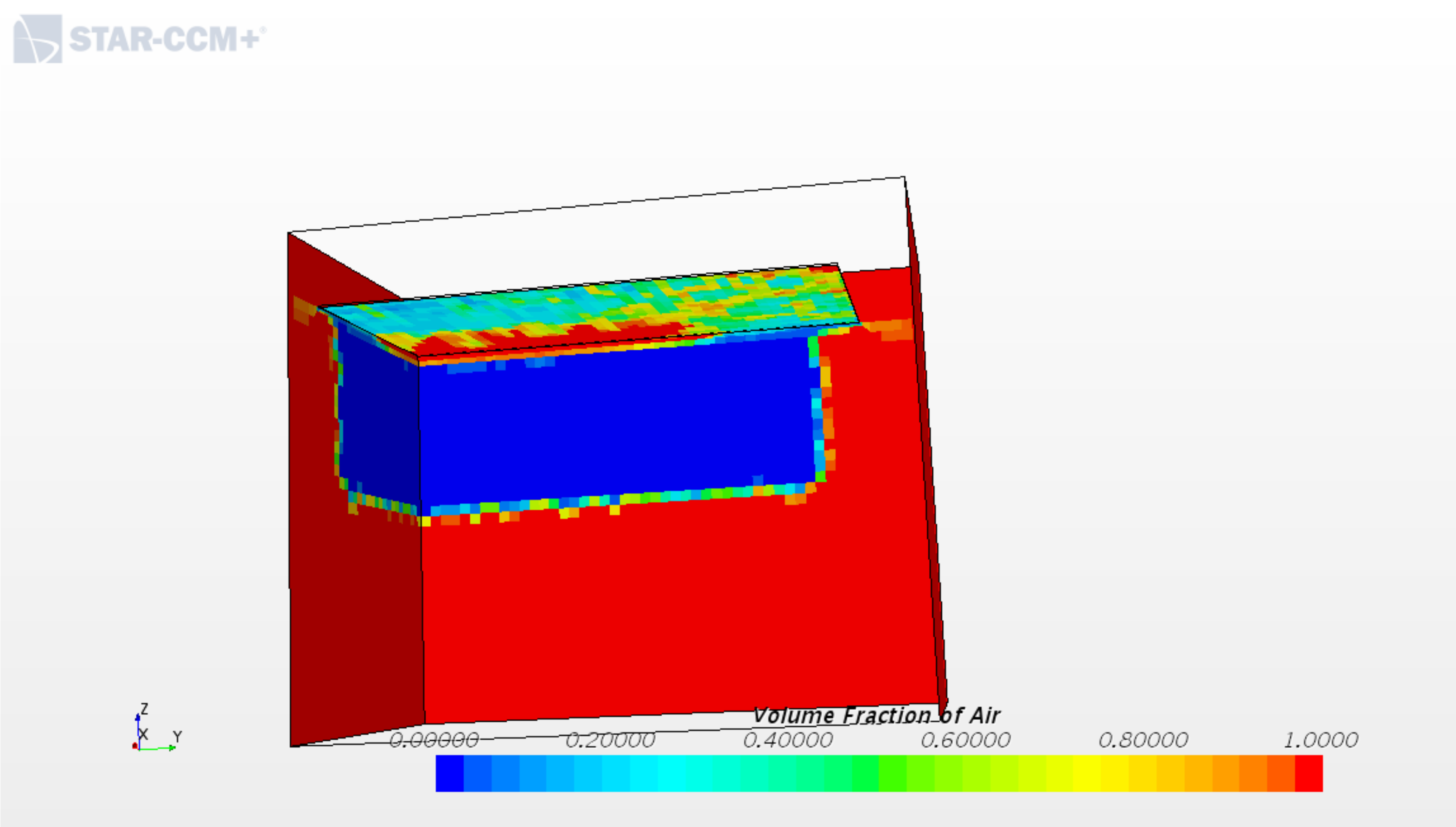

4 m/s	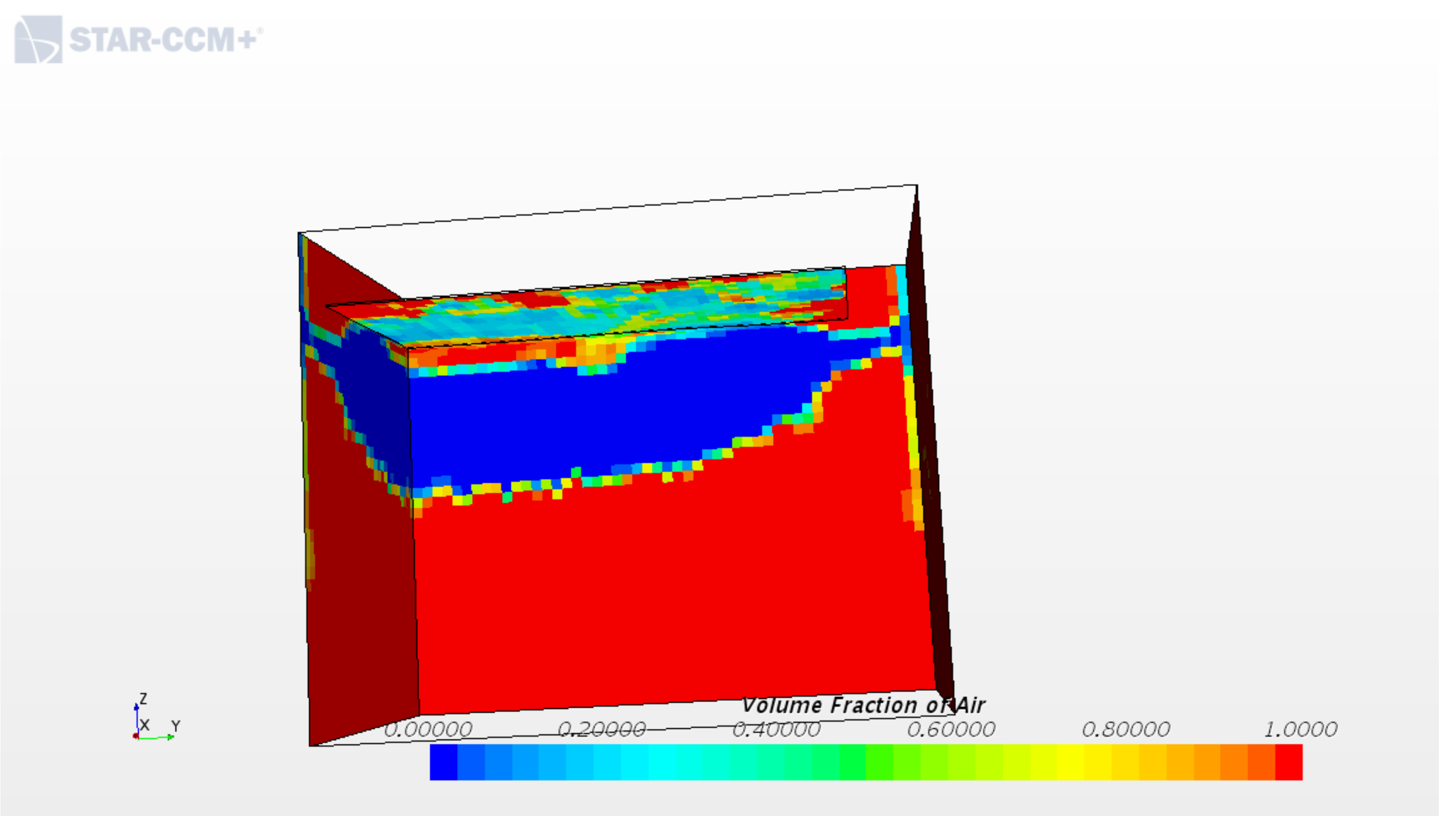STAR-CCM+
Volume Fraction of Air
0.00000
0.20000
0.40000
0.60000
0.80000
1.0000
Z
X
Y

8 m/s	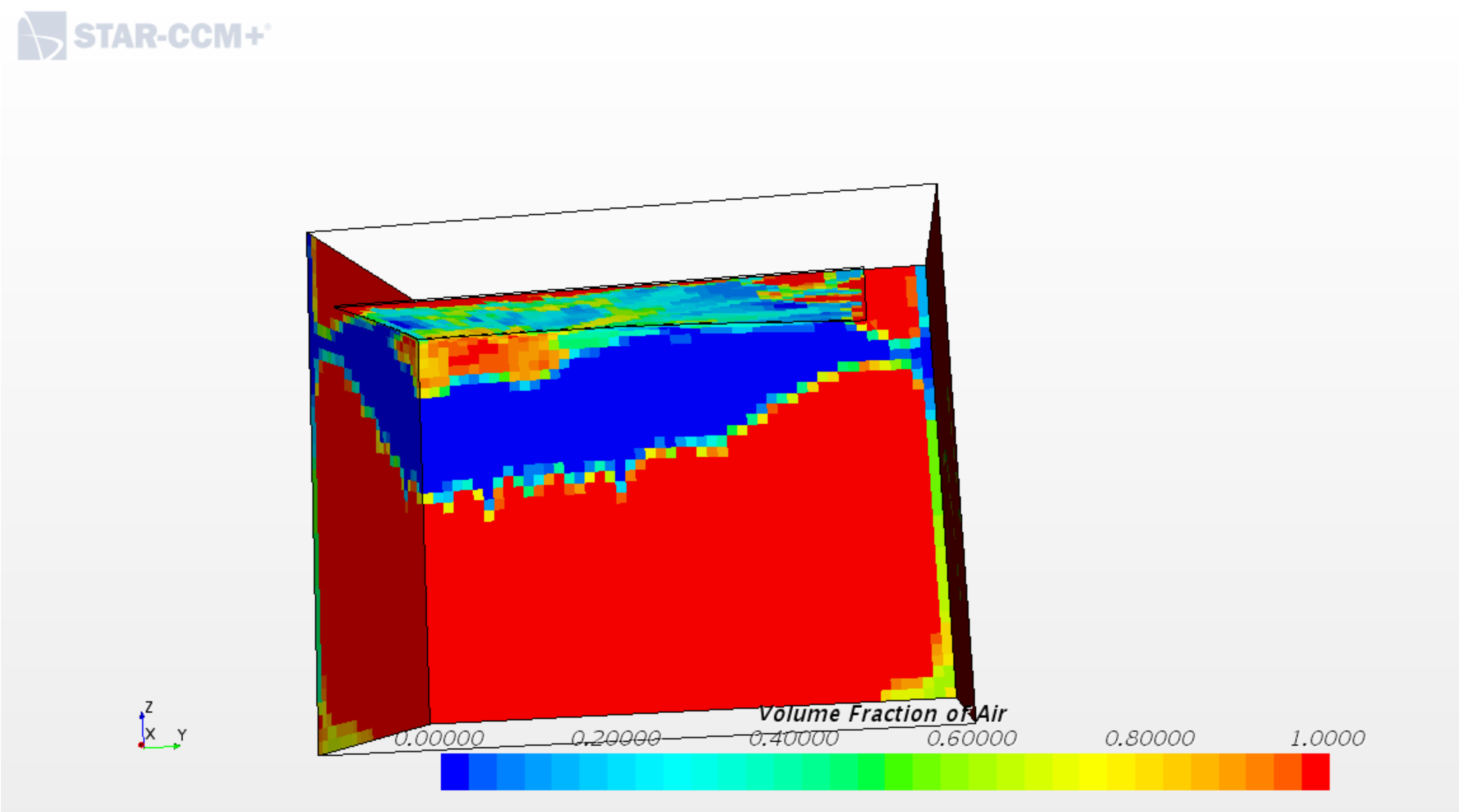STAR-CCM+
Volume Fraction of Air
0.00000
0.20000
0.40000
0.60000
0.80000
1.0000
Z
X
Y

APPENDIX XII: SETTING AIR AS COMPRESSIBLE & WATER AS COMPRESSIBLE (Volume Fraction of Water)

1 m/s	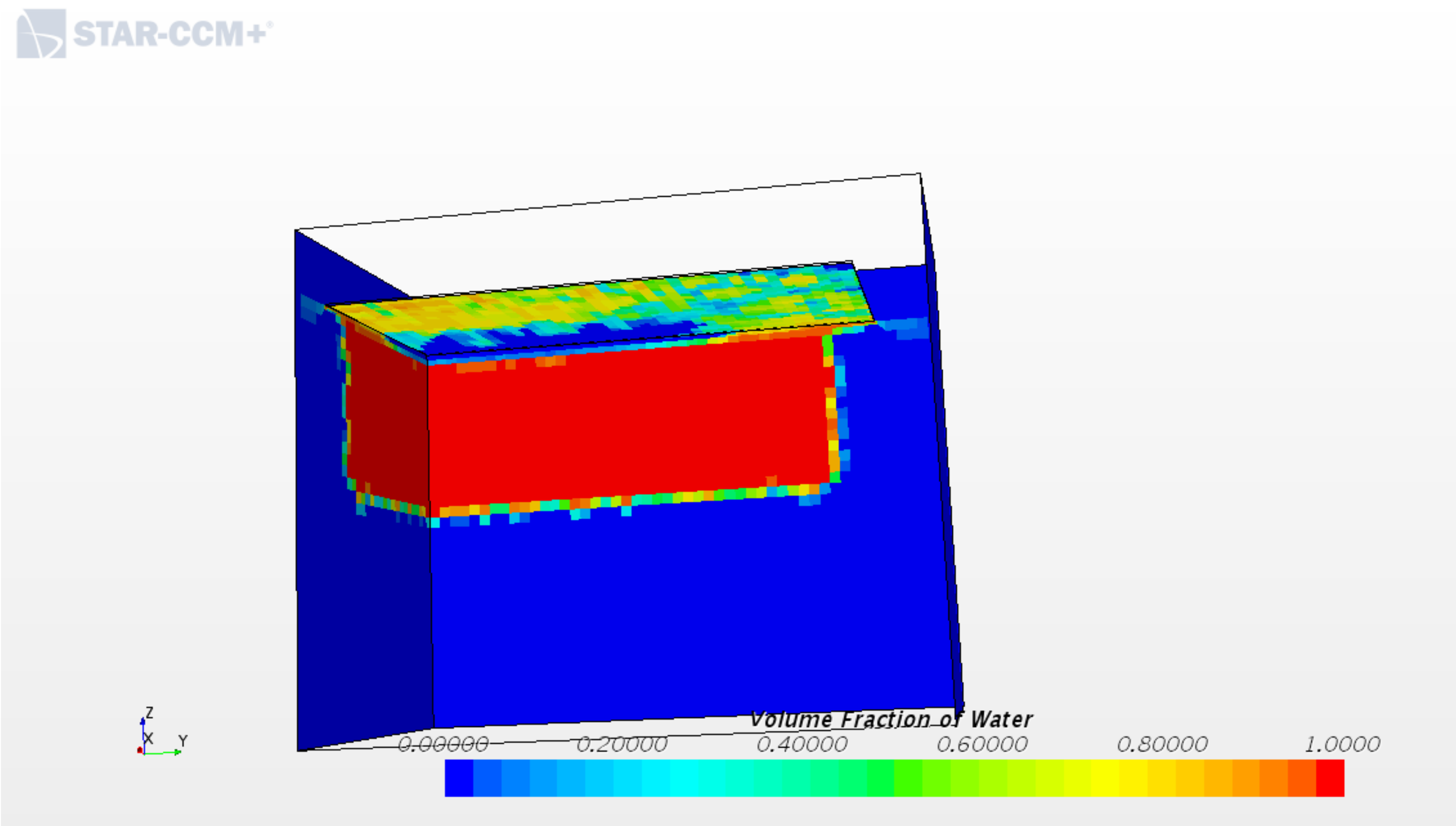

4 m/s	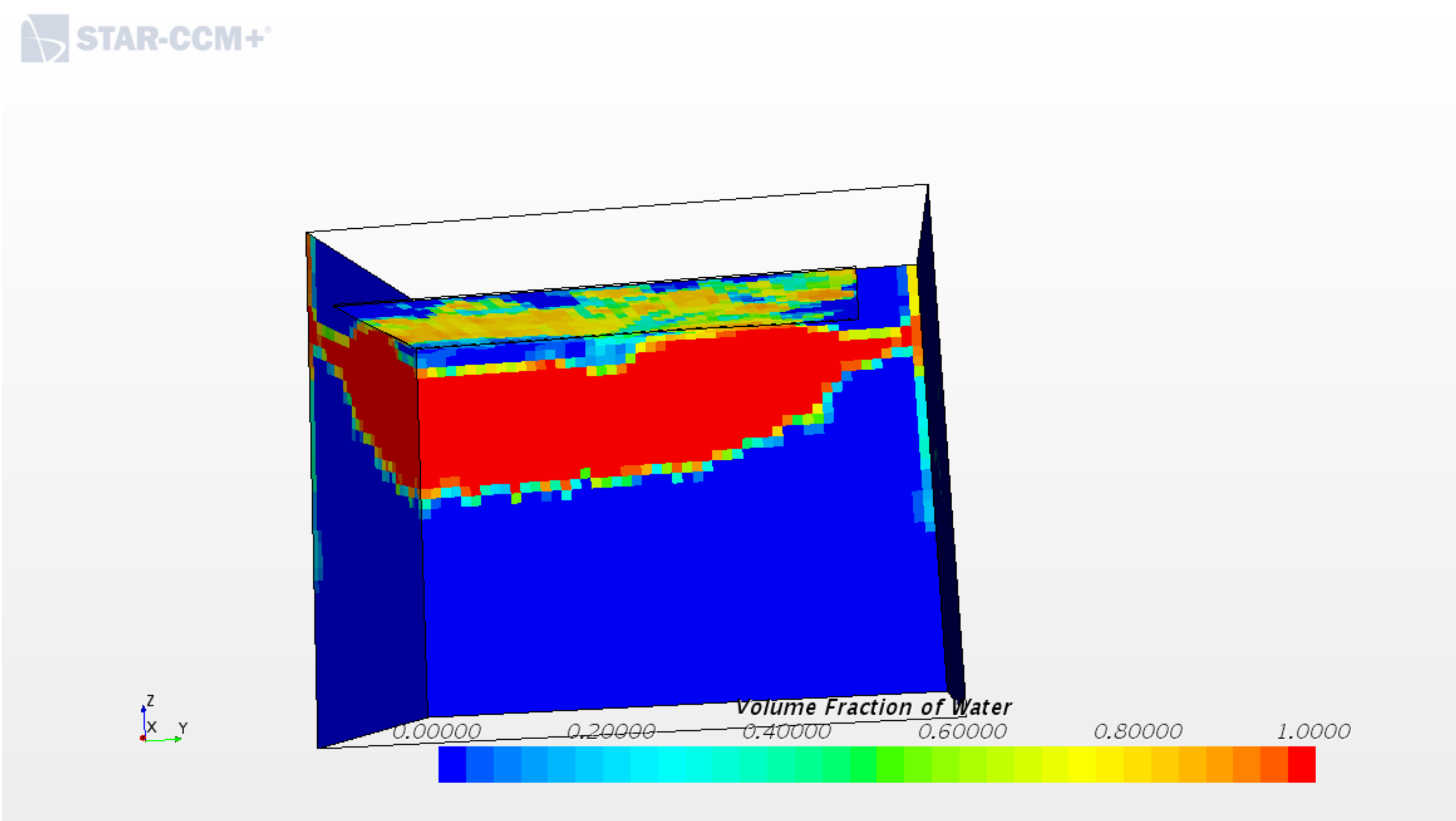Volume Fraction of Water 0.00000 0.20000 0.40000 0.60000 0.80000 1.0000 Z X Y

8 m/s	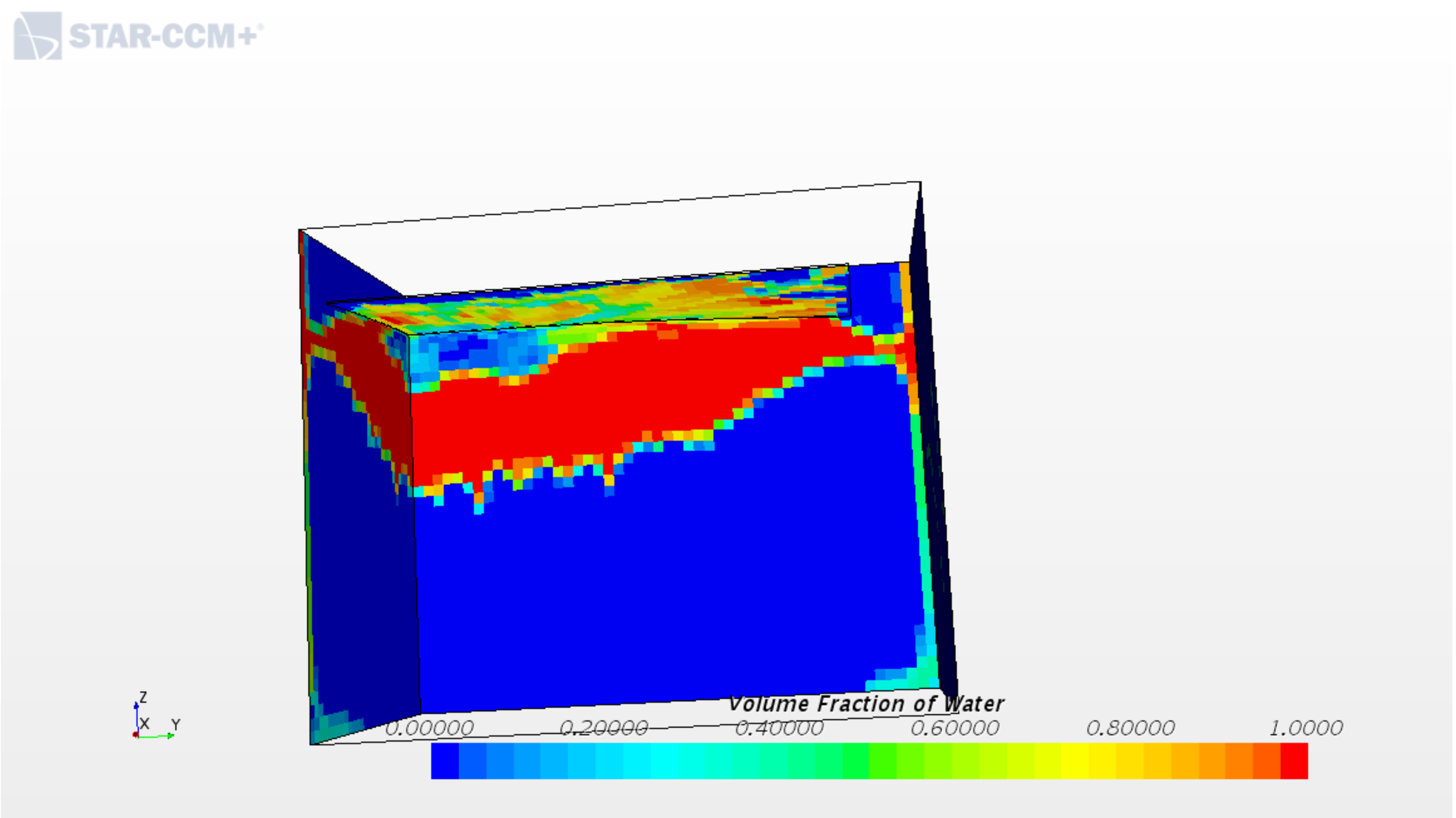STAR-CCM+ Volume Fraction of Water 0.00000 0.20000 0.40000 0.60000 0.80000 1.0000 Z X Y

APPENDIX XIII: SETTING AIR AS COMPRESSIBLE & WATER AS COMPRESSIBLE (Pressure Distribution)

1 m/s	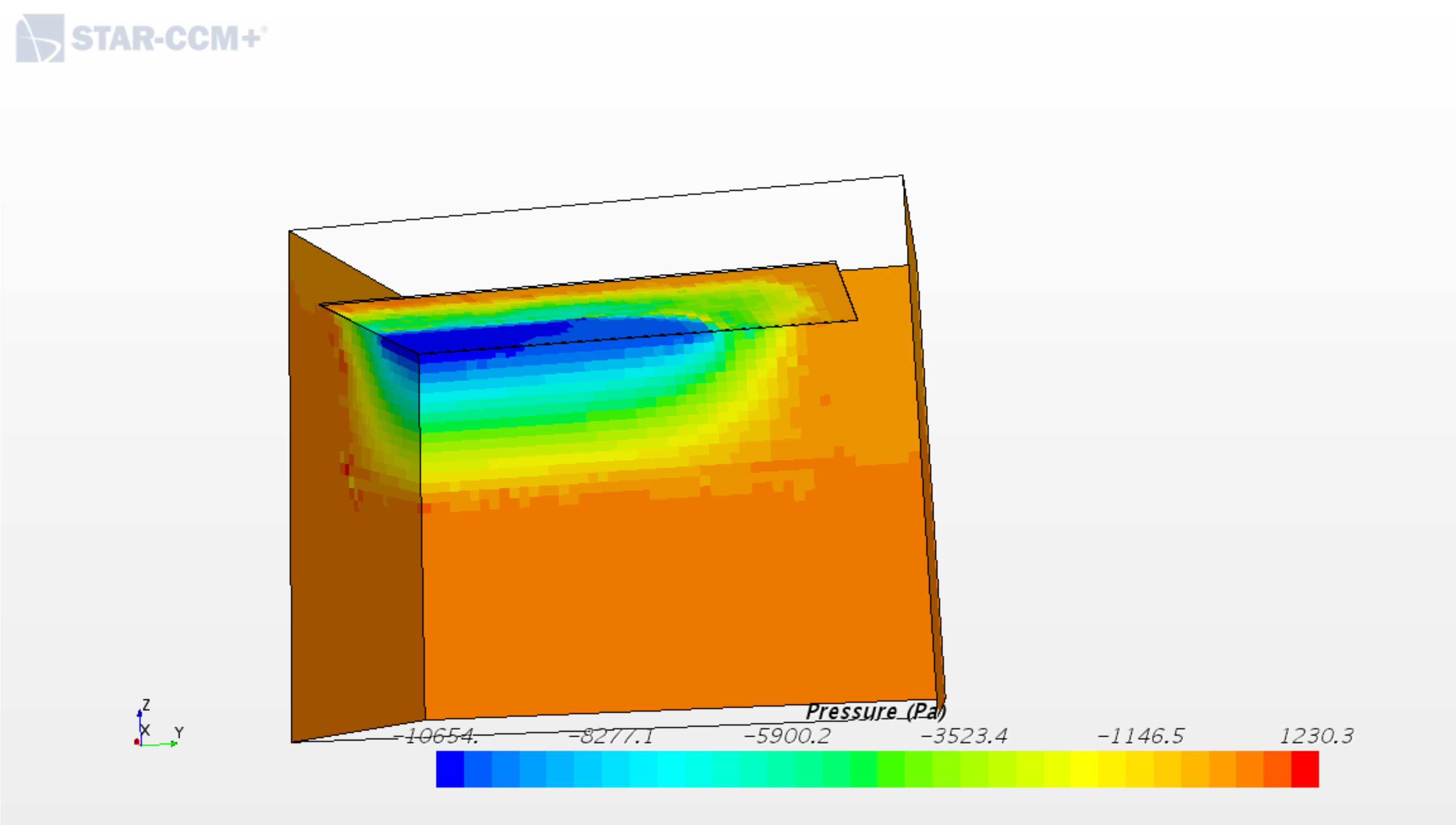

4 m/s	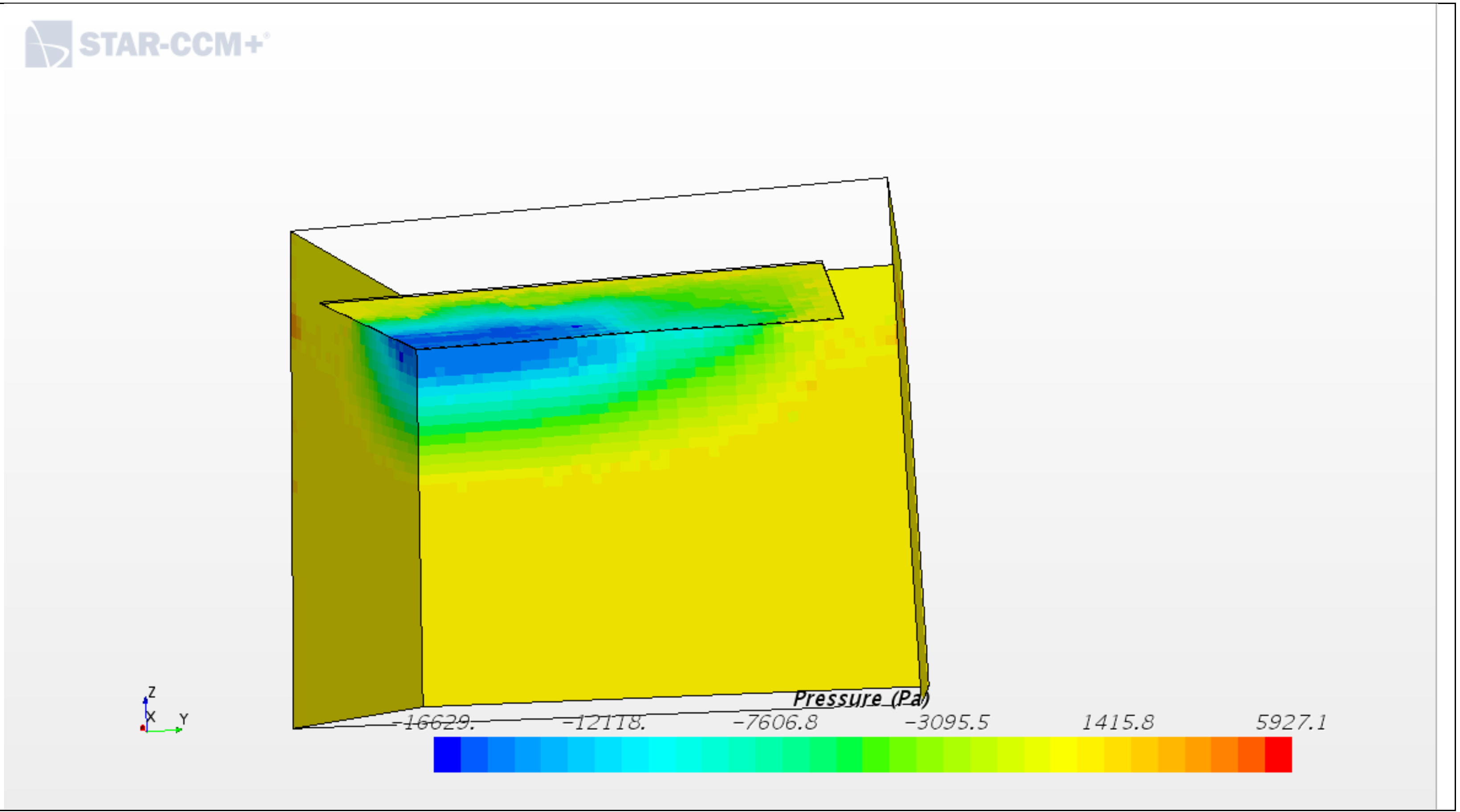STAR-CCM+ Pressure (Pa) -16629. -12118. -7606.8 -3095.5 1415.8 5927.1 Z X Y

8 m/s	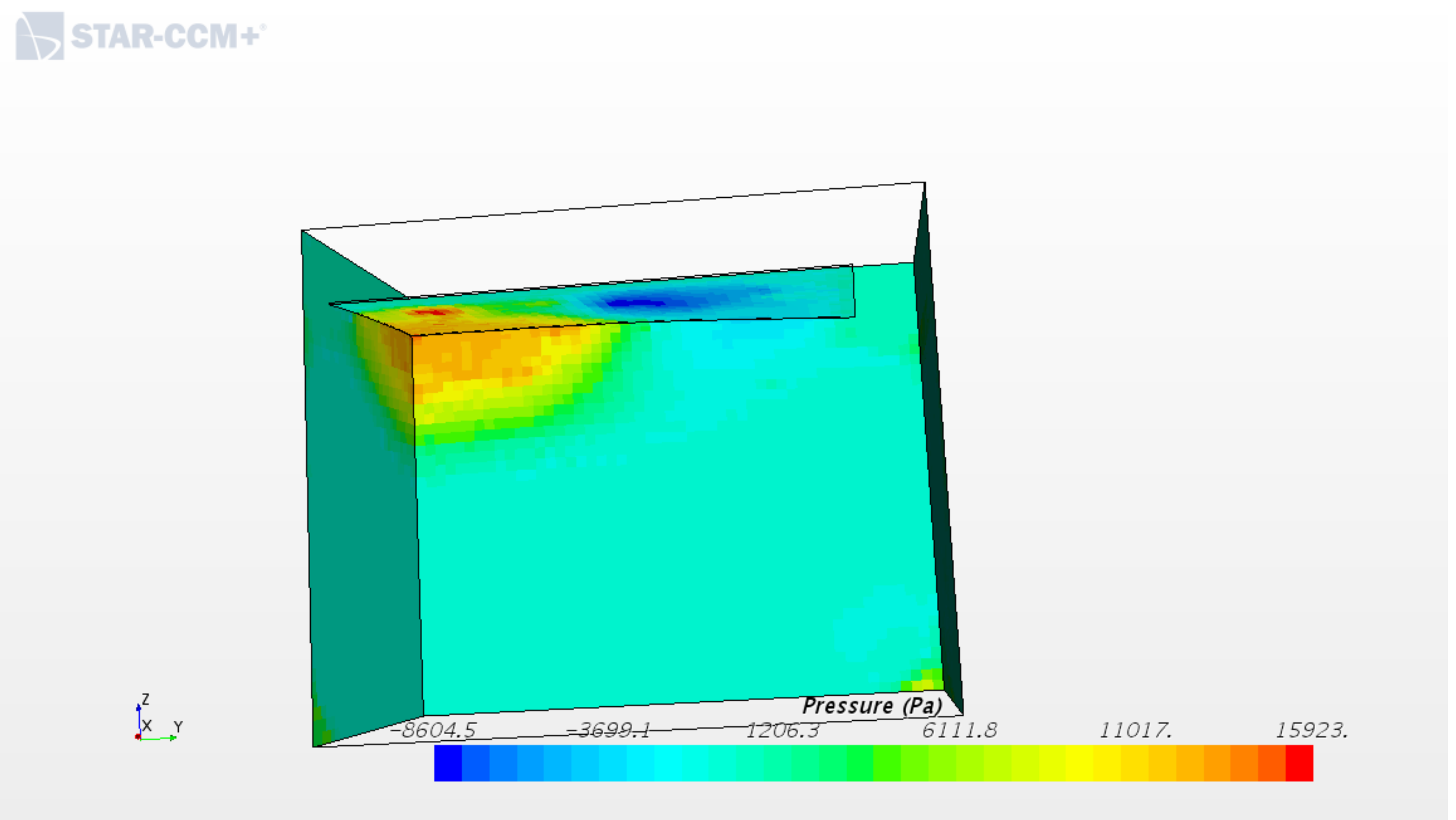 STAR-CCM+ Pressure (Pa) -8604.5 -3699.1 1206.3 6111.8 11017. 15923. Z X Y

APPENDIX XIV: SETTING AIR AS COMPRESSIBLE & WATER AS COMPRESSIBLE (ABAQUS Solution on Plate)

1 m/s	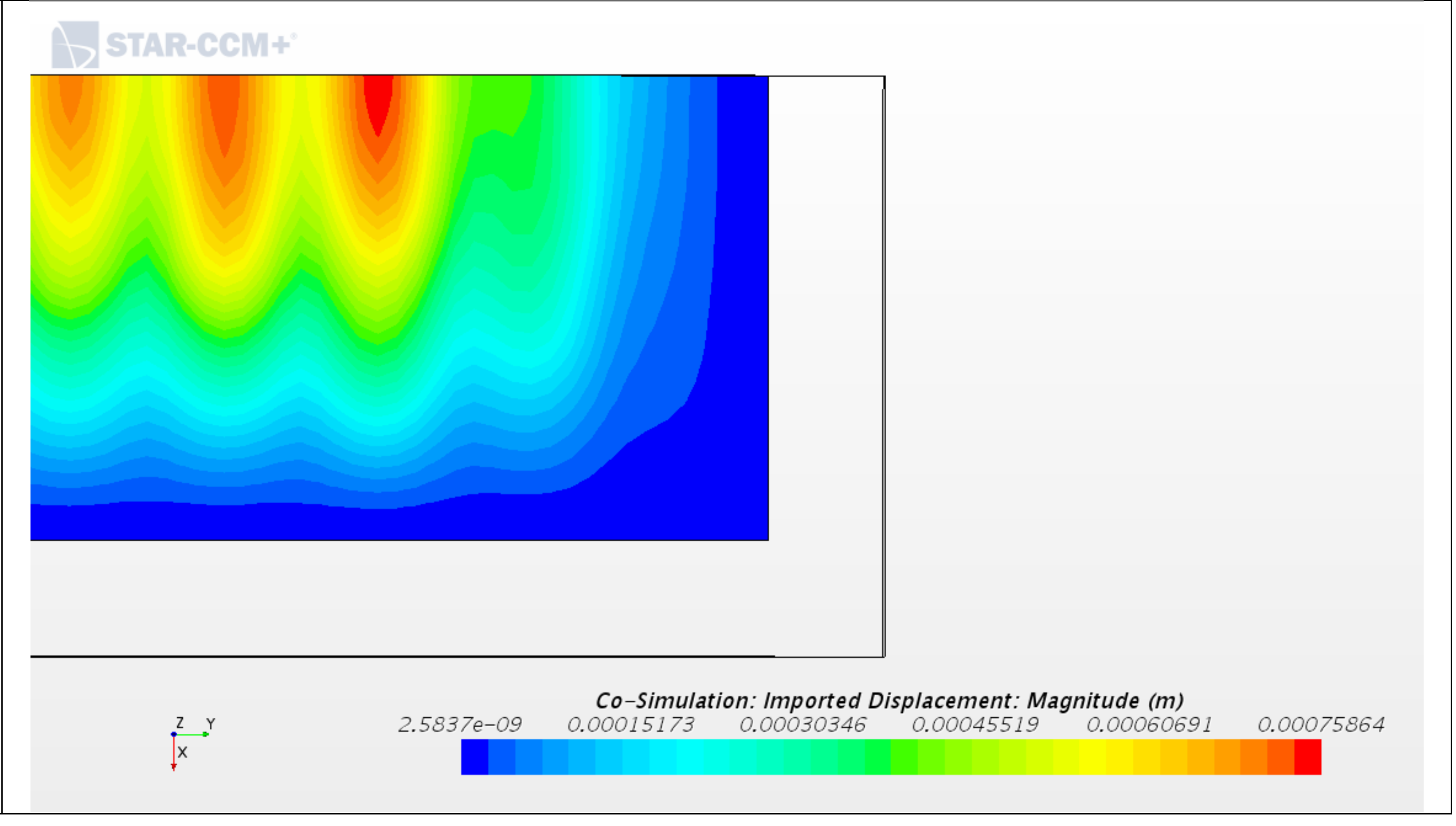

4 m/s	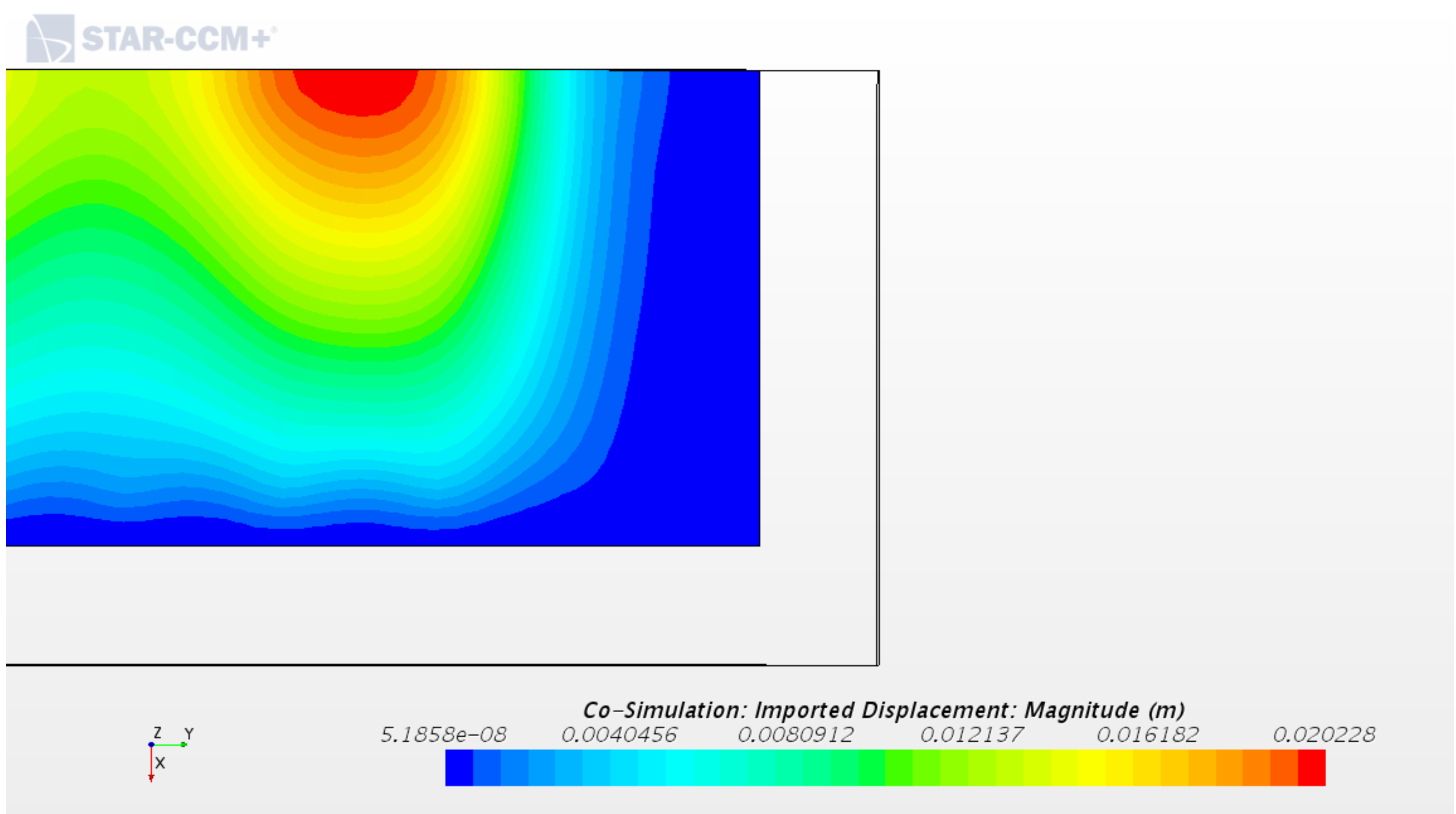STAR-CCM+ Co-Simulation: Imported Displacement: Magnitude (m) 5.1858e-08 0.0040456 0.0080912 0.012137 0.016182 0.020228 Z Y X

8 m/s	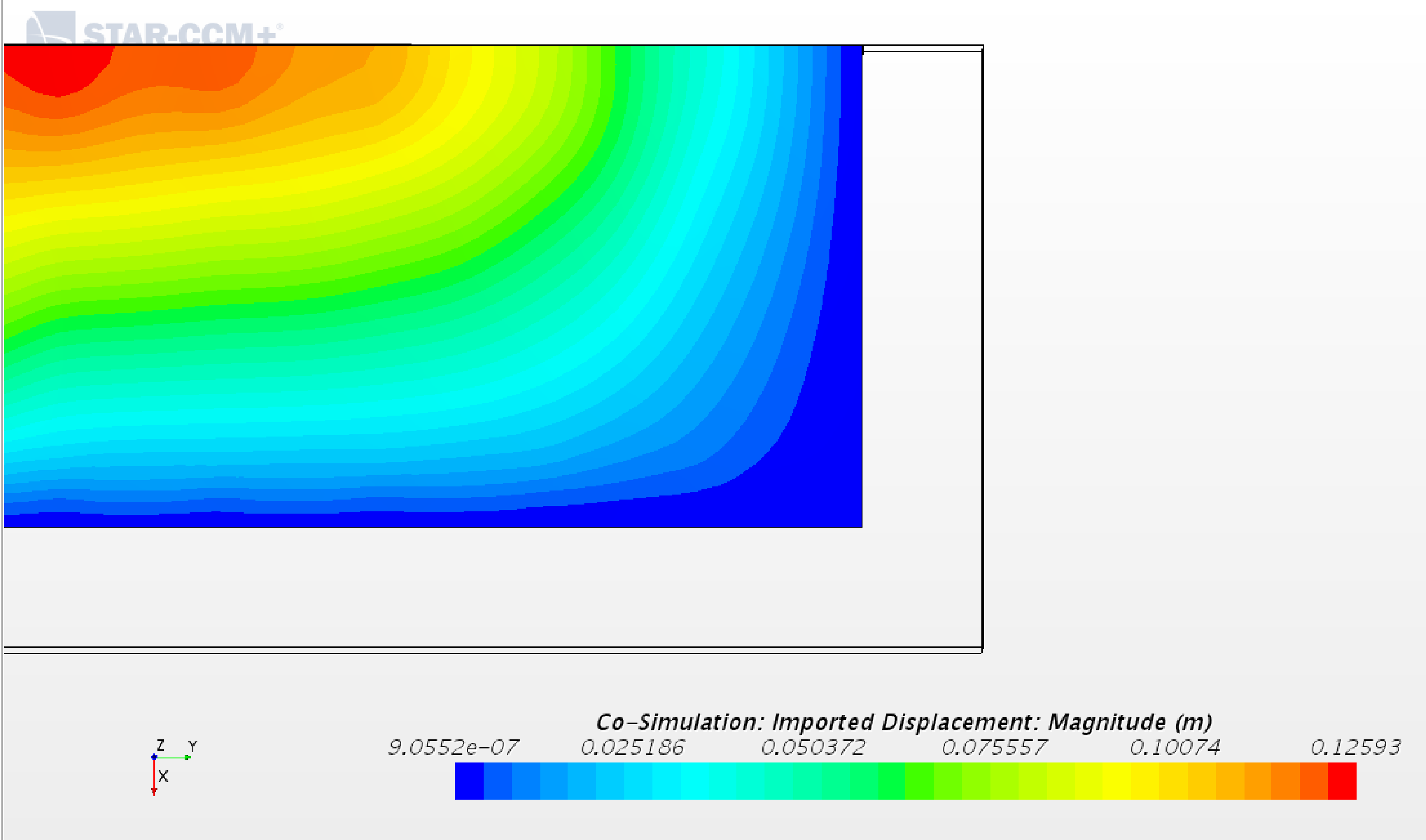STAR-CCM+ Co-Simulation: Imported Displacement: Magnitude (m) 9.0552e-07 0.025186 0.050372 0.075557 0.10074 0.12593 Z Y X

APPENDIX XV: SETTING AIR AS COMPRESSIBLE & WATER AS INCOMPRESSIBLE (Force Monitor Plot)

1 m/s	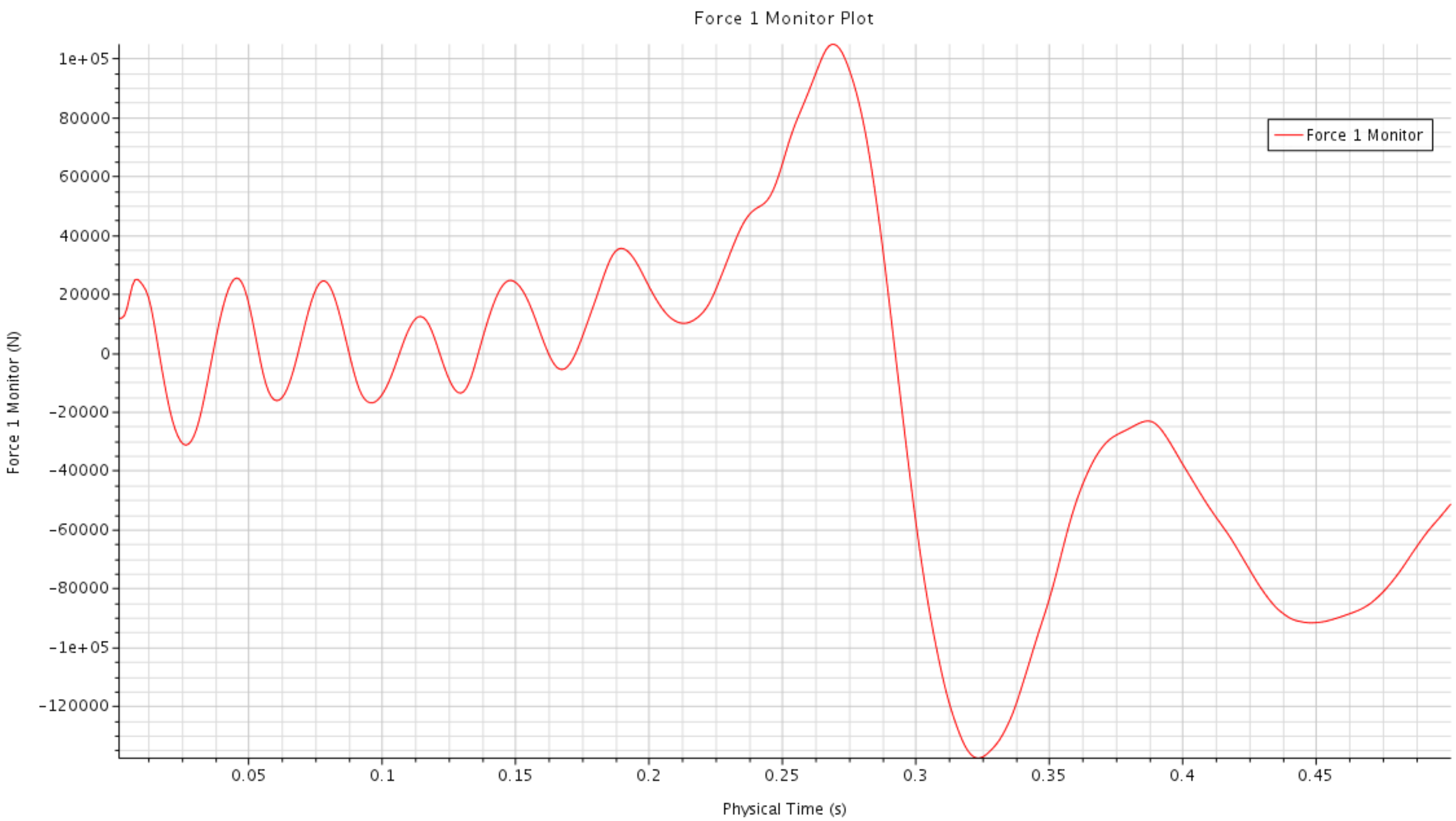

4 m/s	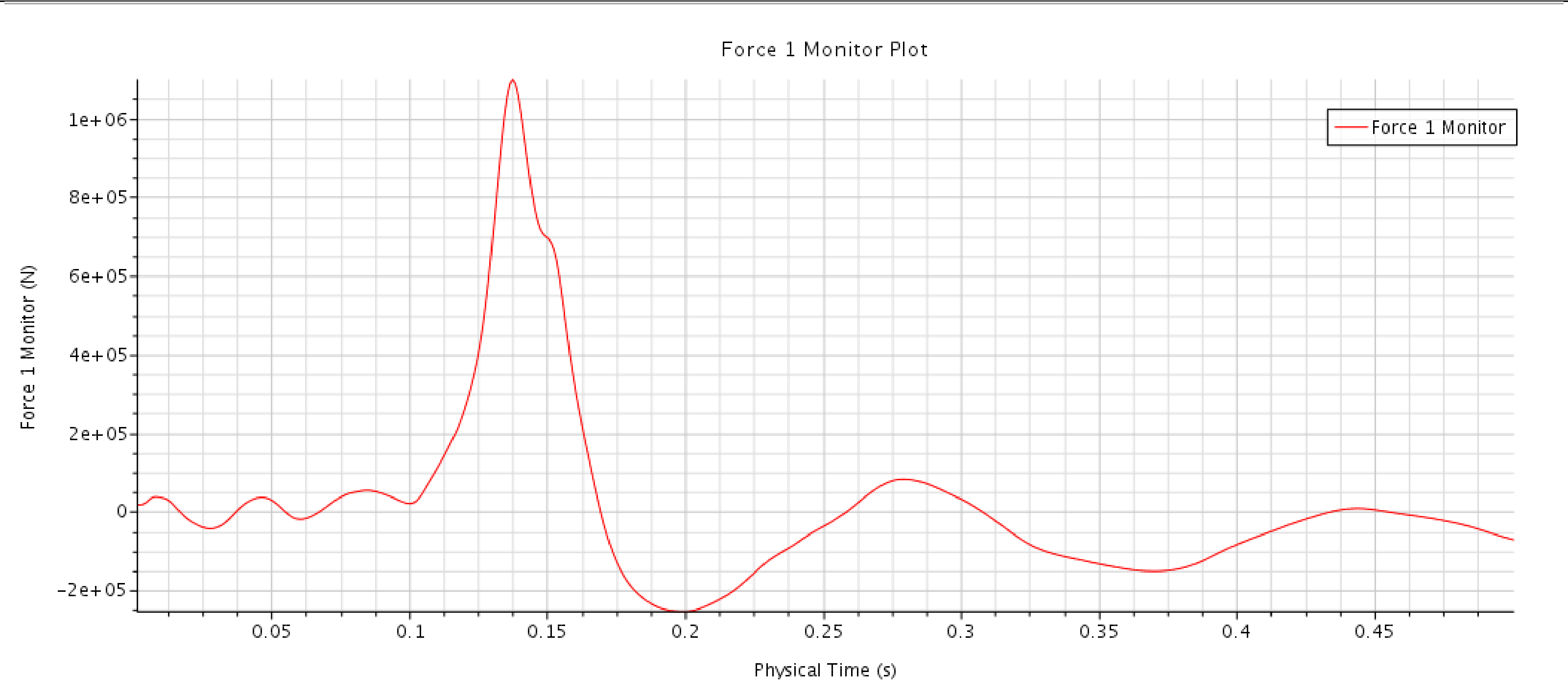Force 1 Monitor Plot Force 1 Monitor 1e+06 8e+05 6e+05 4e+05 2e+05 0 -2e+05 Force 1 Monitor (N) 0.05 0.1 0.15 0.2 0.25 0.3 0.35 0.4 0.45 Physical Time (s)

8 m/s	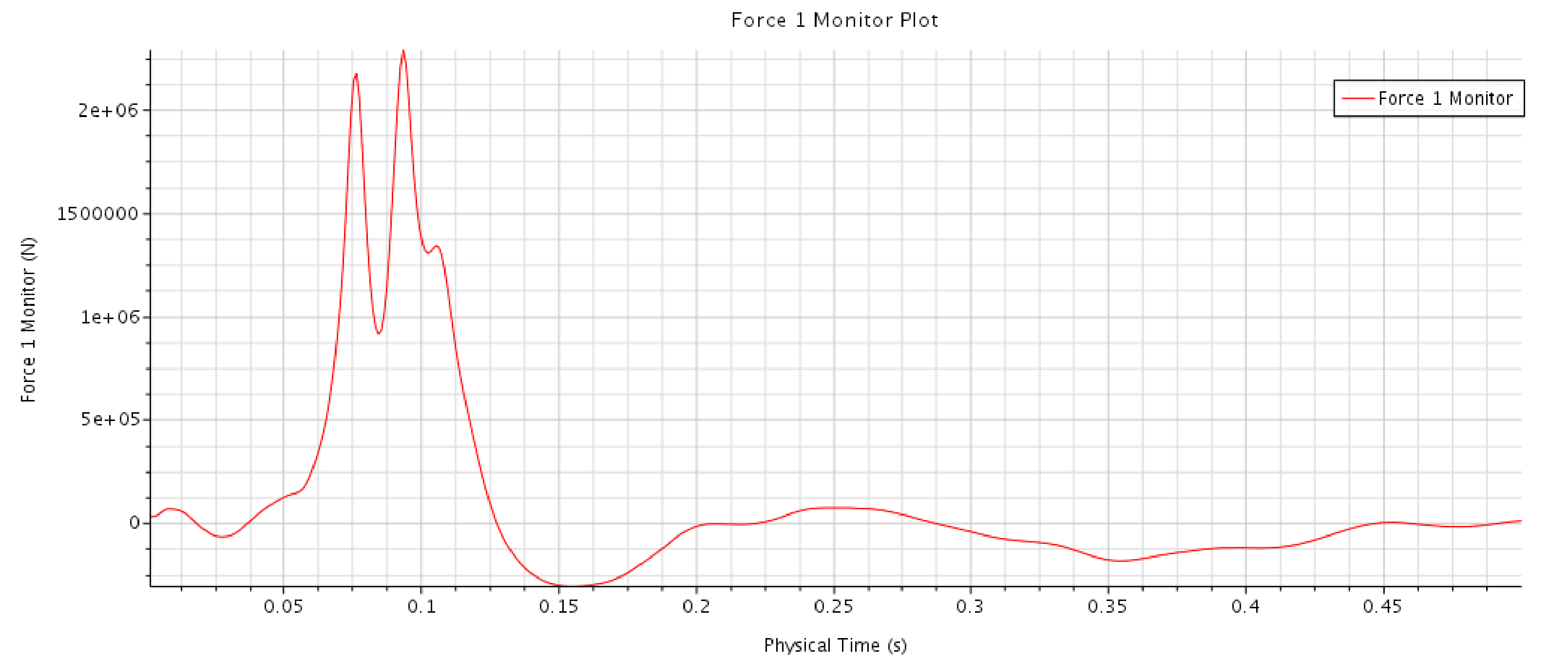Force 1 Monitor Plot Force 1 Monitor 2e+06 1500000 1e+06 5e+05 0 Force 1 Monitor (N) 0.05 0.1 0.15 0.2 0.25 0.3 0.35 0.4 0.45 Physical Time (s)

APPENDIX XVI: SETTING AIR AS COMPRESSIBLE & WATER AS INCOMPRESSIBLE (Point Monitor Plot)

1 m/s	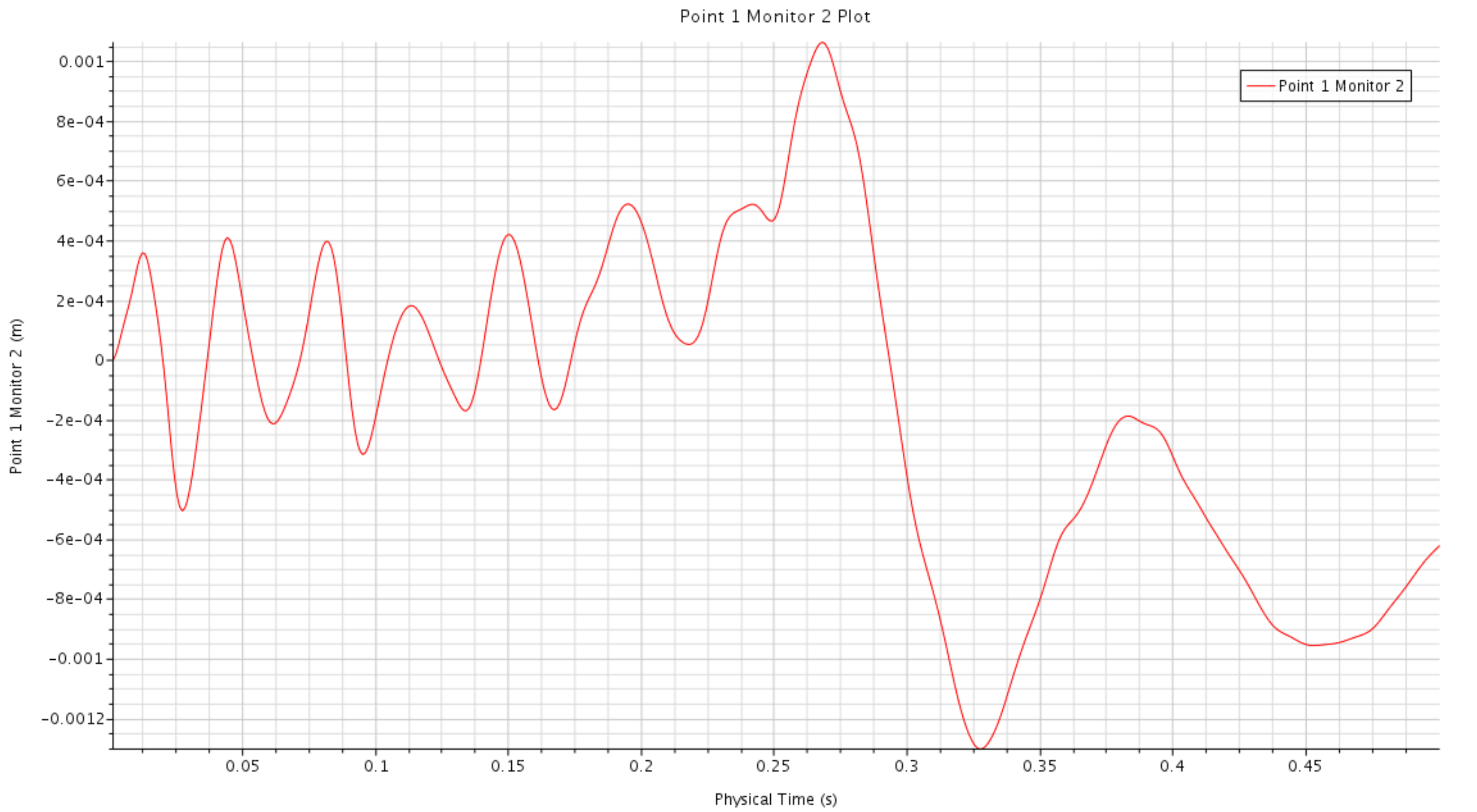

4 m/s	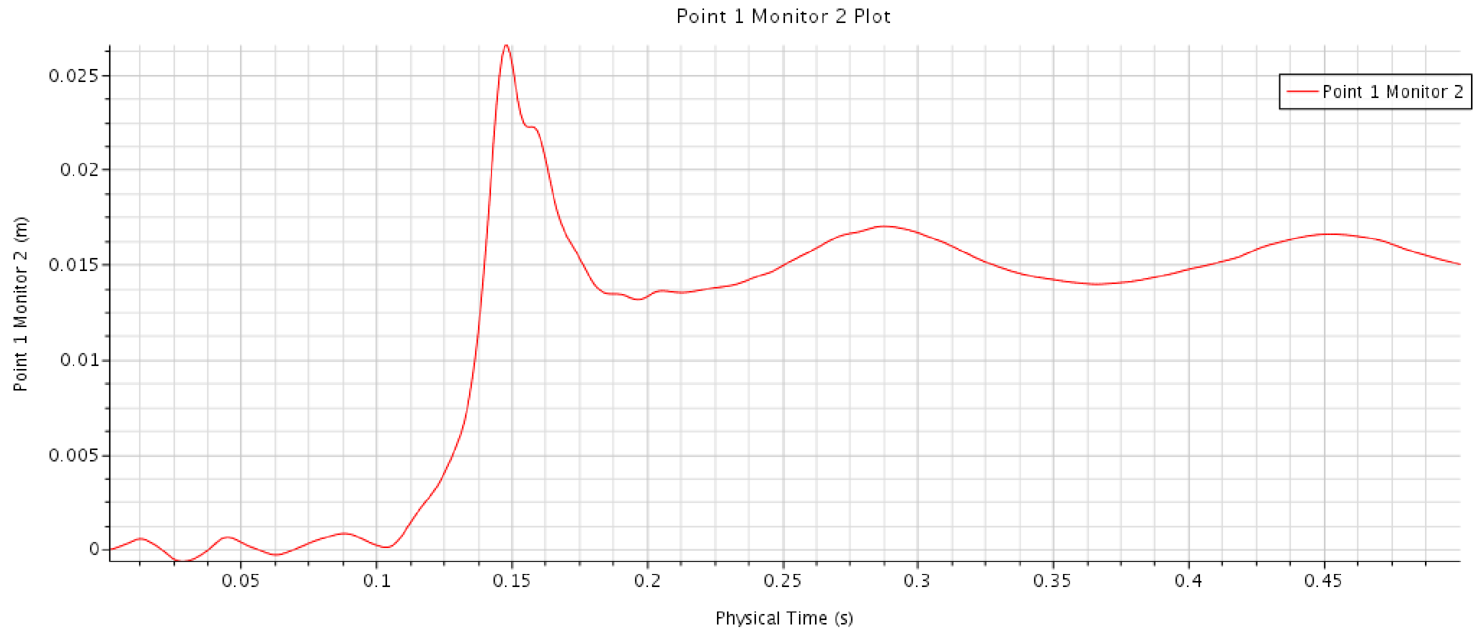Point 1 Monitor 2 Plot
Point 1 Monitor 2
Point 1 Monitor 2 (m)
Physical Time (s)
0.025
0.02
0.015
0.01
0.005
0
0.05
0.1
0.15
0.2
0.25
0.3
0.35
0.4
0.45

8 m/s	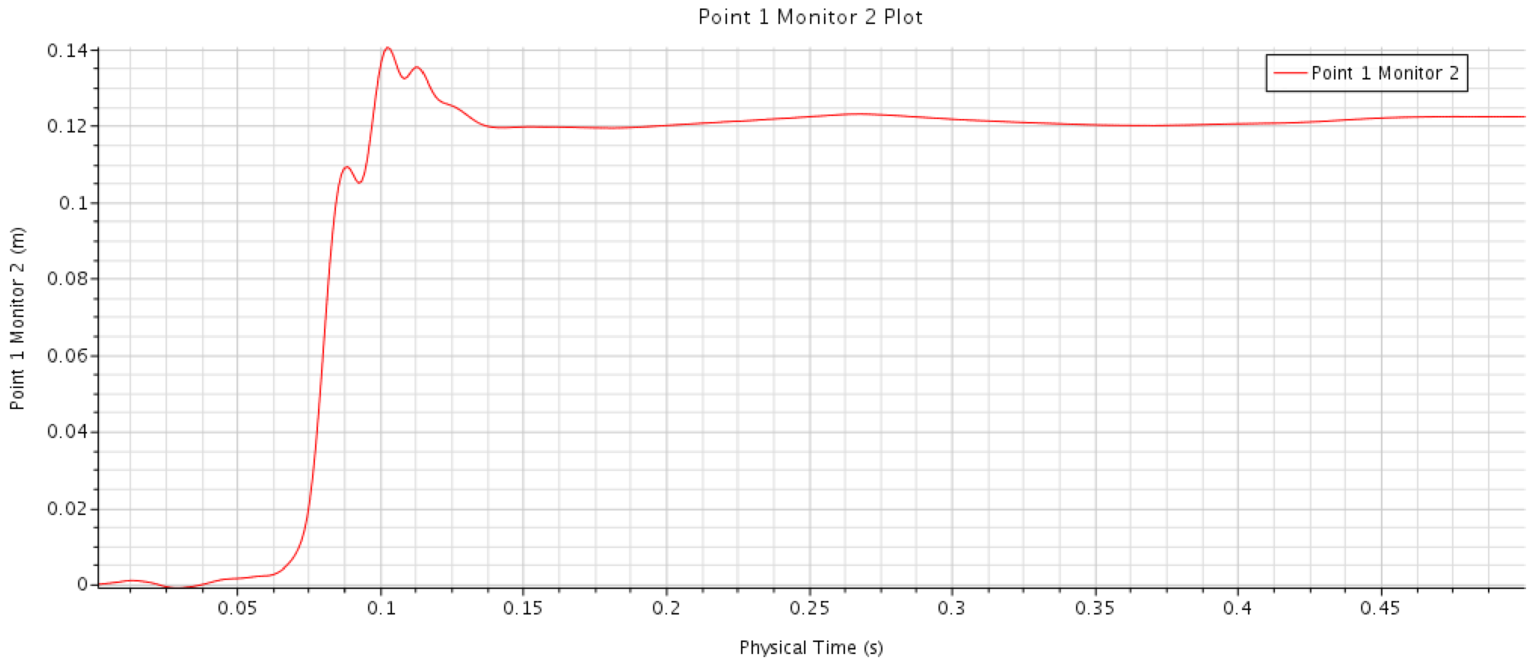 Point 1 Monitor 2 Plot Point 1 Monitor 2 Point 1 Monitor 2 (m) 0.14 0.12 0.1 0.08 0.06 0.04 0.02 0 0.05 0.1 0.15 0.2 0.25 0.3 0.35 0.4 0.45 Physical Time (s)

APPENDIX XVII: SETTING AIR AS COMPRESSIBLE & WATER AS INCOMPRESSIBLE (Vector Plot)

1 m/s	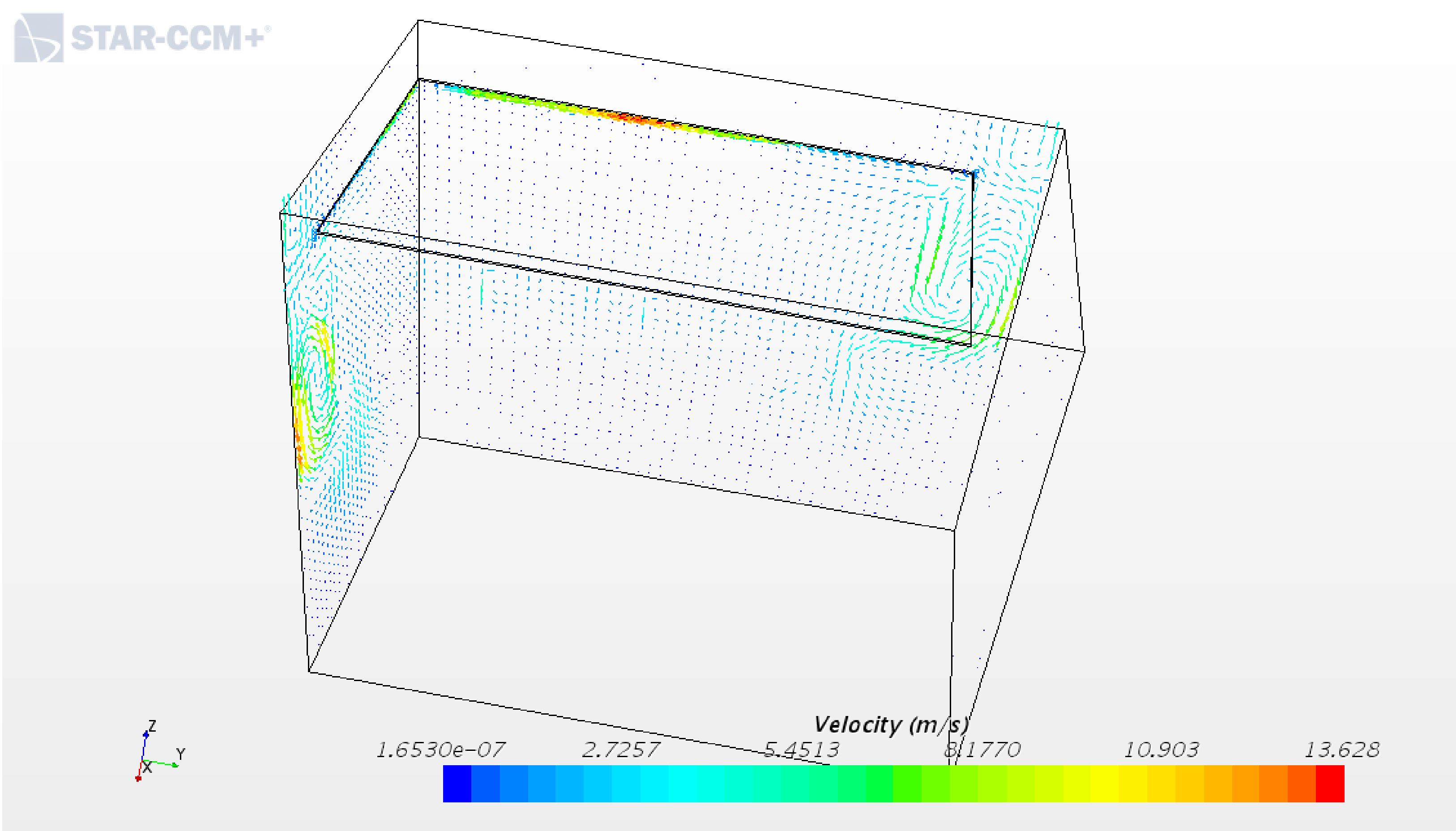

4 m/s	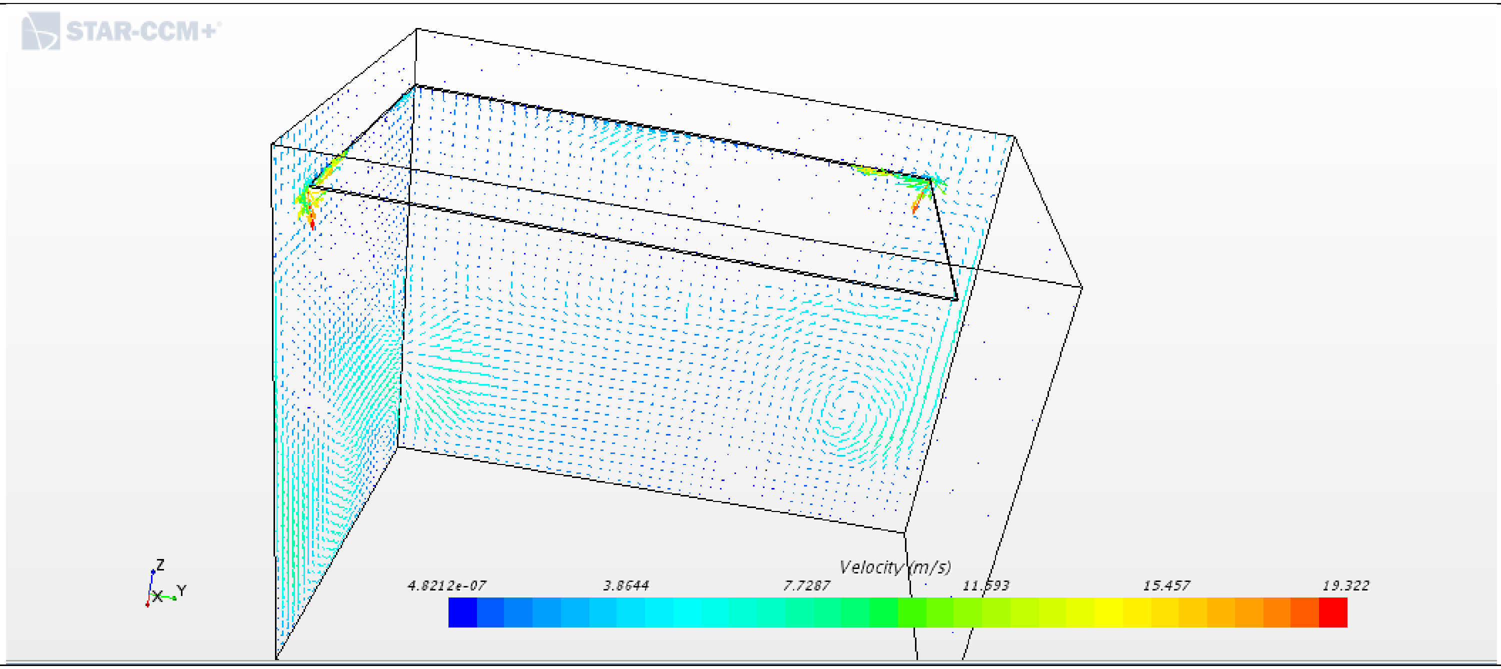Velocity (m/s) 4.8212e-07 3.8644 7.7287 11.593 15.457 19.322 Z X Y

8 m/s	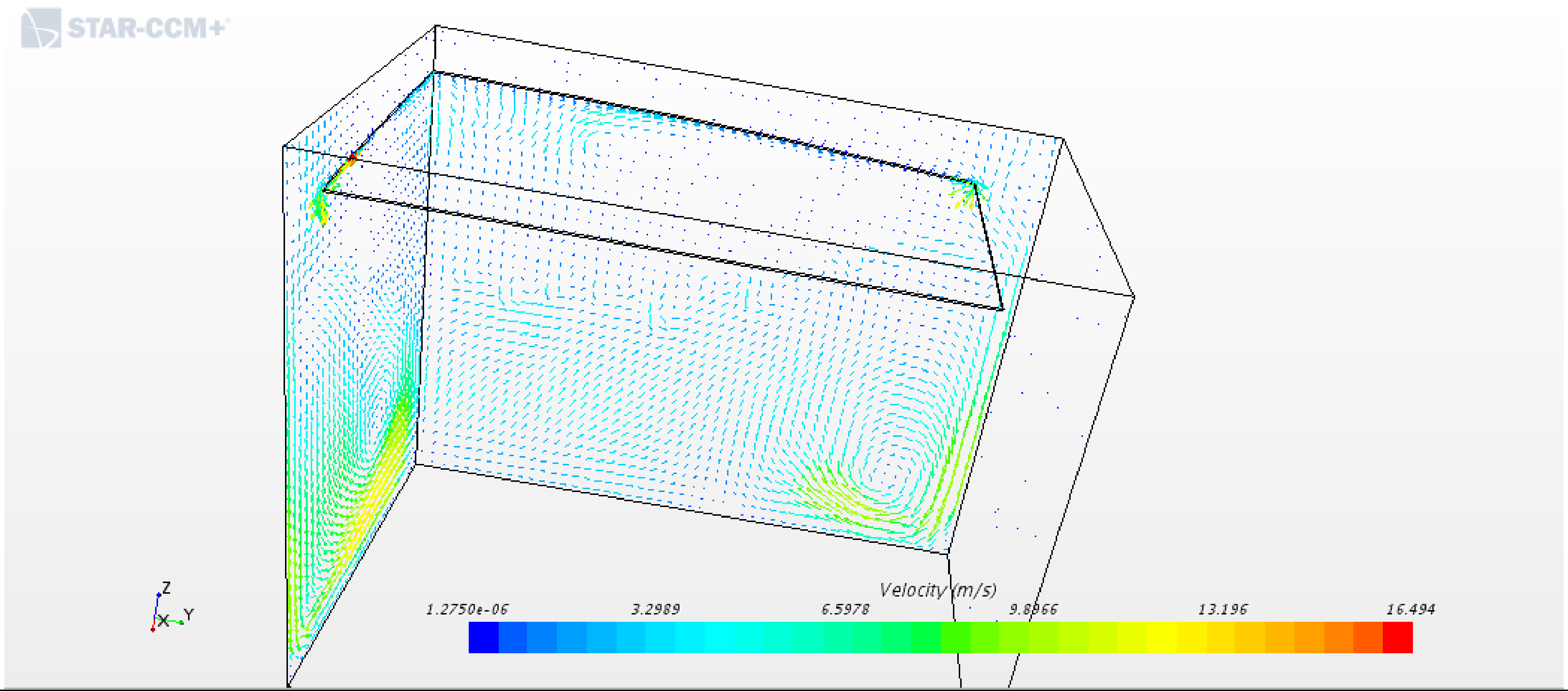STAR-CCM+ Velocity (m/s) 1.2750e-06 3.2989 6.5978 9.8966 13.196 16.494 Z X Y

APPENDIX XVIII: SETTING AIR AS COMPRESSIBLE & WATER AS INCOMPRESSIBLE (Volume Fraction of Air)

1 m/s	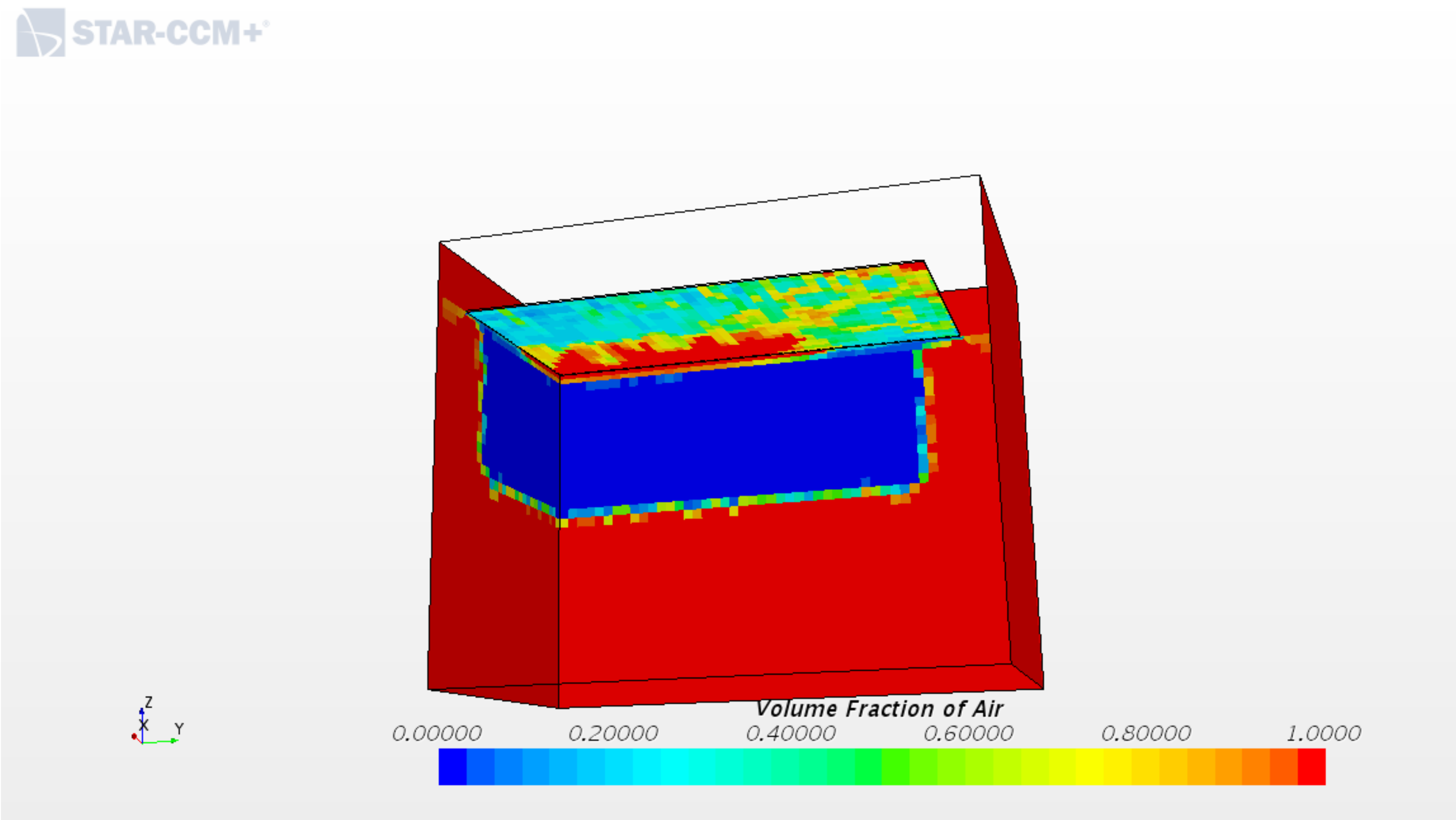

4 m/s	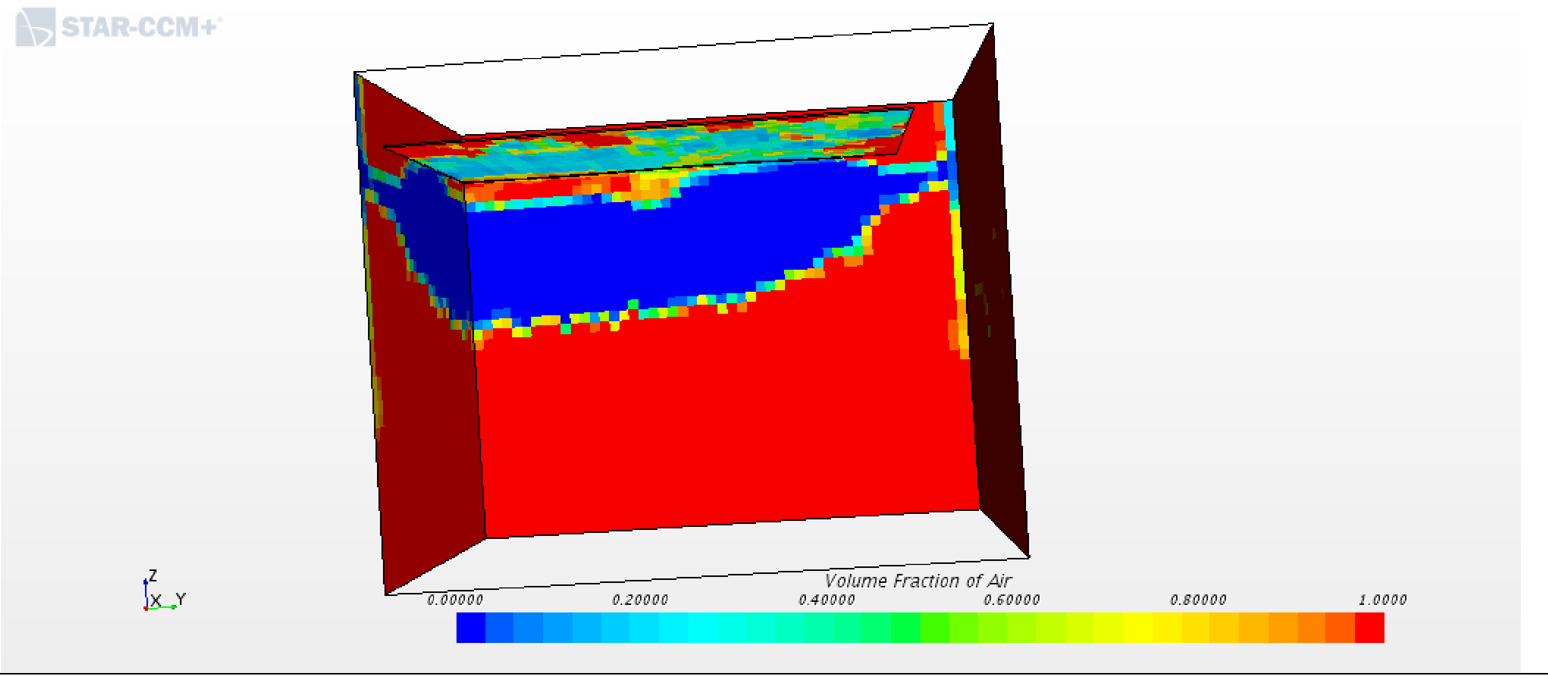STAR-CCM+ Volume Fraction of Air 0.00000 0.20000 0.40000 0.60000 0.80000 1.0000 Z X Y

8 m/s	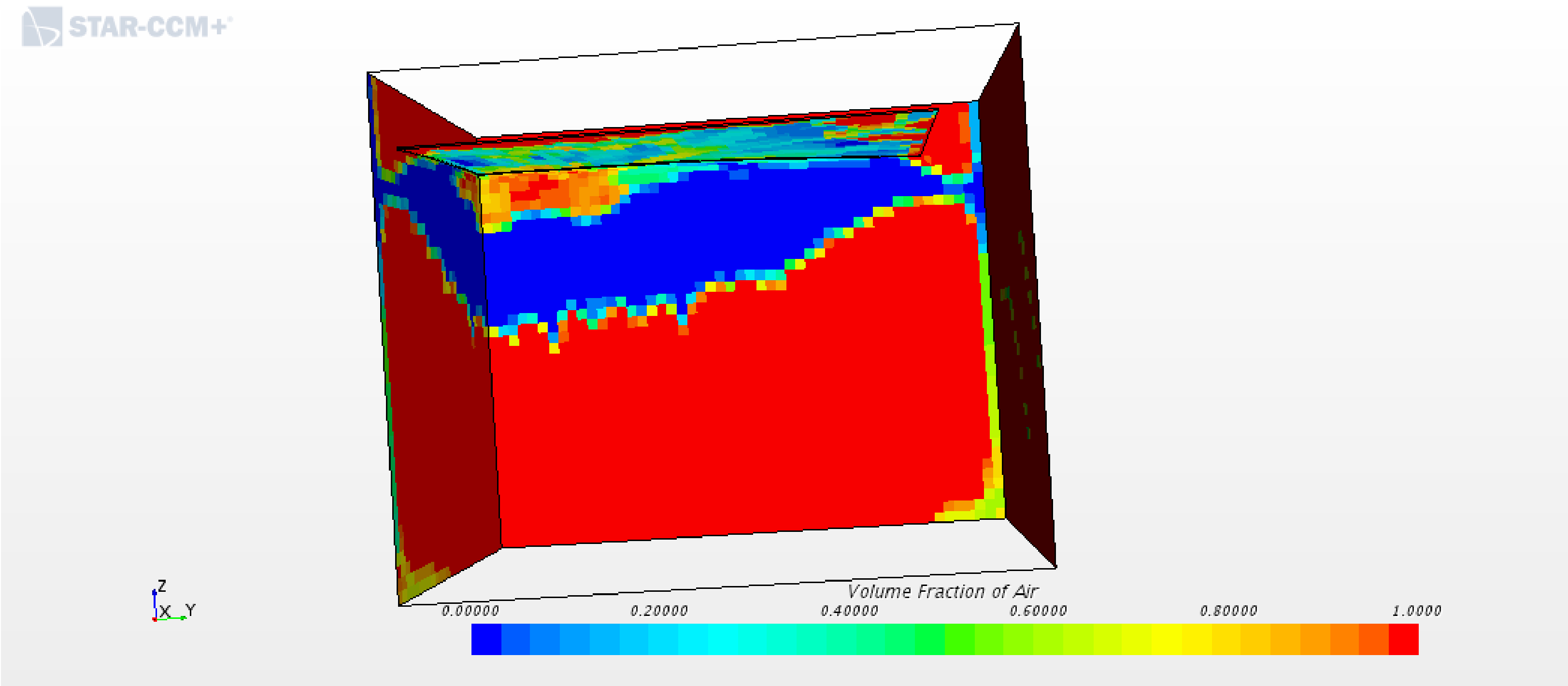STAR-CCM+ Volume Fraction of Air 0.00000 0.20000 0.40000 0.60000 0.80000 1.0000 Z X Y

APPENDIX XIX: SETTING AIR AS COMPRESSIBLE & WATER AS INCOMPRESSIBLE (Volume Fraction of Water)

1 m/s	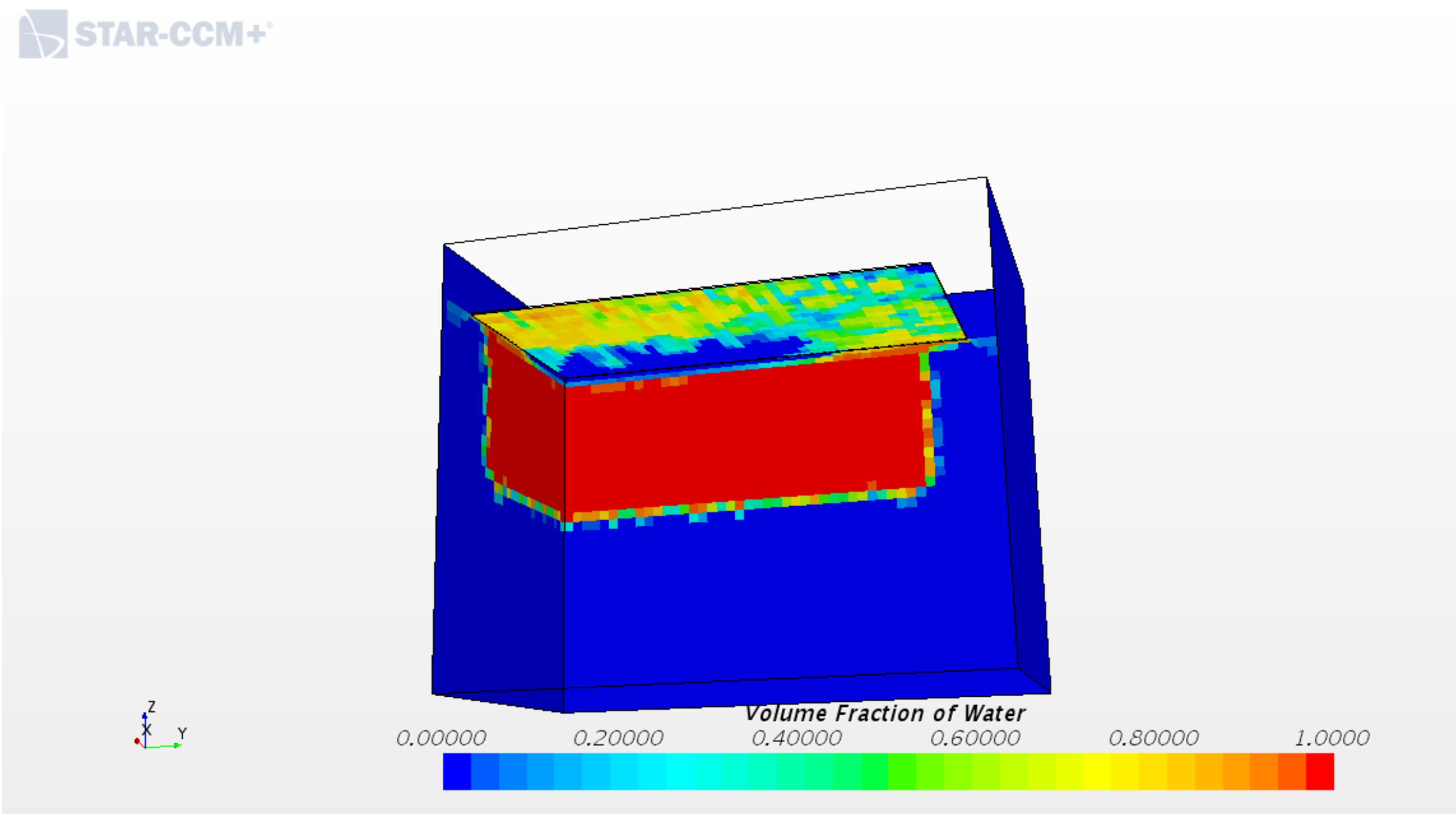

4 m/s		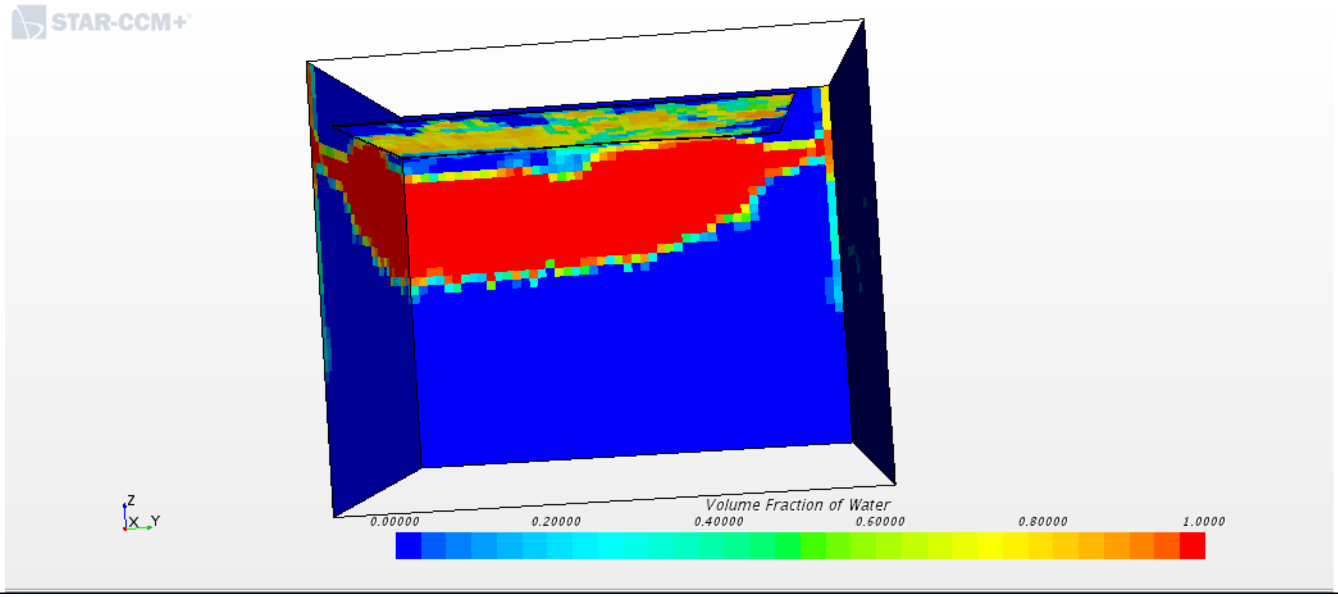 STAR-CCM+ Volume Fraction of Water 0.00000 0.20000 0.40000 0.60000 0.80000 1.0000 Z X Y

8 m/S	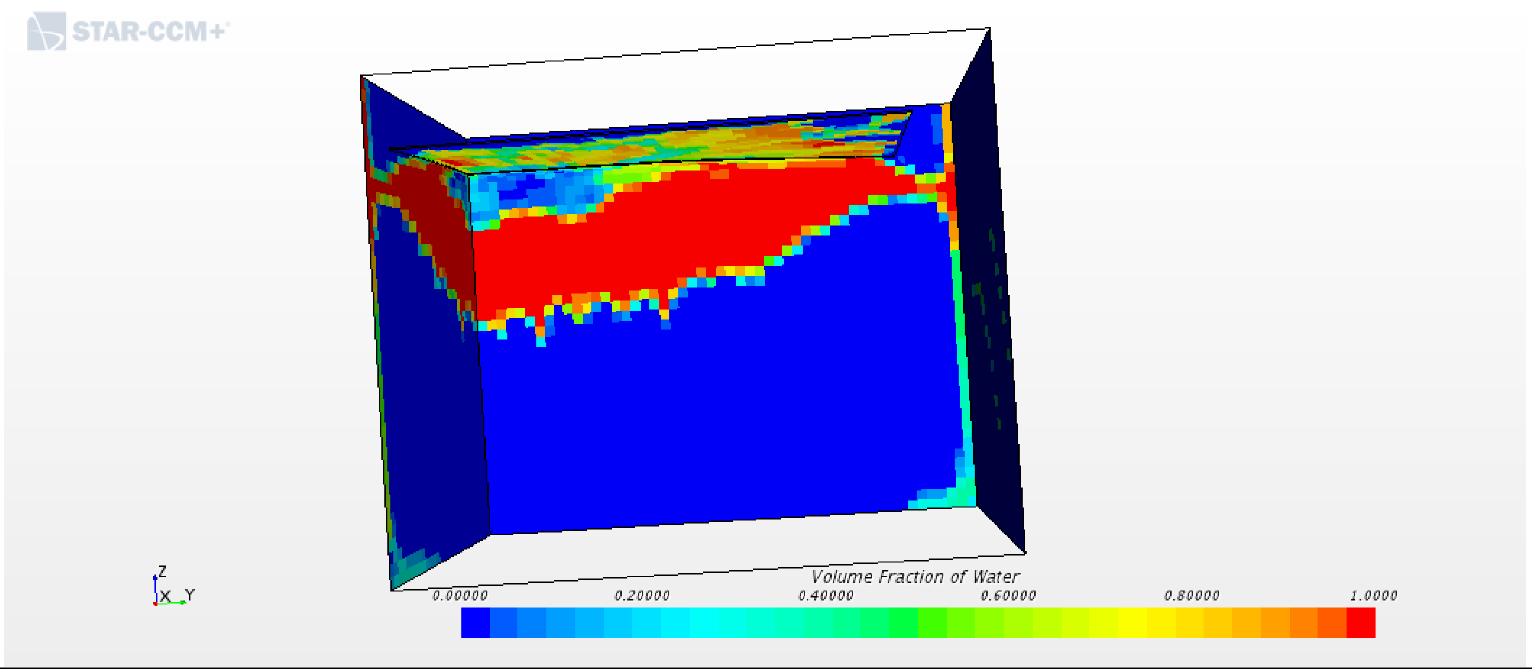 STAR-CCM+ Volume Fraction of Water 0.00000 0.20000 0.40000 0.60000 0.80000 1.0000 Z X Y

APPENDIX XX: SETTING AIR AS COMPRESSIBLE & WATER AS INCOMPRESSIBLE (Pressure Distribution)

1 m/s	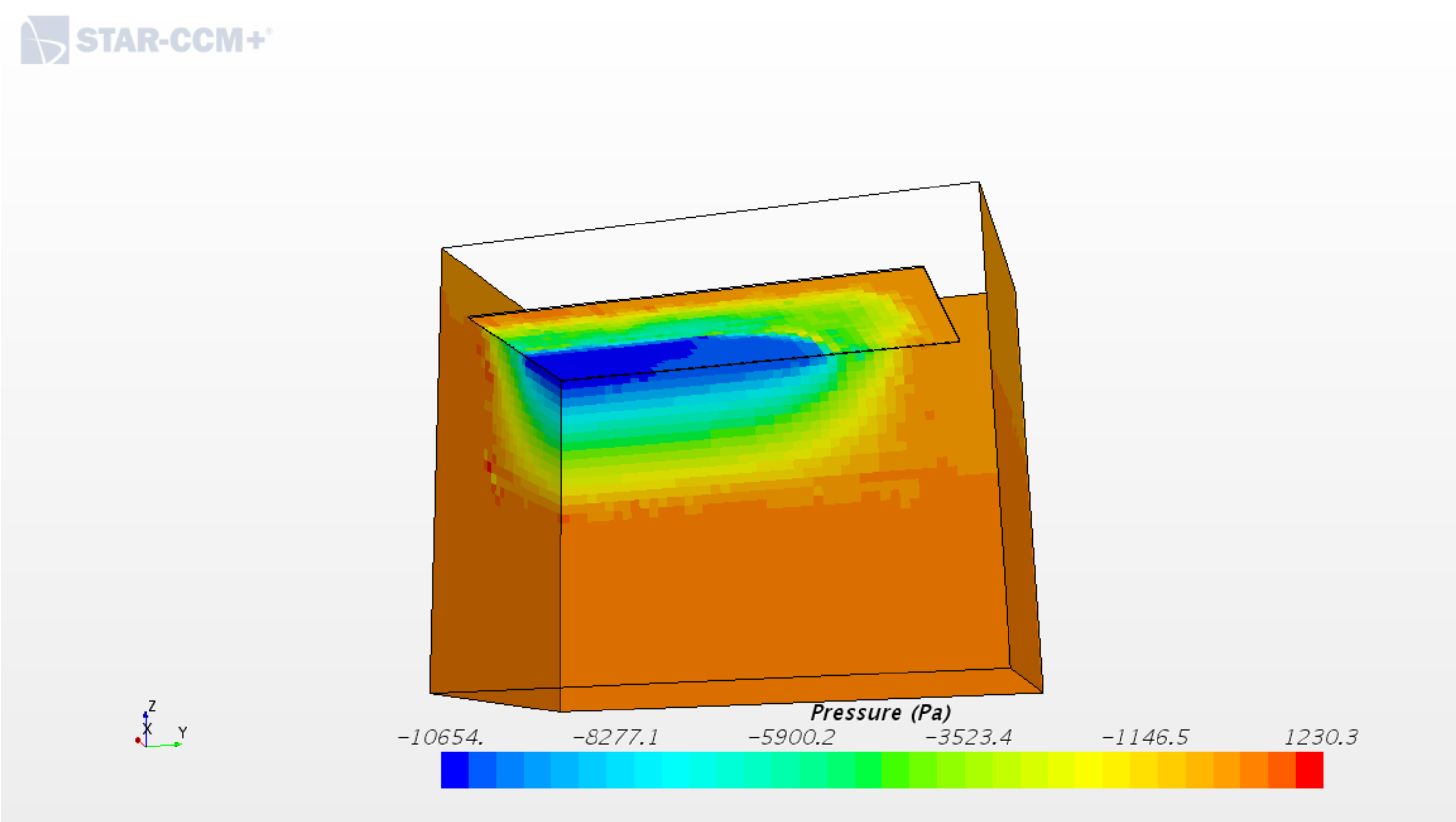

4 m/s	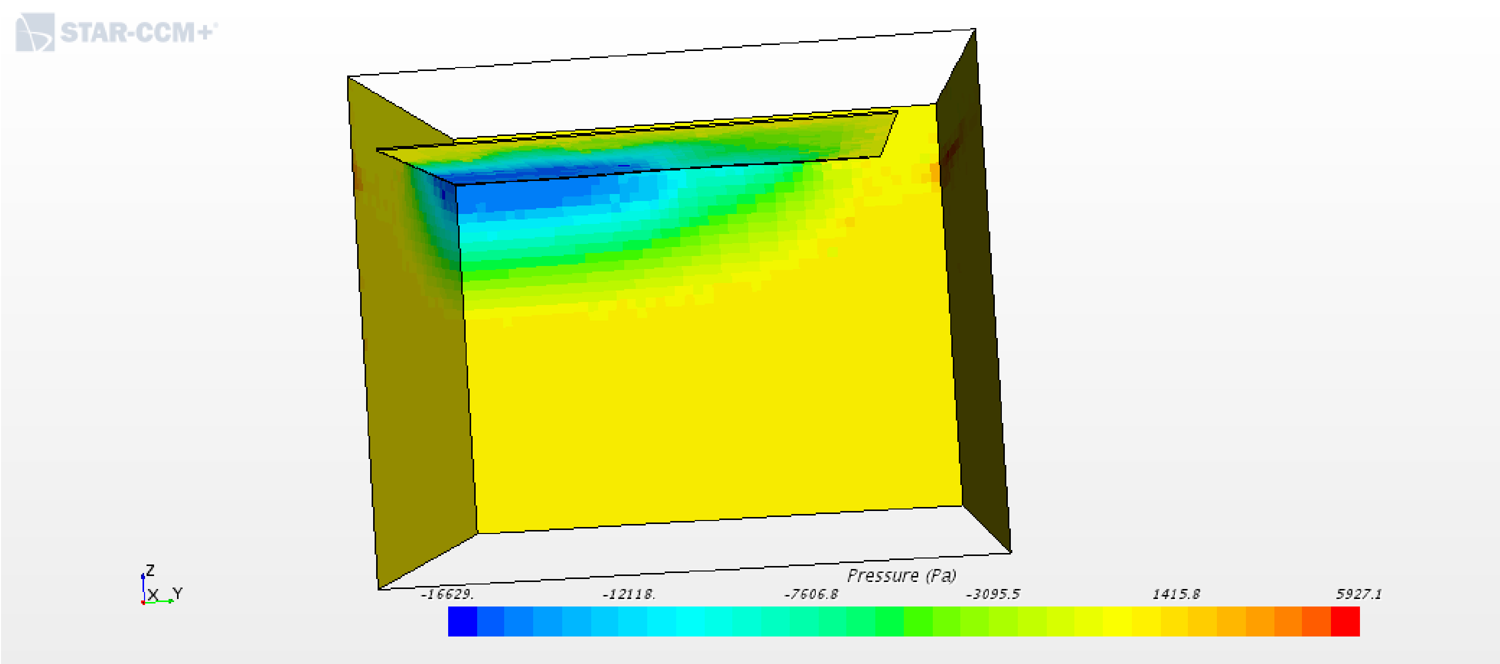STAR-CCM+ Pressure (Pa) -16629. -12118. -7606.8 -3095.5 1415.8 5927.1 Z X Y

8 m/s	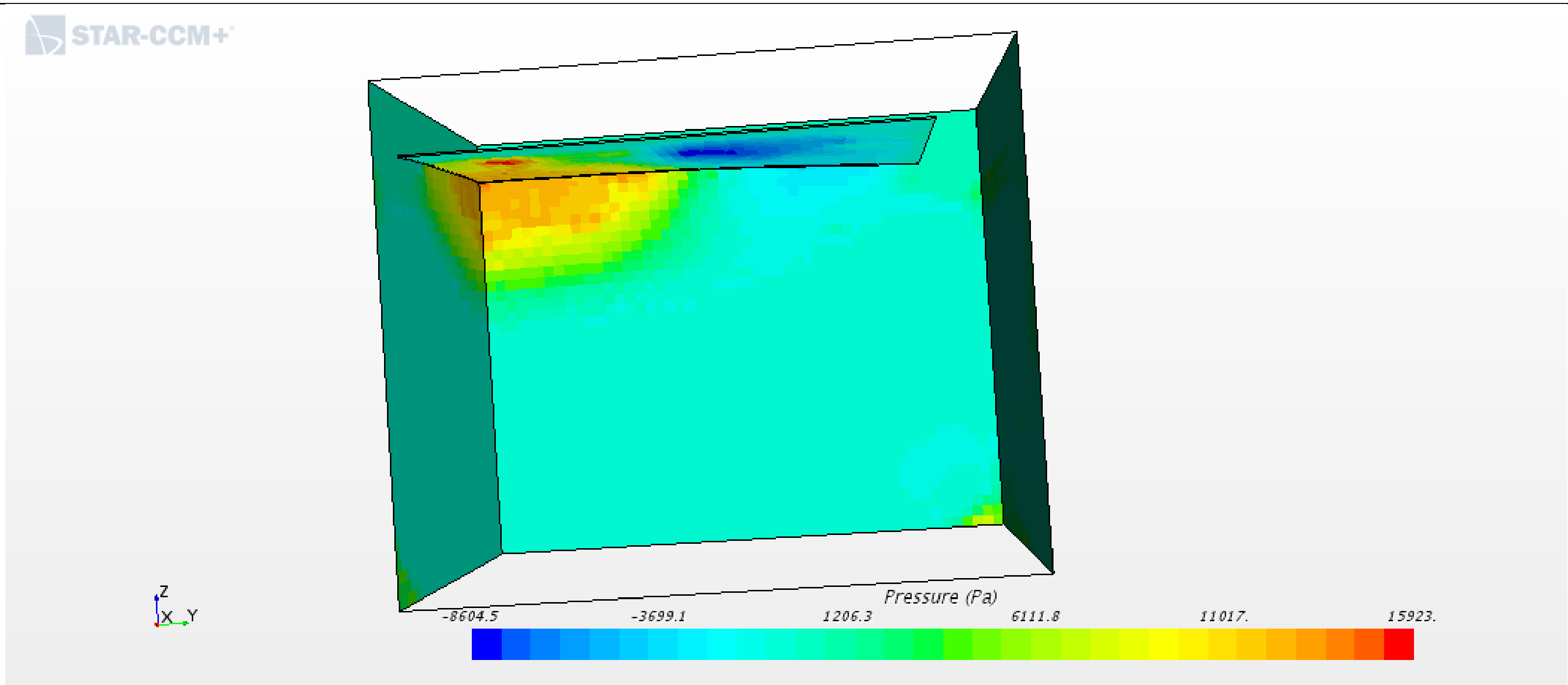 STAR-CCM+ Pressure (Pa) -8604.5 -3699.1 1206.3 6111.8 11017. 15923. Z X Y

APPENDIX XXI: SETTING AIR AS COMPRESSIBLE & WATER AS INCOMPRESSIBLE (ABAQUS Solution on Plate)

1 m/s	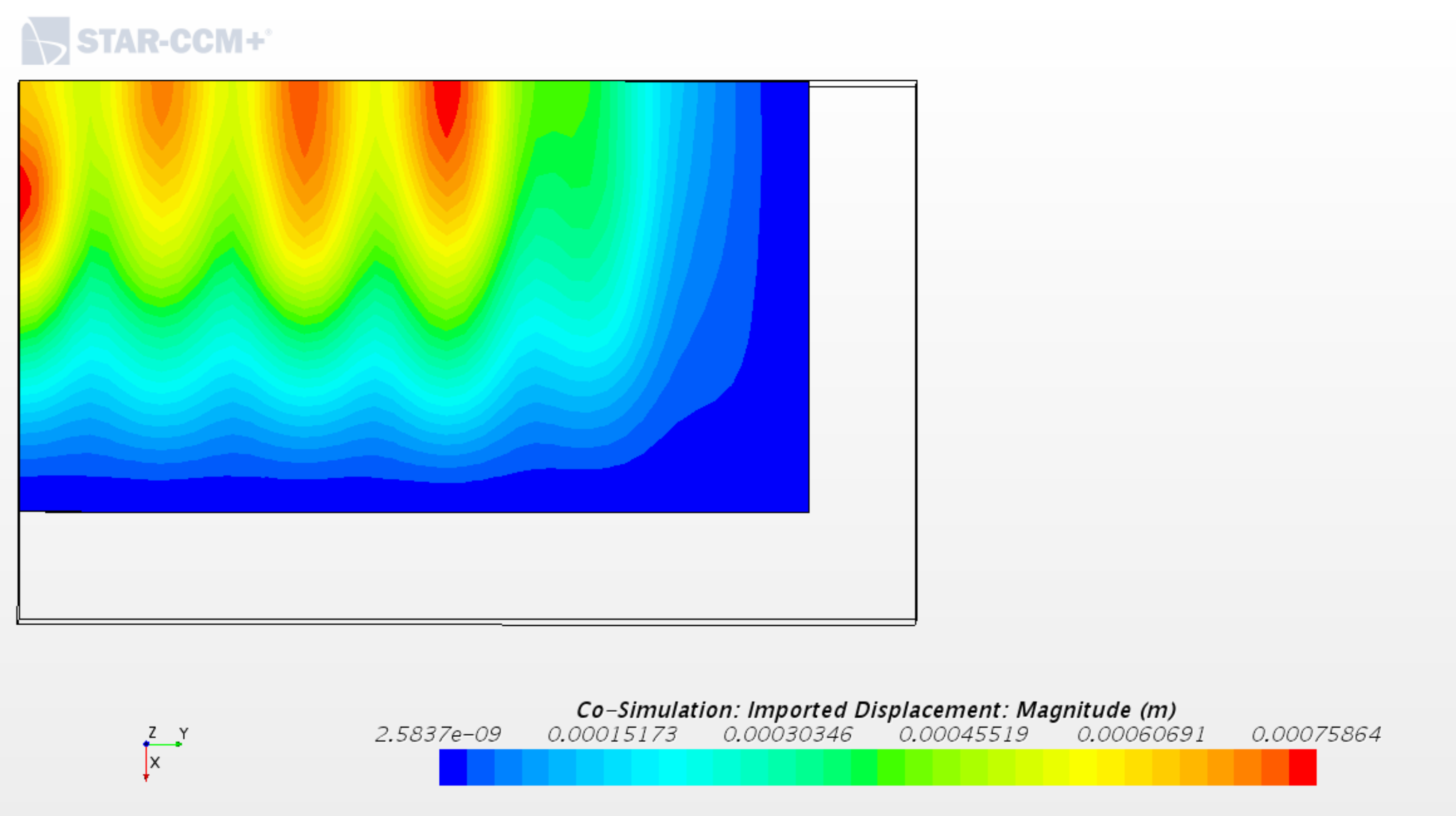

4 m/s	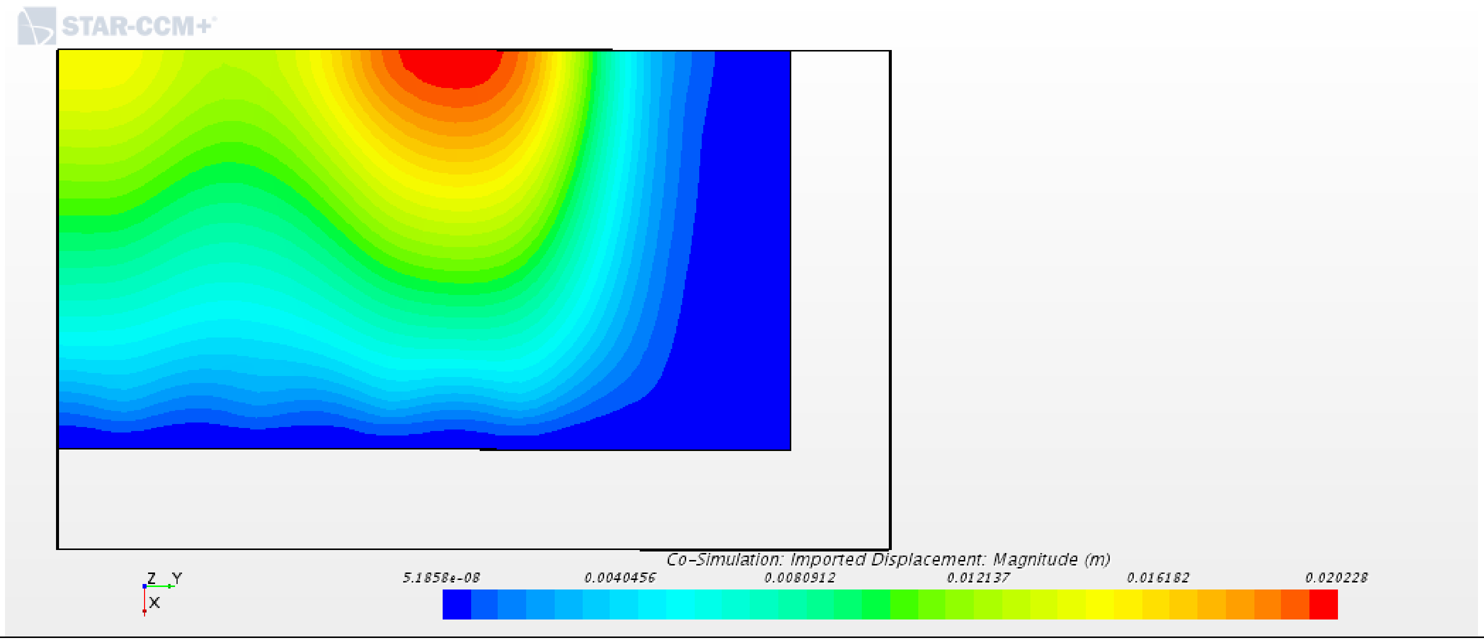STAR-CCM+ Co-Simulation: Imported Displacement: Magnitude (m) 5.1858e-08 0.0040456 0.0080912 0.012137 0.016182 0.020228 Z Y X

8 m/s	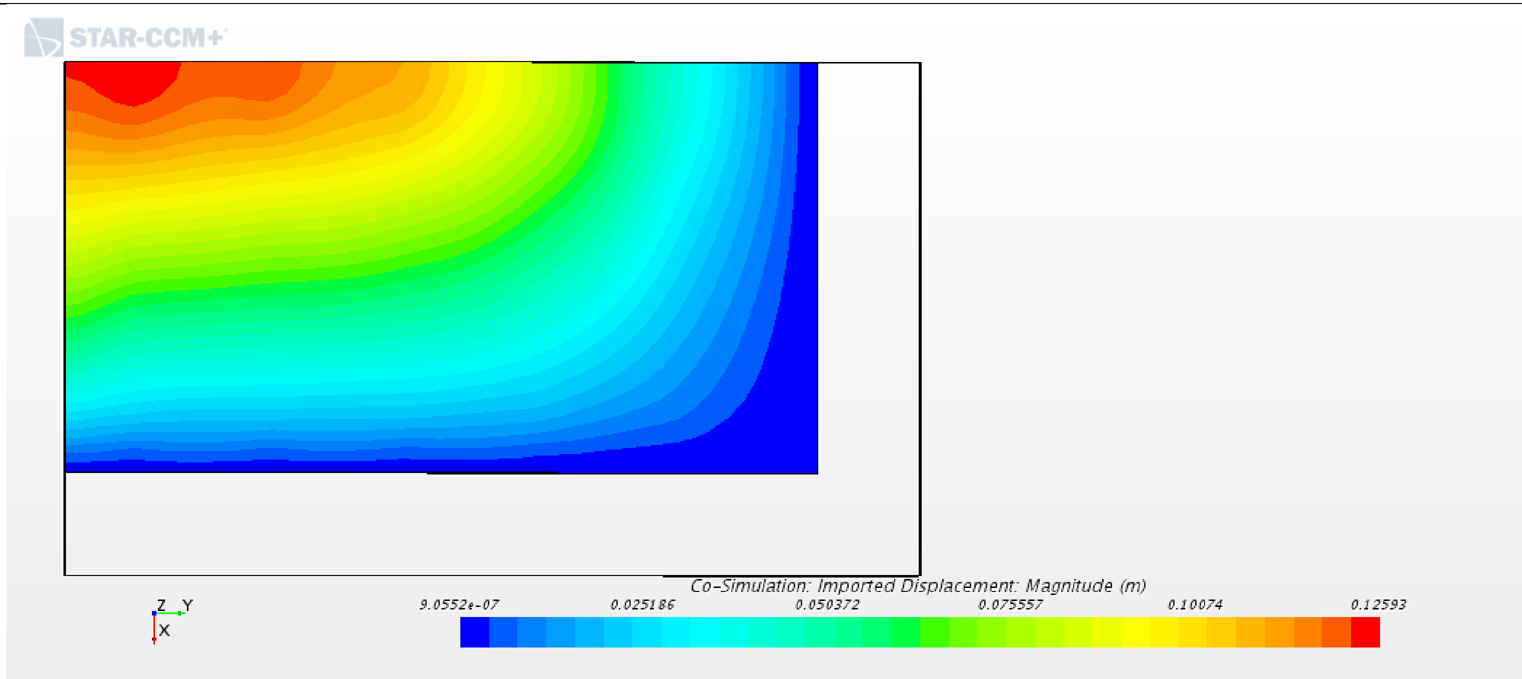 STAR-CCM+ Co-Simulation: Imported Displacement: Magnitude (m) 9.0552e-07 0.025186 0.050372 0.075557 0.10074 0.12593 Z Y X

APPENDIX XXII: SETTING AIR AS INCOMPRESSIBLE & WATER AS INCOMPRESSIBLE (Force Monitor Plot)

4 m/s	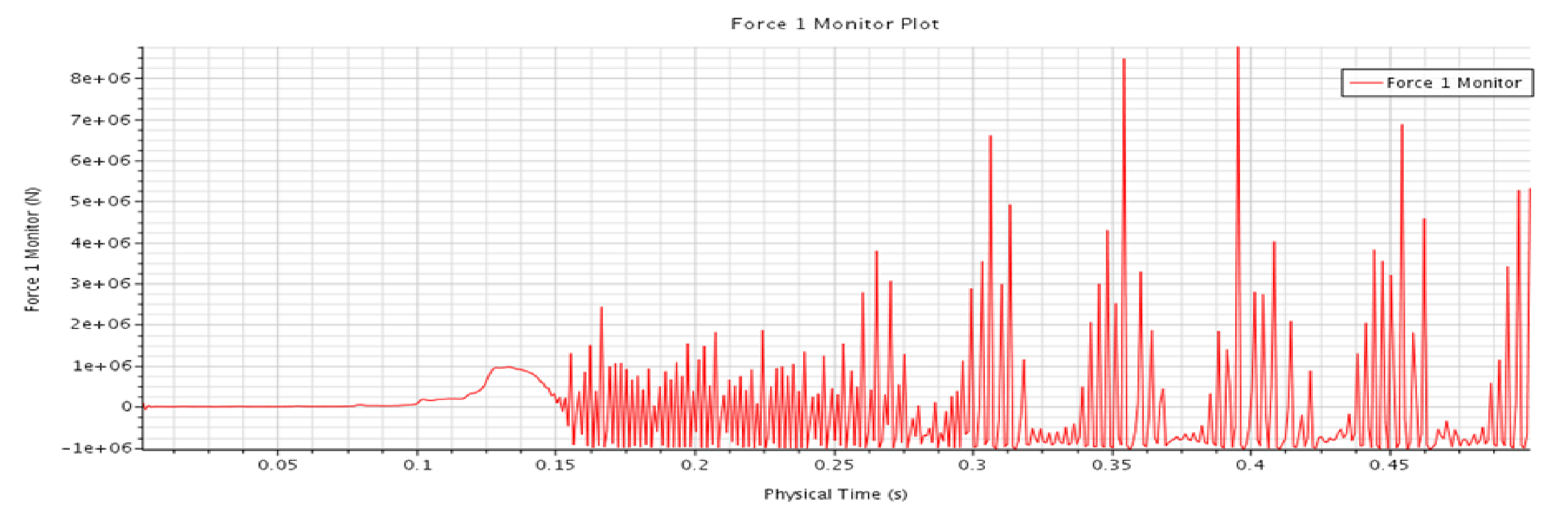

8 m/s	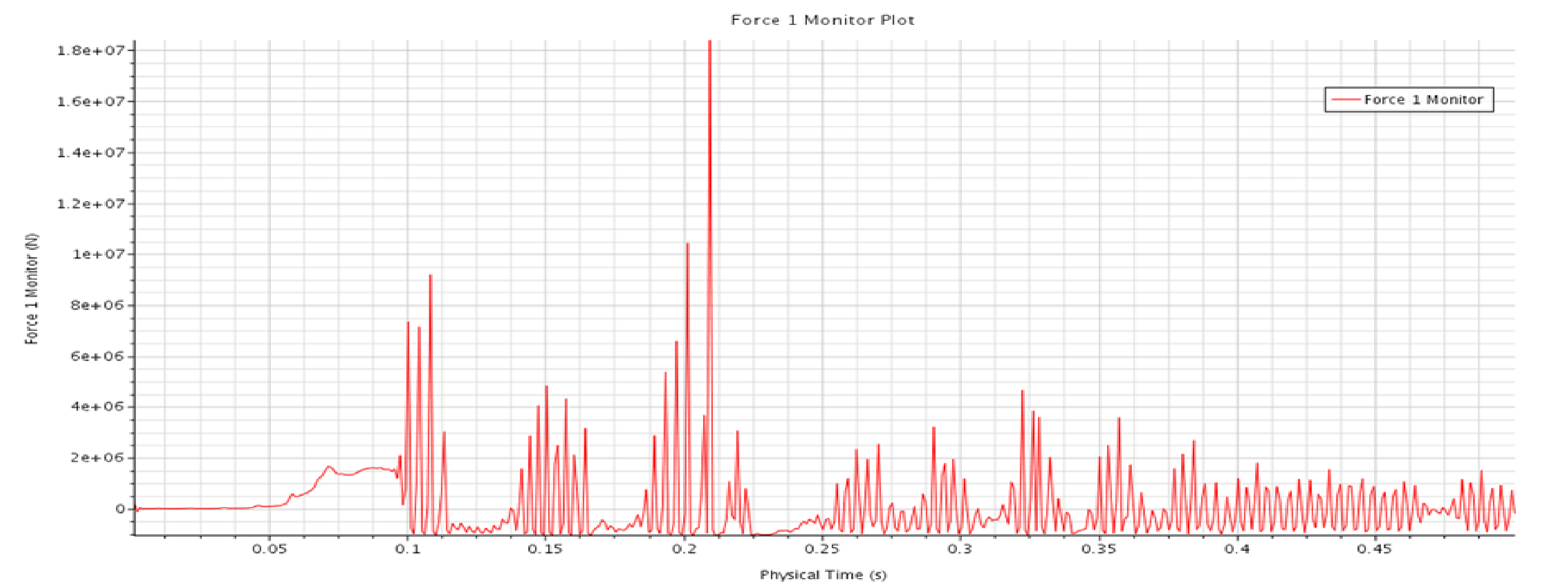Force 1 Monitor Plot 1.8e+07 1.6e+07 1.4e+07 1.2e+07 1e+07 8e+06 6e+06 4e+06 2e+06 0 Force 1 Monitor (N) Force 1 Monitor 0.05 0.1 0.15 0.2 0.25 0.3 0.35 0.4 0.45 Physical Time (s)

APPENDIX XXIII: SETTING AIR AS COMPRESSIBLE & WATER AS INCOMPRESSIBLE (Point Monitor Plot)

4 m/s	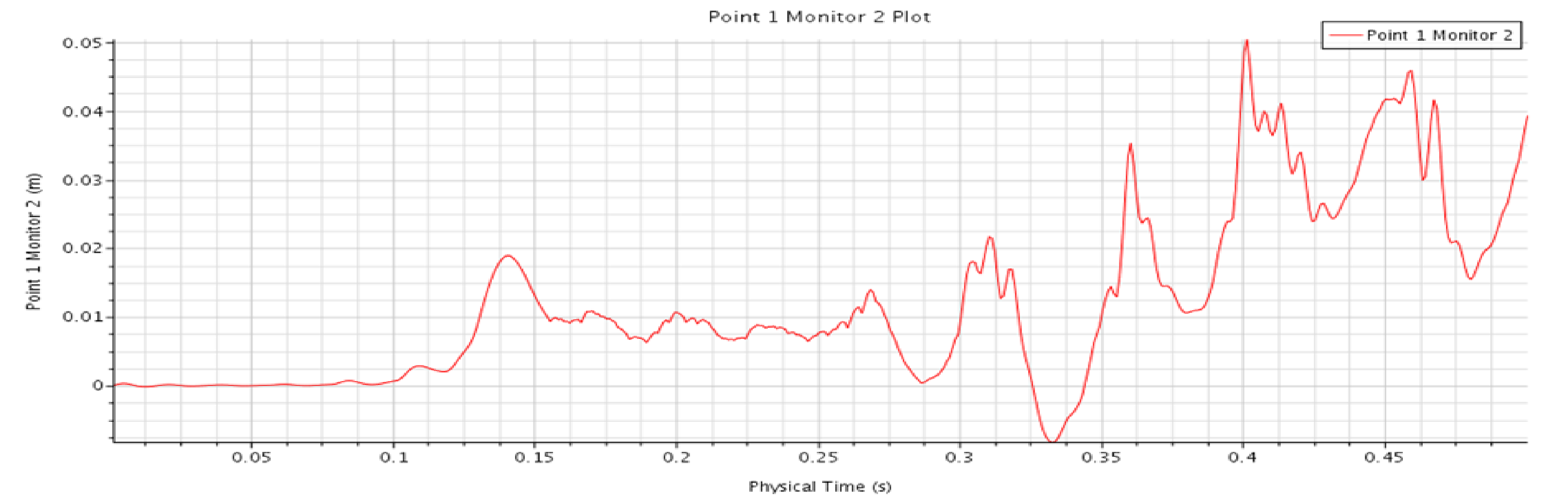

8 m/s	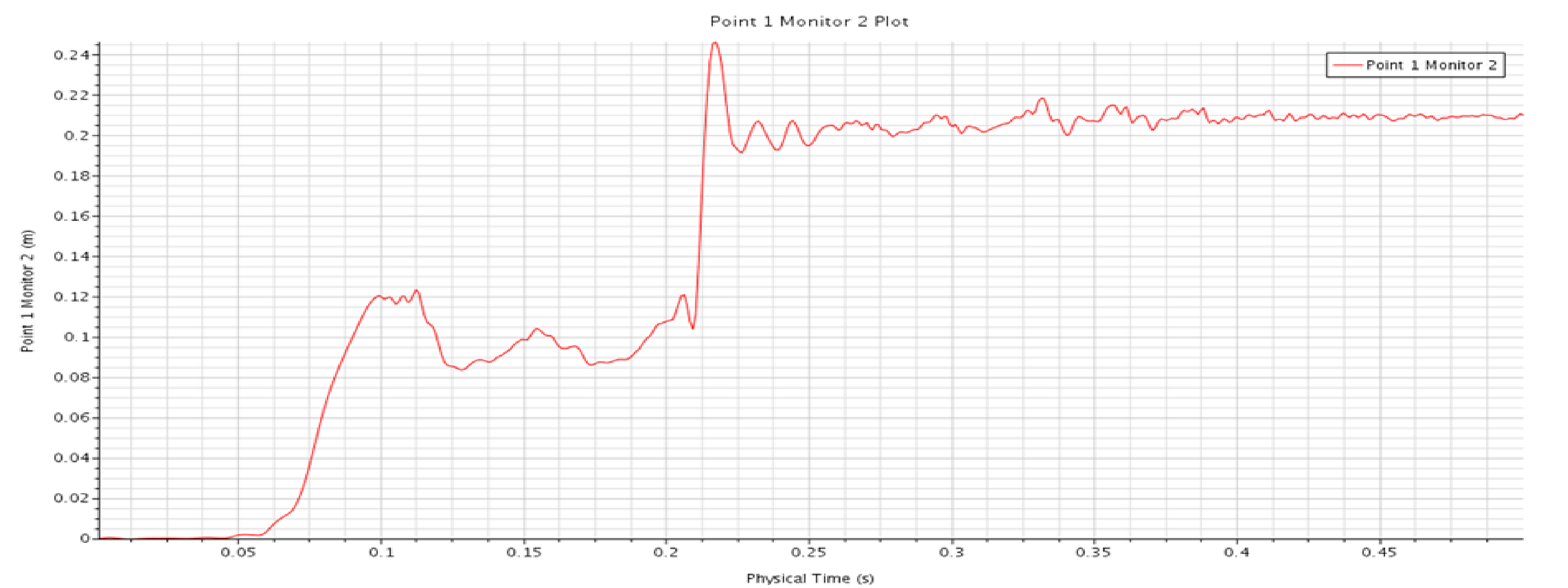Point 1 Monitor 2 Plot Point 1 Monitor 2 Point 1 Monitor 2 (m) Physical Time (s) 0.24 0.22 0.2 0.18 0.16 0.14 0.12 0.1 0.08 0.06 0.04 0.02 0 0.05 0.1 0.15 0.2 0.25 0.3 0.35 0.4 0.45

APPENDIX XXIV: SETTING AIR AS COMPRESSIBLE & WATER AS INCOMPRESSIBLE (Vector Plot)

4 m/s	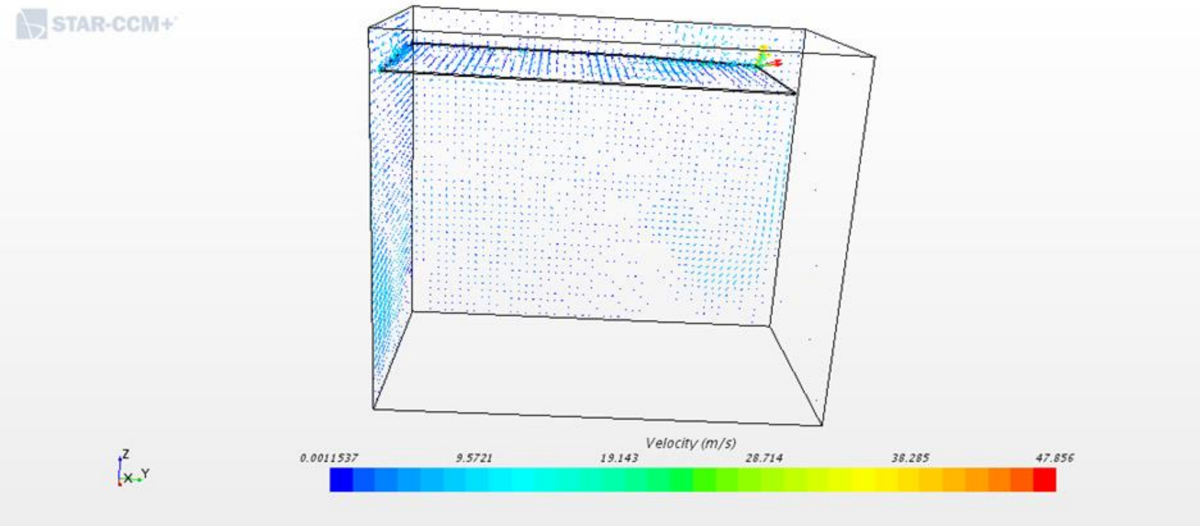

8 m/s	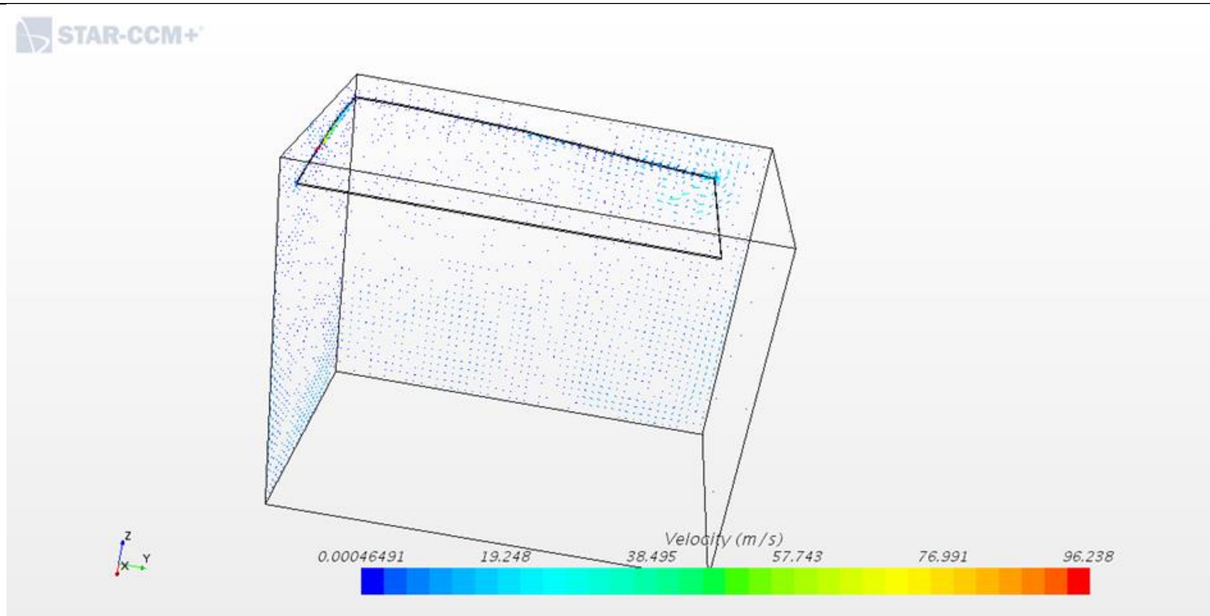STAR-CCM+ Velocity (m/s) 0.00046491 19.248 38.495 57.743 76.991 96.238 Z X Y

APPENDIX XXV: SETTING AIR AS COMPRESSIBLE & WATER AS INCOMPRESSIBLE (Volume Fraction of Air)

4 m/s	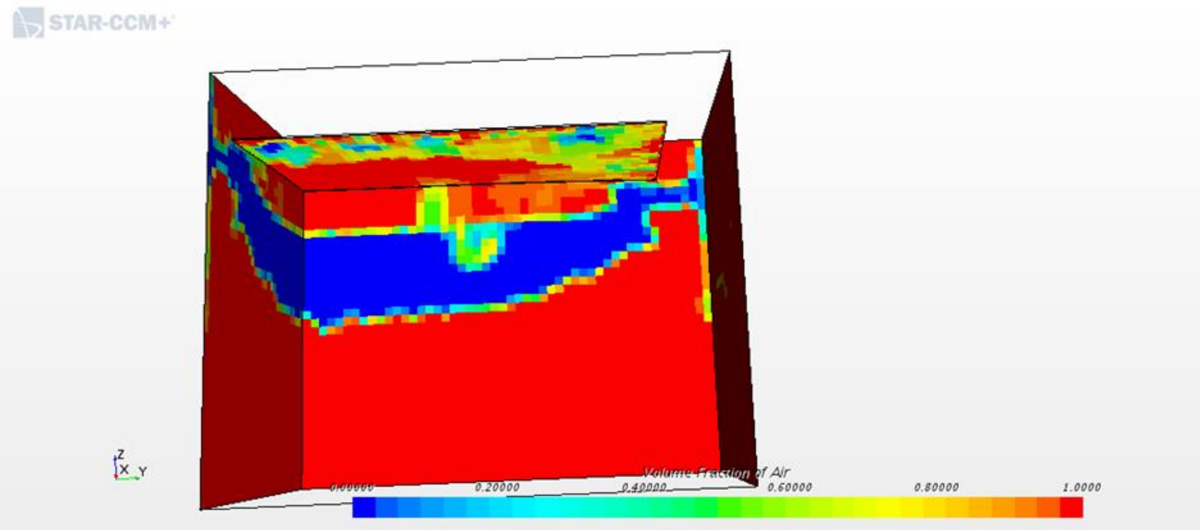

8 m/s	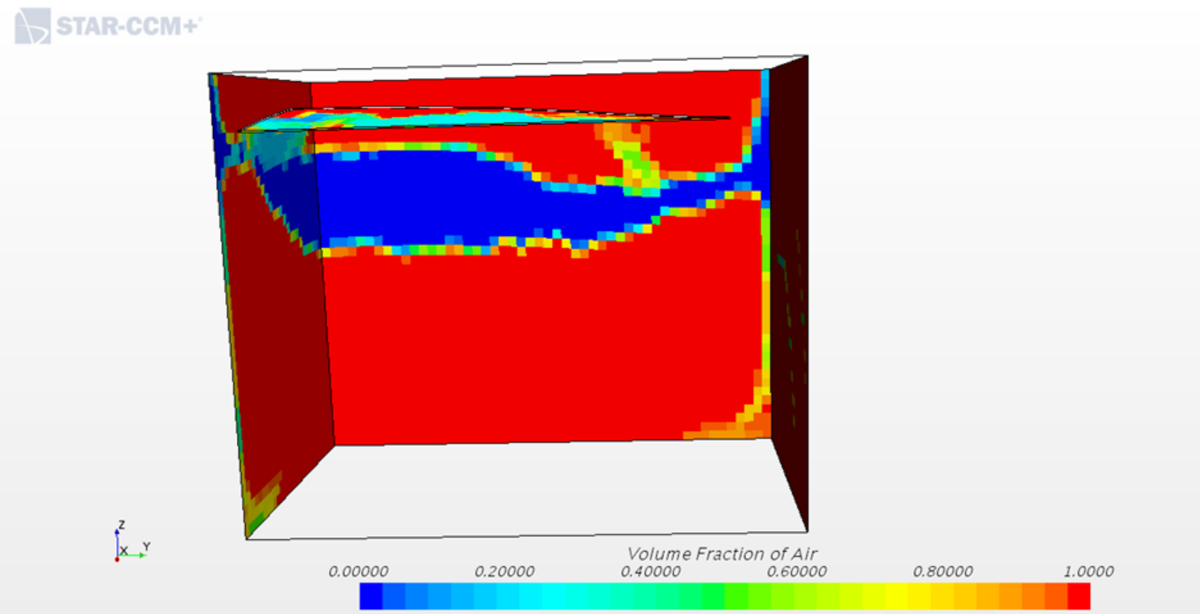 STAR-CCM+ Volume Fraction of Air 0.00000 0.20000 0.40000 0.60000 0.80000 1.0000 Z X Y

APPENDIX XXVI: SETTING AIR AS COMPRESSIBLE & WATER AS INCOMPRESSIBLE (Volume Fraction of Water)

4 m/s	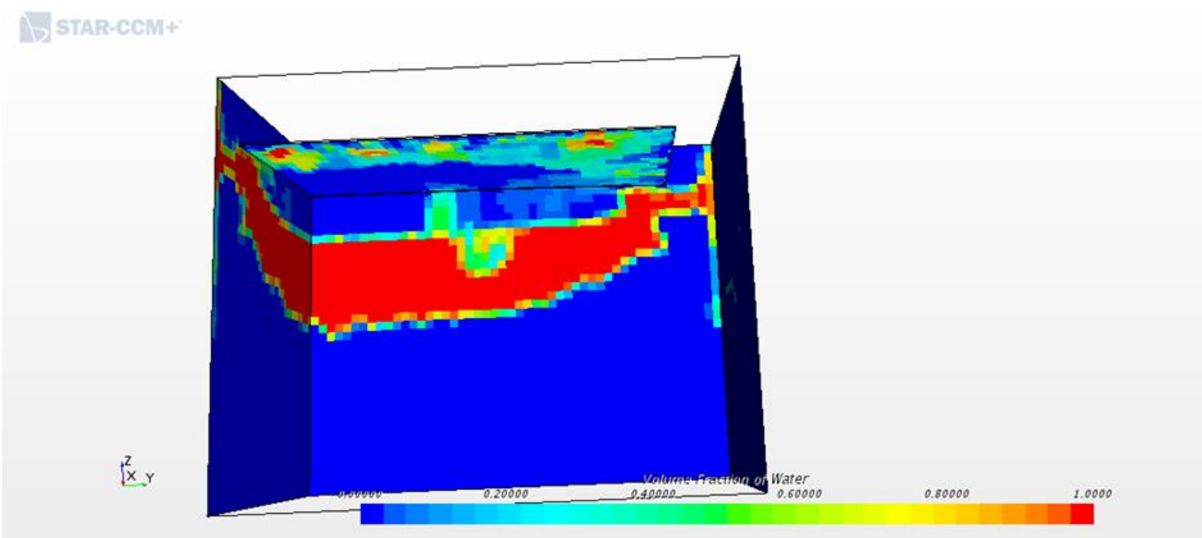

8 m/s	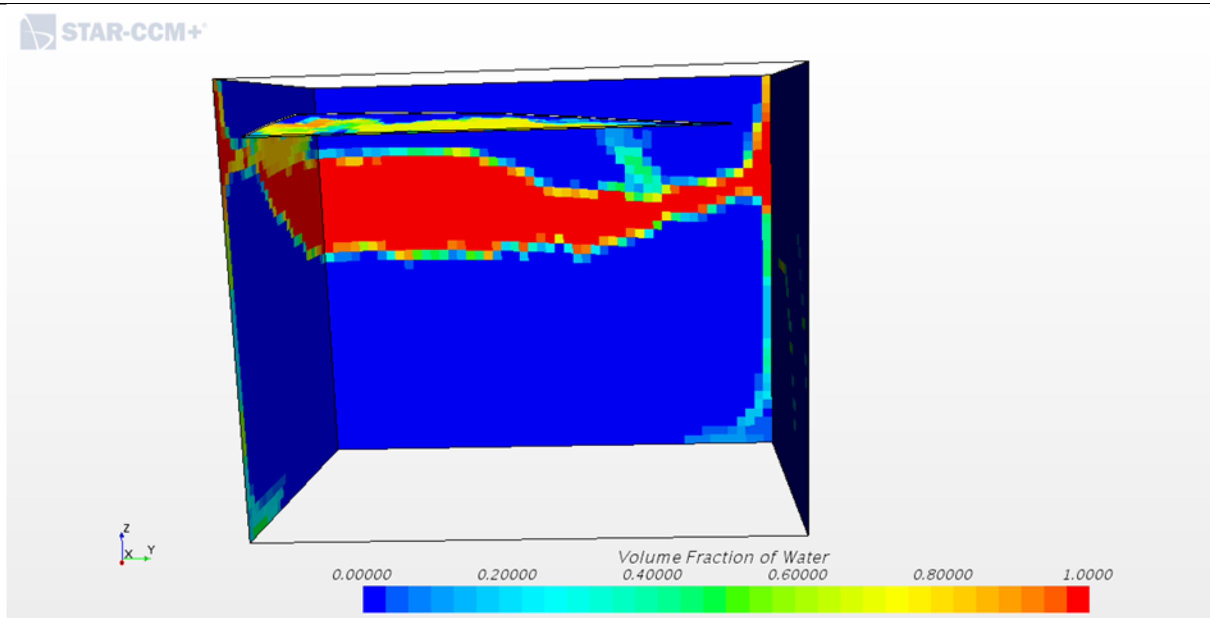STAR-CCM+ Z X Y Volume Fraction of Water 0.00000 0.20000 0.40000 0.60000 0.80000 1.0000

APPENDIX XXVII: SETTING AIR AS COMPRESSIBLE & WATER AS INCOMPRESSIBLE (Pressure Distribution)

4 m/s	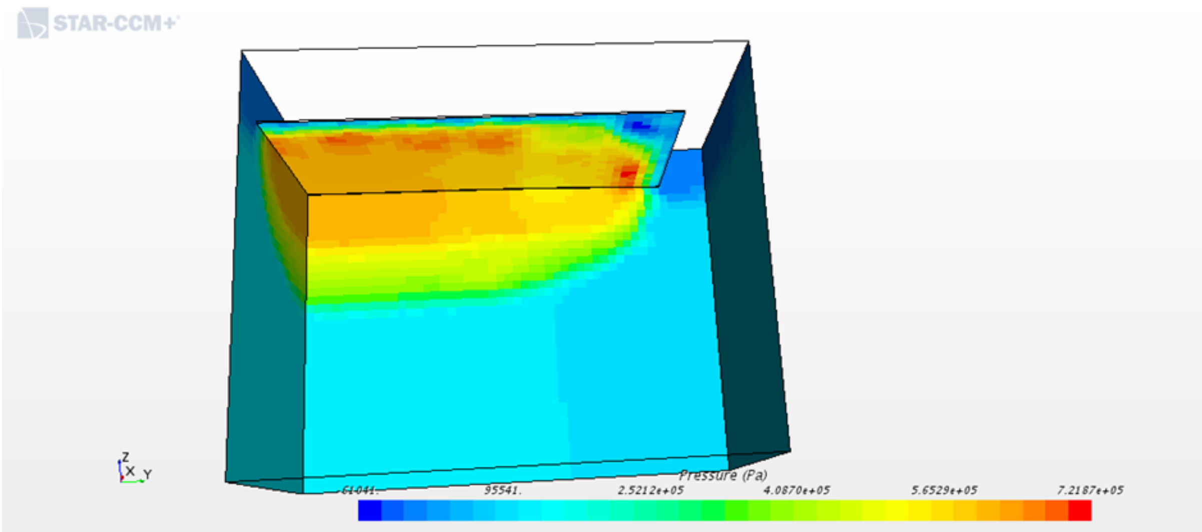

8 m/s	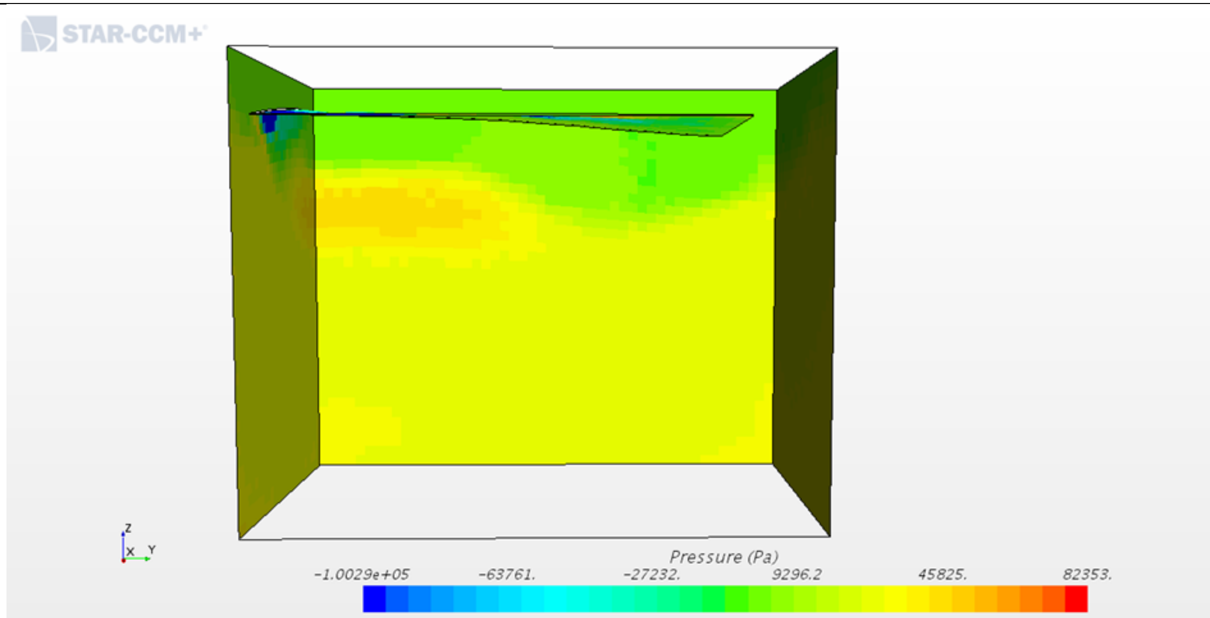Pressure (Pa) -1.0029e+05 -63761. -27232. 9296.2 45825. 82353.

APPENDIX XXVIII: SETTING AIR AS COMPRESSIBLE & WATER AS INCOMPRESSIBLE (ABAQUS Solution on Plate)

4 m/s	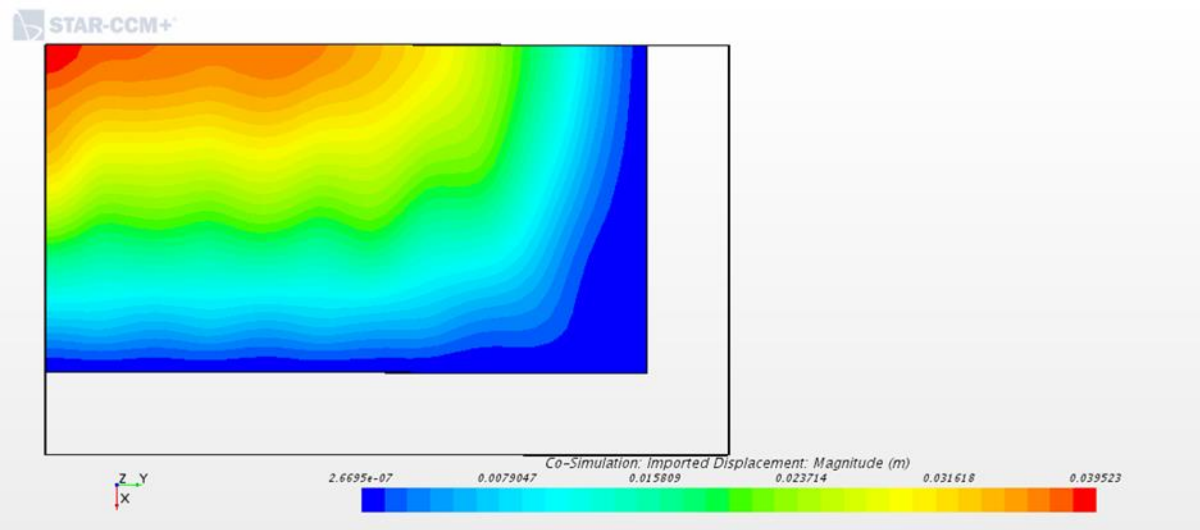

8 m/s		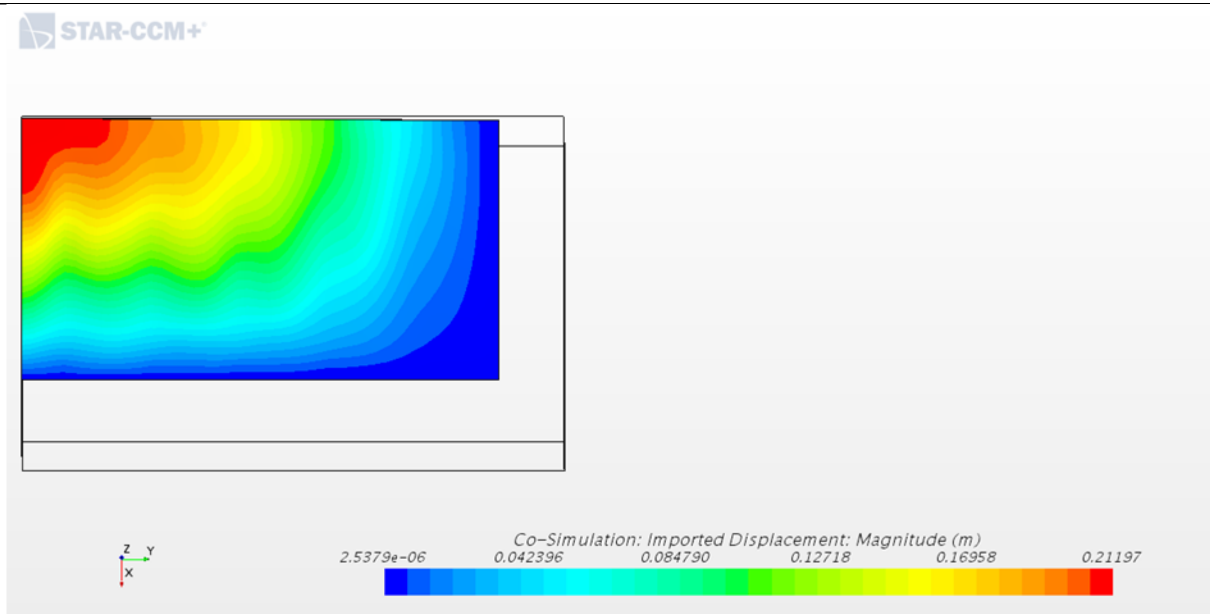STAR-CCM+
Co-Simulation: Imported Displacement: Magnitude (m)
2.5379e-06
0.042396
0.084790
0.12718
0.16958
0.21197
Z
Y
X

APPENDIX XXIX: 1° DEADRISE, WATER INCOMPRESSIBLE, AIR COMPRESSIBLE

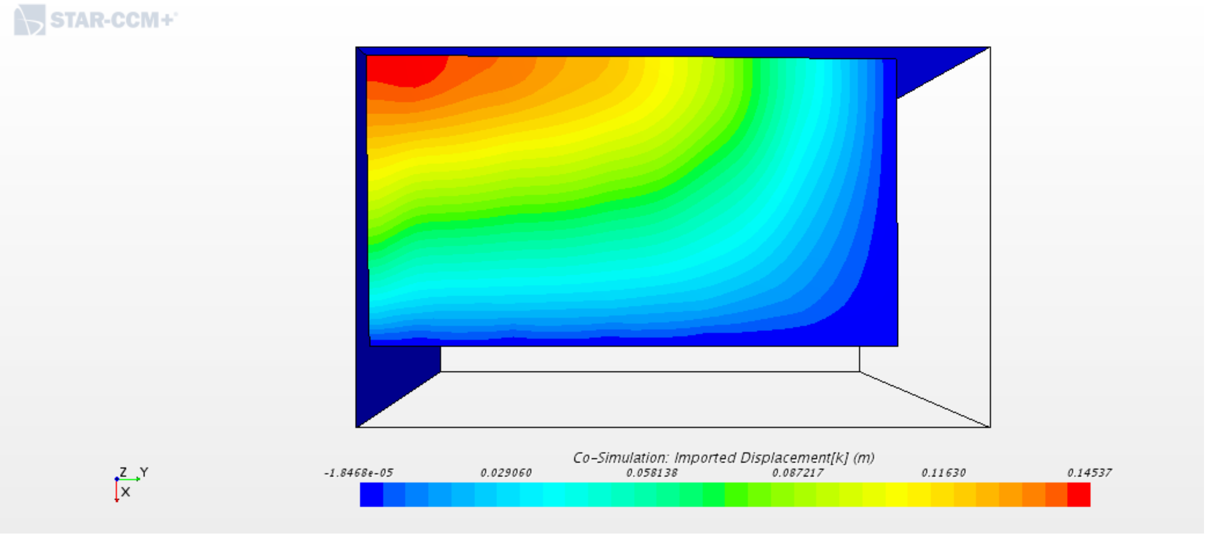

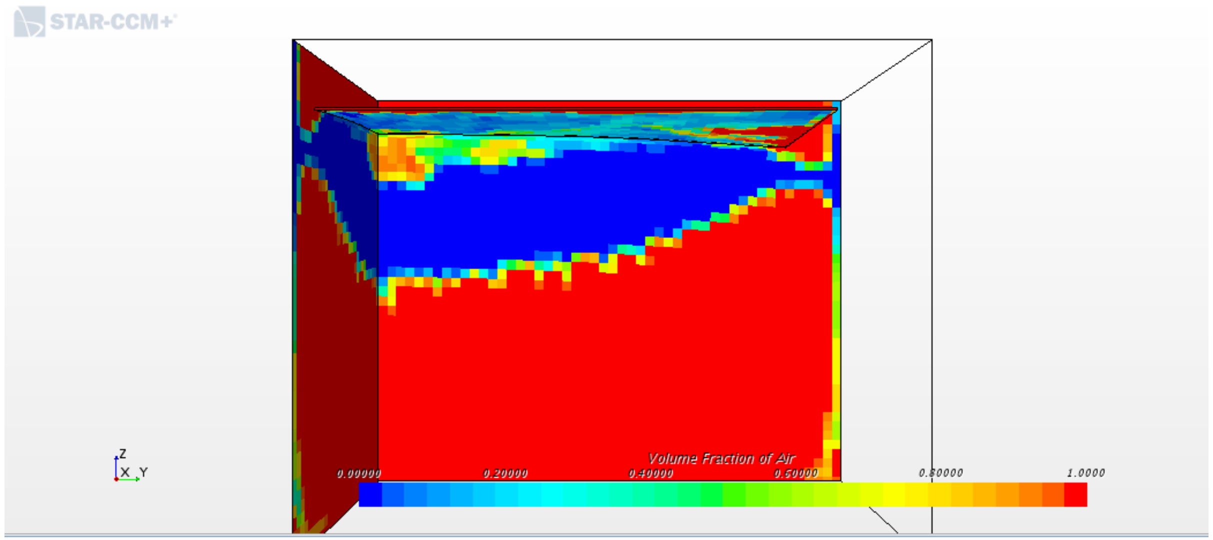

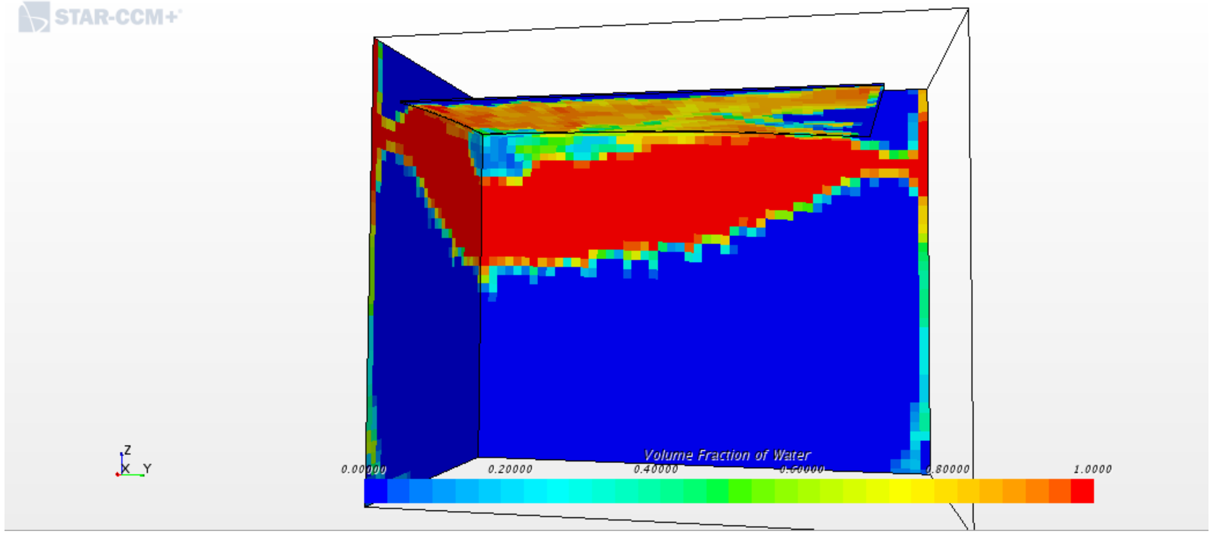
STAR-CCM+
Volume Fraction of Water
0.00000
0.20000
0.40000
0.80000
1.0000
Z
X
Y

APPENDIX XXX: 2° DEADRISE, WATER COMPRESSIBLE, AIR COMPRESSIBLE

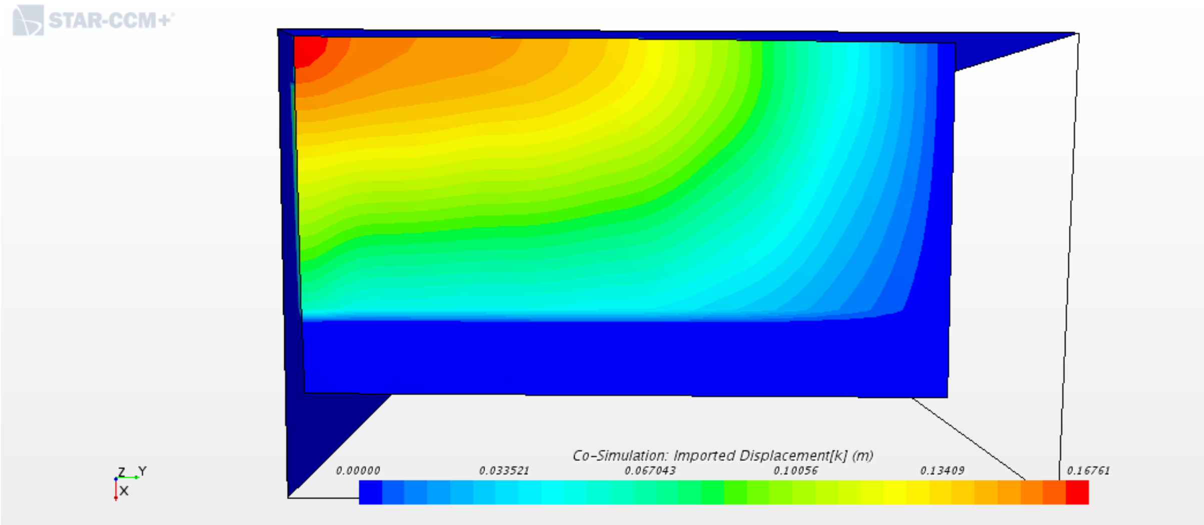

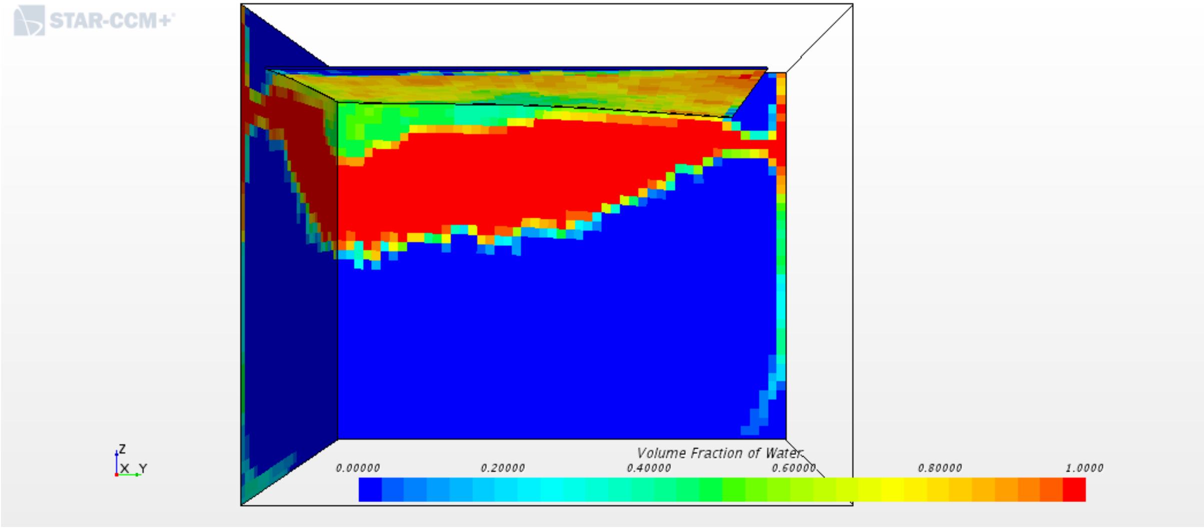
STAR-CCM+
Volume Fraction of Water
0.00000
0.20000
0.40000
0.60000
0.80000
1.0000

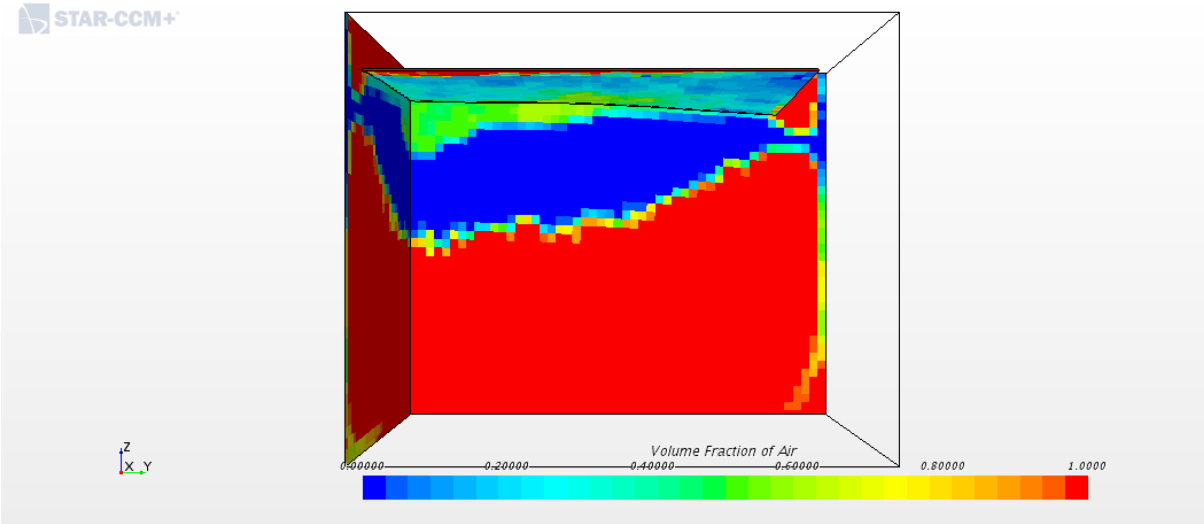
STAR-CCM+
Volume Fraction of Air
0.00000
0.20000
0.40000
0.60000
0.80000
1.0000

APPENDIX XXXI: 2° DEADRISE, WATER COMPRESSIBLE, AIR INCOMPRESSIBLE

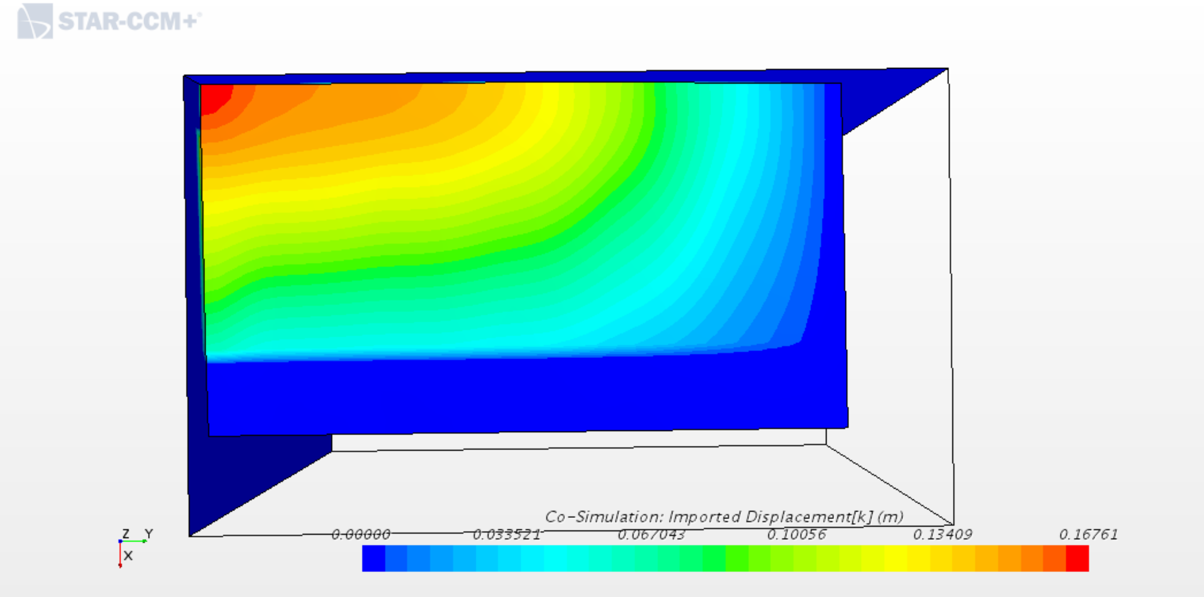

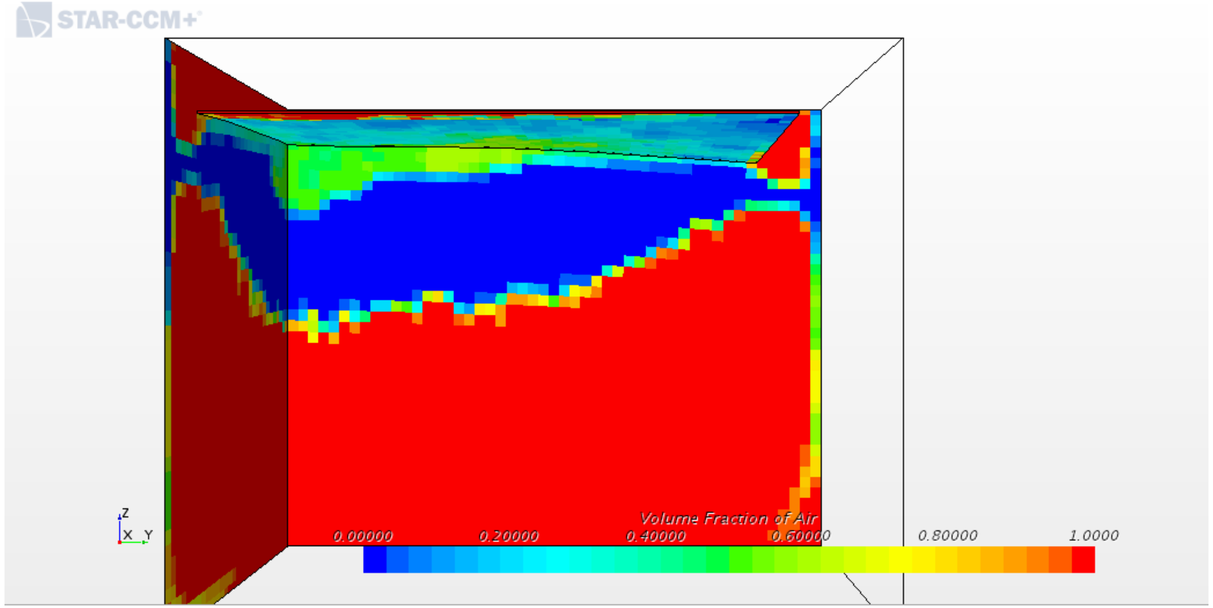

STAR-CCM+
Volume Fraction of Air
0.00000
0.20000
0.40000
0.60000
0.80000
1.0000
Z
X
Y

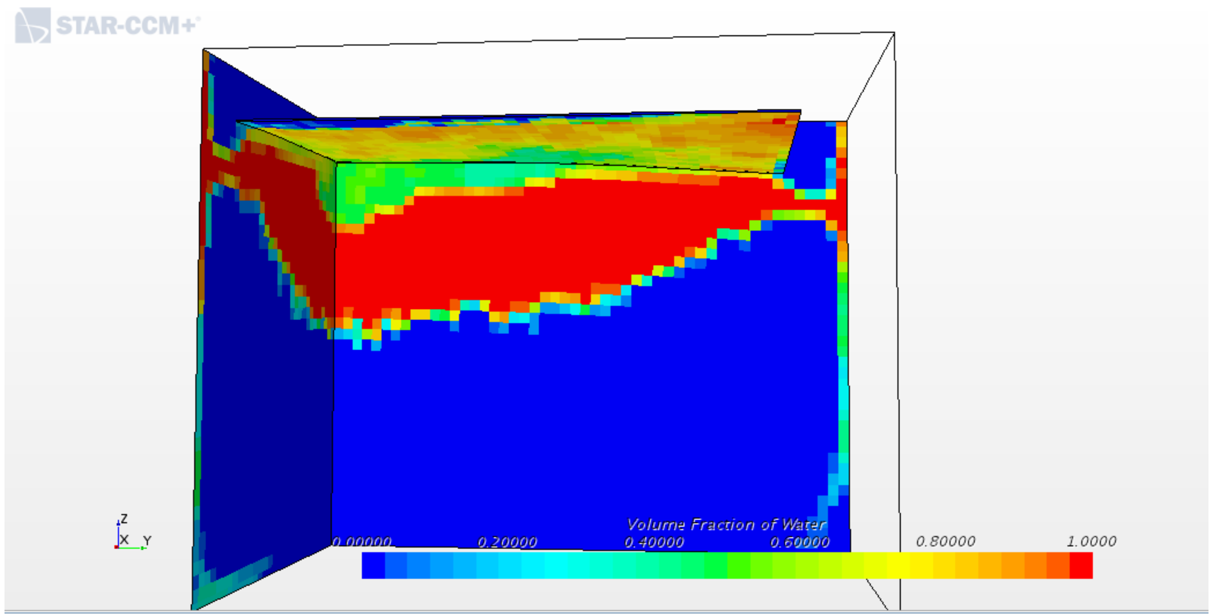

STAR-CCM+
Volume Fraction of Water
0.00000
0.20000
0.40000
0.60000
0.80000
1.0000
Z
X
Y

APPENDIX XXXII: 2° DEADRISE, WATER INCOMPRESSIBLE, AIR COMPRESSIBLE

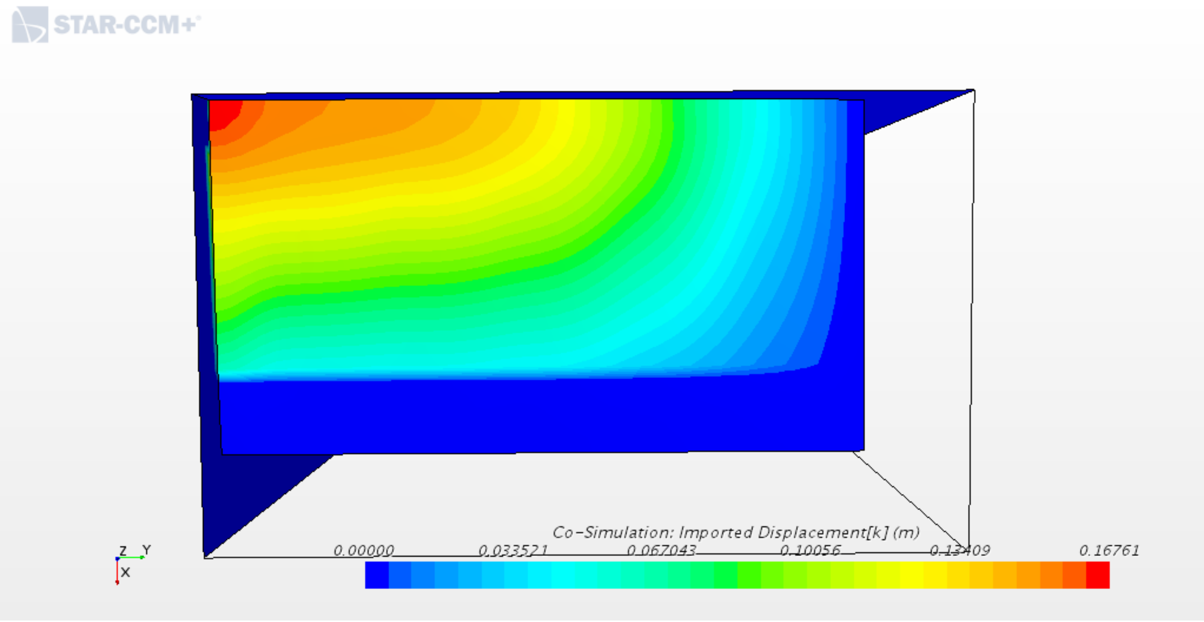

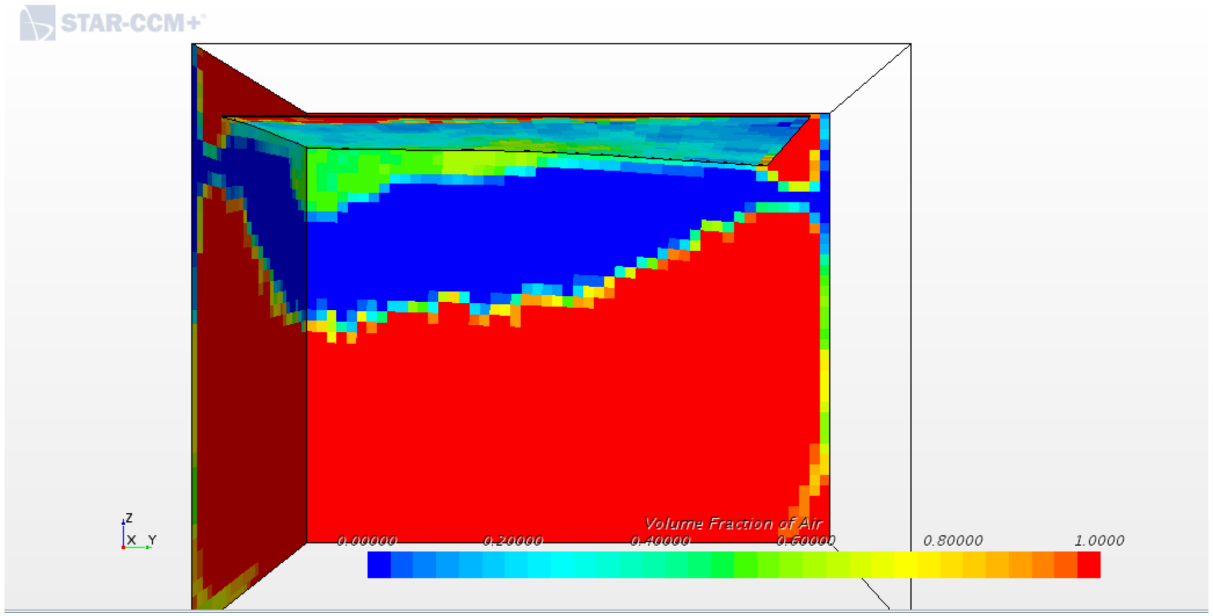
STAR-CCM+
Volume Fraction of Air
0.00000
0.20000
0.40000
0.60000
0.80000
1.0000
Z
X
Y

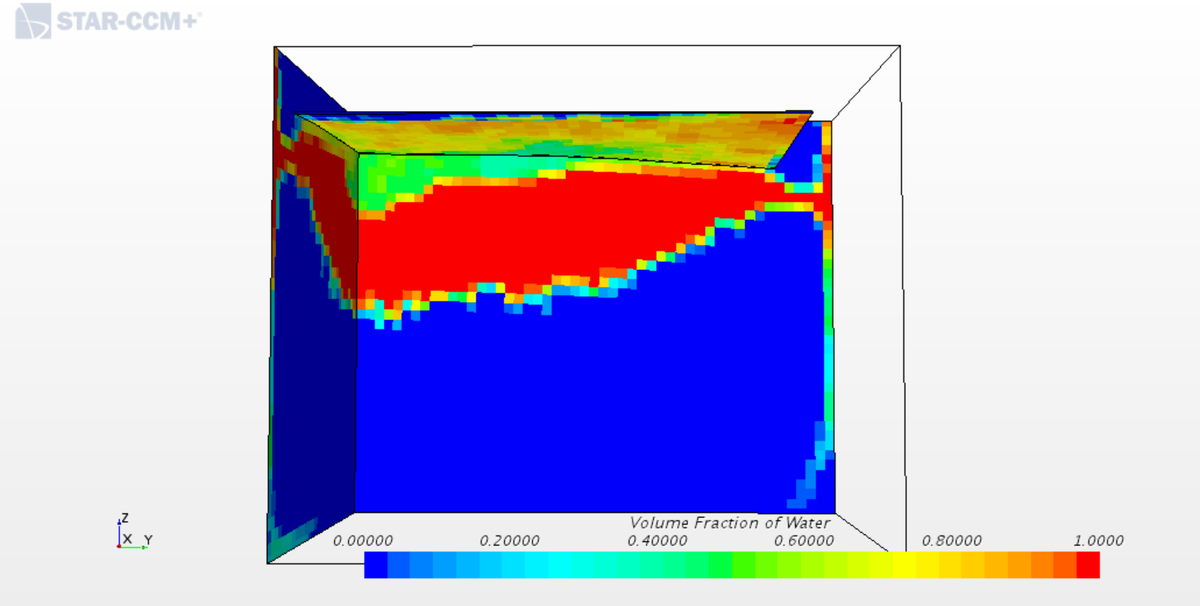
STAR-CCM+
Volume Fraction of Water
0.00000
0.20000
0.40000
0.60000
0.80000
1.0000
Z
X
Y

APPENDIX XXXIII: 5° DEADRISE, WATER COMPRESSIBLE, AIR INCOMPRESSIBLE

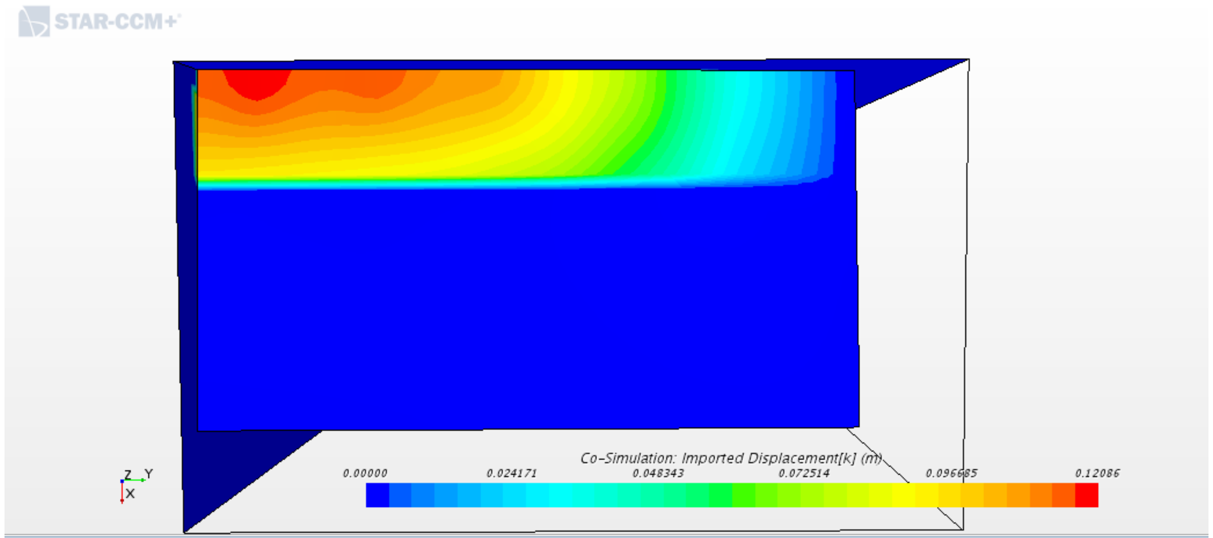

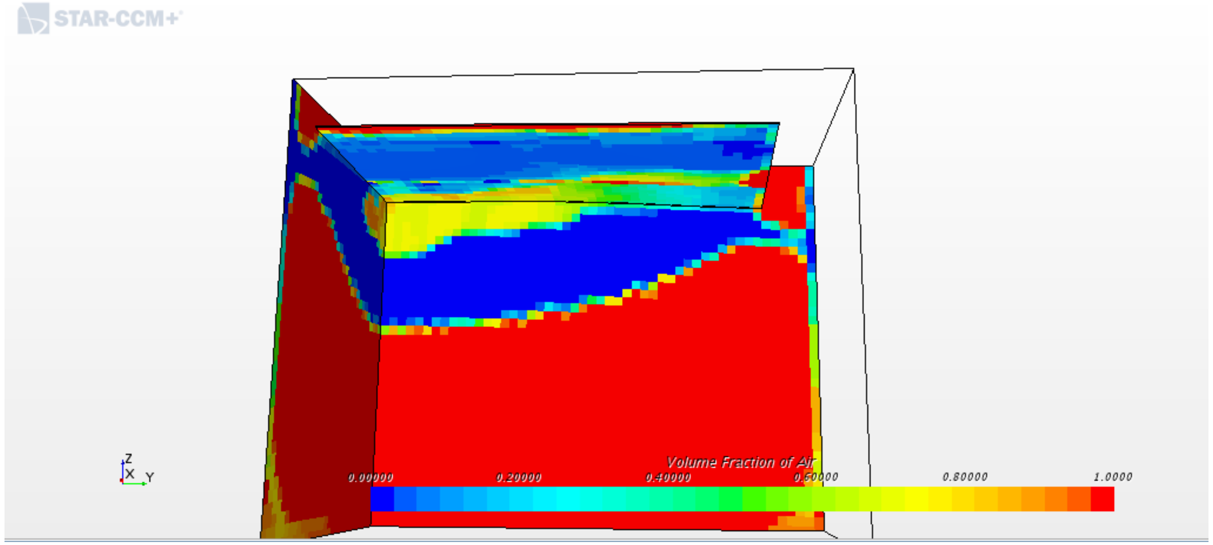
STAR-CCM+
Volume Fraction of Air
0.00000
0.20000
0.40000
0.60000
0.80000
1.0000

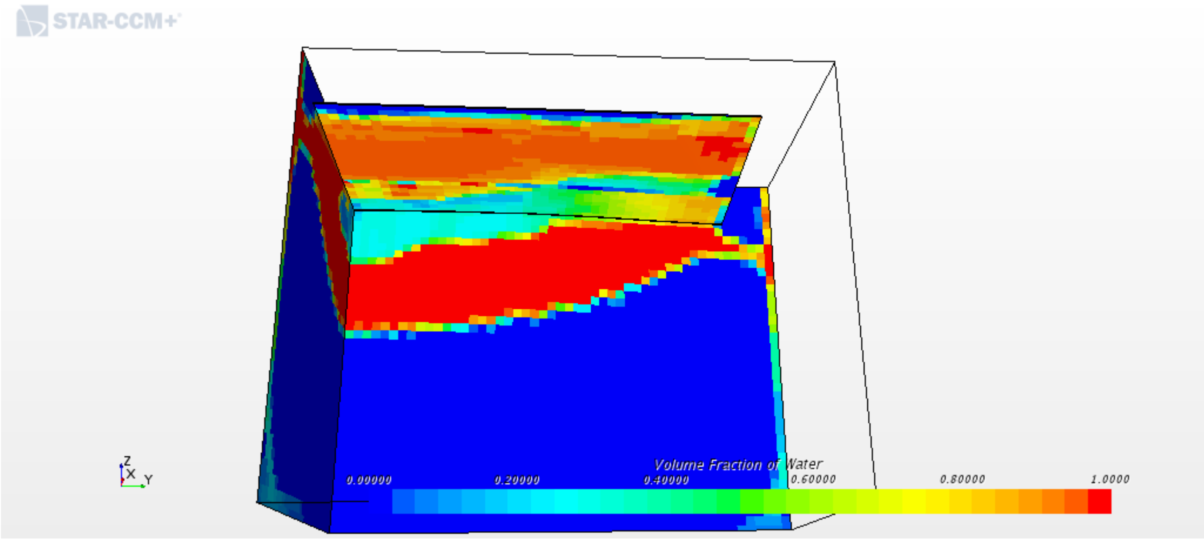
STAR-CCM+
Volume Fraction of Water
0.00000
0.20000
0.40000
0.60000
0.80000
1.0000